

Cathode Ray Tubes:

Getting Down to Basics

TEKTRONIX, INC.
Test & Measurement Training

**Cathode Ray Tubes:
Getting Down to Basics**

068-0313-00


Copyright (C) 1989, Tektronix, Inc. All rights reserved. Printed in the U.S.A., Tektronix products are covered by U.S. and foreign patents, issued and pending. Information in this publication supersedes that in all previously published material. Specification and price change privileges reserved. TEKTRONIX, TEK, SCOPE-MOBILE and  are registered trademarks of Tektronix, Inc. TELEQUIPMENT is a registered trademark of Tektronix U.K. Limited.

TABLE OF CONTENTS

	Page
Electron Optics	1
The Triode Section	5
Unblanking	11
Focus and Astigmatism Lens	17
The Deflection System	19
Acceleration Schemes	33
Space Charge Repulsion Effect and Trace Width	39
Phosphors	43
Human Eye Response	45
Luminance Characteristics of Phosphors	47
Spectral Response	51
Photographic Writing Speed	53
Phosphor Burning	57
Aluminized Tubes	59
Graticules	61
Trace Alignment	63
Special CRT Types - Dual Beam	65
Special CRT Types - Dual Gun	67
Special CRT Types - 7612D	69
Special CRT Types - 7912	83
Special CRT Types - 7104	89
Storage Tube Basics	93
Bistable Phosphor-Target Tube Construction	97
Operating Characteristics of the Phosphor-Target Tube	103
Bistable Storage Oscilloscope Features	113
Features of the Transfer Storage Oscilloscope	127
Storage Writing Speed	131

FORWARD

This book was written to serve three major purposes:

1. To understand the interaction and interdependence between the CRT and electronic circuitry in measurement devices having CRTs. The cathode-ray tube (CRT), as the output or display section of oscilloscopes, graphics terminals and other measurement devices, requires understanding in isolating a malfunctioning electronic circuit, the design of circuitry that interfaces with the CRT is dependent upon the requirements of the CRT and before these circuits can be fully analyzed the requirements of the CRT must be known. The proper operation of the various controls and adjustments directly associated with the display requires an understanding of the probable effect upon the CRT.
2. To understand the basic theory or principles of CRT design and operation. In today's world of solid-state devices the principles of operation of vacuum devices is relatively unknown. This book is an attempt to give the engineer, technician or other reader a basic understanding of CRT operation.
3. To consolidate previous CRT-technical documents under one cover. Over the past 30 years there have been a number of CRT theory booklets and technical reports written by Tektronix covering CRT design and theory of operation; some were published and now are out-of-date and no longer in print, others were never published.

I wish to acknowledge those whose publications have been used in this book and whose efforts continue to advance the performance of cathode-ray tubes.

Vernon L. Isaac
CRT Product Assurance Manager
Tektronix, Inc.

ELECTRON OPTICS

The electrons emitted by the heated cathode are acted upon by the electric field between the cathode, grid, and first anode. This field can be represented by lines showing where the potential of the field is constant. These lines are called equipotential lines and their effect on an electron passing through them depends on their shape, the voltage difference between them, their spacing, the velocity of the electron, and whether the electron is traveling in the direction of increasing or decreasing potential.

The CRT axis is used as a reference for describing the path of an electron. This axis is the center line of the tube or, in other words, the shortest straight line from the cathode to the faceplate. An electron's velocity can be separated into two components, axial velocity and radial velocity. Figure 1-1 shows an electron with its velocity separated into these two components. Both components are referenced to the CRT axis. The radial component is perpendicular to the CRT axis and the axial component is parallel to the axis.

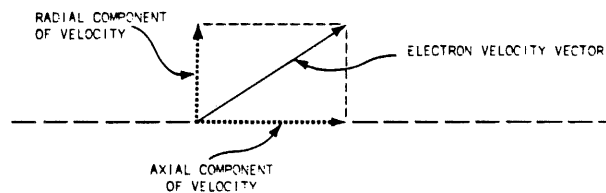


Figure 1-1

The action of an electrostatic electron lens is based on the fact that the force acting upon an electron traveling in the field is in a direction perpendicular or normal to the lines of equal potential and in the direction of increasing potential. Figure 1-2 shows an electron passing through equipotential lines. The electron is traveling in the direction of increasing potential. The entrance velocity of the electron is normal to the equipotential lines and the force acting on the electron is normal to the lines in the same direction. Therefore, the velocity vectors add and the axial velocity of the electron is increased. The electron has no radial velocity before entering the field and the field imparts none.

If the field in Figure 1-2 were reversed so that the electron was traveling in the direction of decreasing potential, the force acting on the electron would still be normal to the equipotential lines but in the opposite direction shown. The exit velocity in such a case would be less than the entrance velocity.

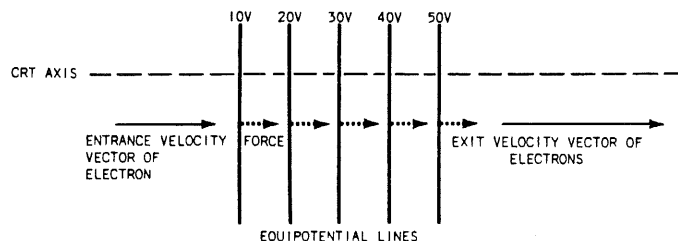


Figure 1-2

Notice that there is no change in the direction of the electron in Figure 1-2, only the velocity of the electron is changed. This will be true for all fields where an electron passes through an equipotential line normal to the line. The electron's velocity will be affected but not its direction.

Figure 1-3 shows an electron passing through a field with equipotential lines parallel to the CRT axis. The force acting on the electron is normal to the line and therefore perpendicular to the electron's entrance-velocity vector. These two vectors are shown in Figure 1-3 and the final velocity vector is shown. The axial velocity of the electron has not changed, but a radial component has been added.

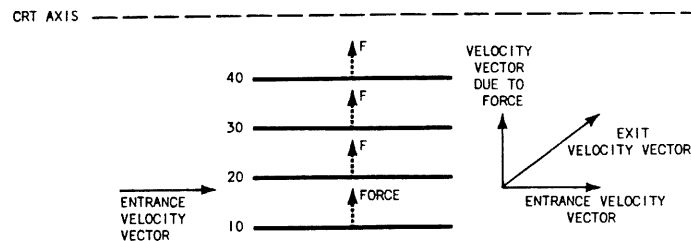


Figure 1-3

An electron passing through equipotential lines at some angle, as shown in Figure 1-4, will have a change in axial velocity but no change in radial velocity. This change in axial velocity will result in a change in direction and velocity. The force acting on the electron is parallel to the axis and therefore the radial component of the electron's velocity is not affected.

The approximate exit direction of an electron can be easily predicted by first resolving its entrance velocity into its axial and radial components and then adding the velocity vector due to the force of the equipotential lines.

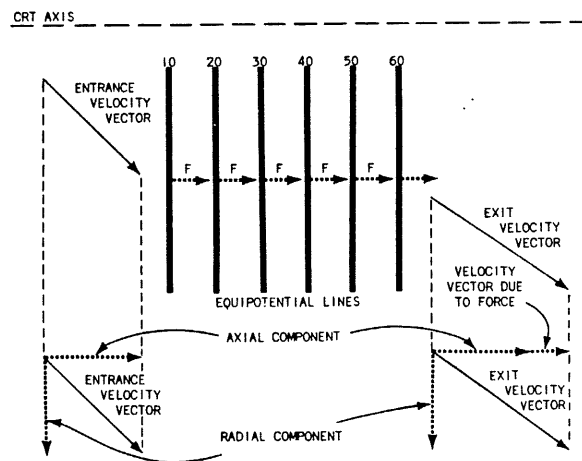


Figure 1-4

Not all equipotential lines are straight. When the equipotential lines are curved, the question which needs answering is whether the lens is convergent or divergent. When determining whether a lens is convergent or divergent in nature, it must first be determined whether the electron is traveling through an increasing or a decreasing potential. An increasing potential situation will be considered first.

An electron passing through a convex equipotential line will be bent toward the axis (Figure 1-5). The effect of the field is convergent. An electron passing through a concave equipotential line will be bent away from the axis (Figure 1-6). The effect of the field is divergent.

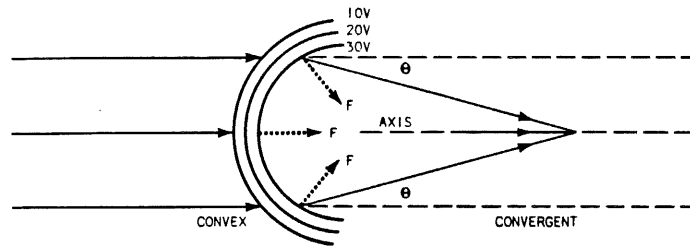


Figure 1-5

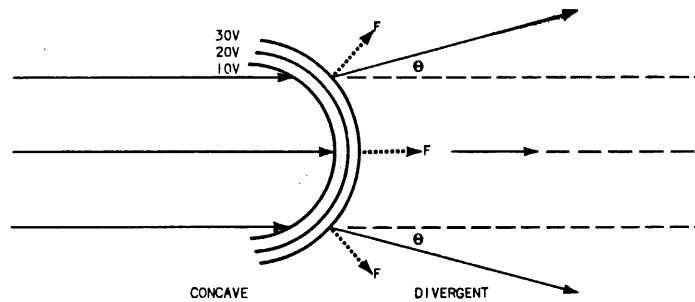


Figure 1-6

The assumption has been made that the electron is traveling in the direction of increasing potential. The size of the angle θ will depend upon the strength of the field, the initial velocity of the electron, and the curvature of the equipotential lines. If the initial electron velocity is increased, the angle will decrease. If the curvature of the field is increased (a smaller circle has a greater curvature), the angle will increase. If the strength of the field is increased the equipotential lines are closer together.

Notice that there is no change in direction of an electron for either field when the original direction of the electron is normal to the equipotential line. When the electron passes through the field normal to the equipotential lines there is no change in direction, only a change in velocity.

The effect of the two lenses is reversed if the electron is traveling in the direction of decreasing potential. Figure 1-7 shows a convex lens that is divergent. The electron has an initial velocity and is passing through a decreasing potential. The velocity of the electron will decrease and the lens will be divergent as shown.

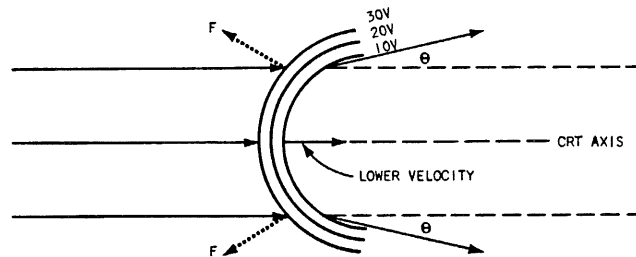


Figure 1-7

THE TRIODE SECTION

The gun section can be divided into two sub-sections, the triode and the focus lens. The triode section of the CRT provides a source of electrons, a means of controlling the number of electrons, and a means for shaping the electrons into a beam.

The triode consists of the cathode, the grid, and the first anode. The cathode consists of a nickel cap coated with barium and strontium oxides. The cathode cylinder is mounted in a ceramic support with the heater held inside by metal leads attached to the ceramic heater mount. A spacer between the cathode assembly and grid cup maintains proper grid to cathode spacing.

The retainer below the cathode support holds the cathode assembly in place and attaches the ceramic heater support to the grid cup.

The cathode spacer and the cathode assembly are placed in the grid cup. The cathode retainer below the cathode is inserted into the grid cup and spot welded in place. The ceramic heater support is held in place by bending the tabs of the cathode retainer. The heater is inserted into the cathode cylinder and its leads welded to tabs mounted on the ceramic heater support. See Figure 2-1.

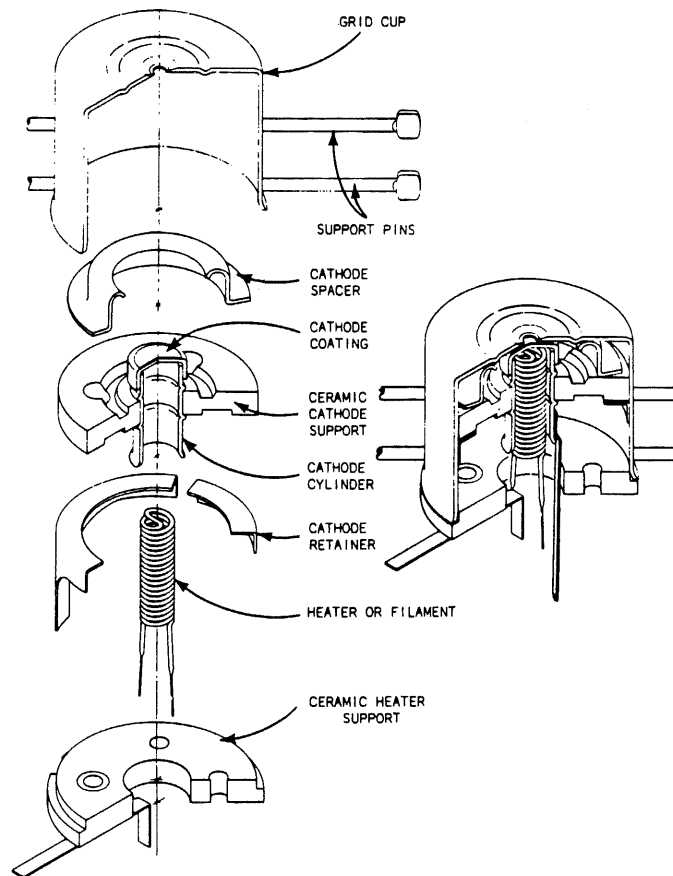


Figure 2-1

The first anode (acceleration) is located in front of the grid and operated several thousand volts more positive than the grid. The grid, as in most triodes, is operated at a more negative voltage than the cathode. The support pins of the first anode and grid cups are pressed into glass rods to maintain proper spacing between the elements.

The equipotential lines are almost straight in the center area and would tend to cause an electron to move parallel to the axis. In the area of the anode aperture the lens is concave; therefore, divergent. The electron velocity at this point is much greater than in the grid aperture and the effect of this divergent lens is slight. The lines are not curved as much as in the grid region so the lens is weaker.

The triode can be divided into three regions when considering the approximate trajectory of an electron through this lens. The first region is the grid-cathode region where the equipotential lines dip towards the cathode through the grid aperture. The second region is between the grid and the anode where the lines are parallel to the grid and anode surfaces. The third region is the anode aperture region where the field penetrates the aperture.

An electron leaving the cathode at some angle less than 90 degrees with respect to the axis and with some velocity due to thermal energy, would immediately experience a decrease in radial velocity and an increase in axial velocity. This would accelerate the electron and bend it toward the axis until it crossed the axis. The point of axis crossover is not the same for all electrons due to the difference in their thermal energy and the initial angle of emission.

As the electron approaches the center region where the equipotential lines are straight (parallel to grid-anode surfaces), it has a radial velocity away from the axis. The axial velocity of the electron will be increasing as it passes through this region but the radial velocity will remain essentially constant. The increase in axial velocity causes the electron to arrive at a trajectory nearly parallel to the axis.

The axial velocity of the electron is higher on entering the anode aperture than it was in the first two regions. The effect of the field on the electron in this region is therefore reduced, but still apparent. The curvature of the field indicates a divergent effect or an increase in radial velocity away from the axis with continued increase in axial velocity.

The electrons emitted from a point on the surface of the cathode, which is off axis, will have a different trajectory and each will experience different forces. Also, one would expect the electrons emitted almost perpendicular to the axis of the triode to cross the axis at a different point than those emitted parallel to the axis.

If the cathode is considered as an infinite number of point sources, the beam will be made up of many rays of electrons crossing the axis at different points.

Electrons which leave different points of the cathode at the same angle, cross at a section of the beam called the crossover. This part of the beam has the least cross-sectional area. The final focused spot seen on the face of a CRT is the image of the crossover and the crossover size determines to a great extent the final spot size.

The size of the crossover and its location along the axis is dependent upon the triode dimensions and voltages. As the control grid voltage is changed to increase or decrease beam current the size and location of the crossover will change; therefore, the focus of the beam.

Remember that the elements shown and the electron beam are three dimensional and are shown in a cross-sectional view. Remember also that the equipotentials represented by lines are actually surfaces.

The equipotential plots of the grid-cathode lens for several values of grid voltage are shown in Figure 2-2. Notice in Figure 2-2A the zero equipotential line does not reach through the grid aperture and touch the cathode. Electrons emitted from the cathode with only slight thermal velocity are prevented by a retarding field from reaching an equipotential line equal to or greater than the cathode potentials. The voltage required to bring about this condition is the cutoff voltage. Figure 2-2B, C, and D show tubes in various stages of conduction, depending on the grid voltage.

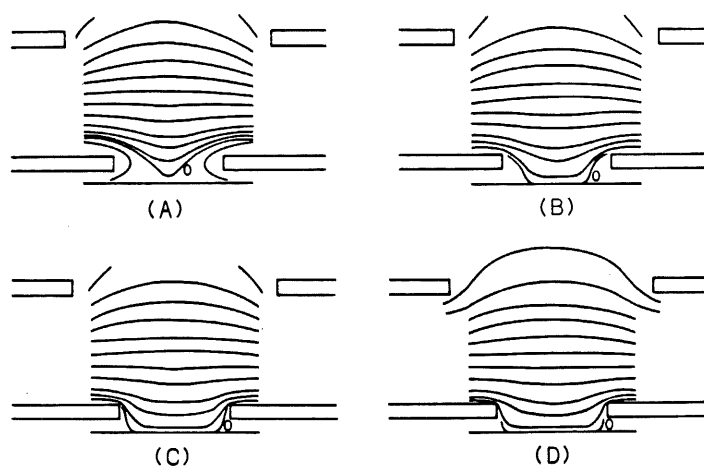


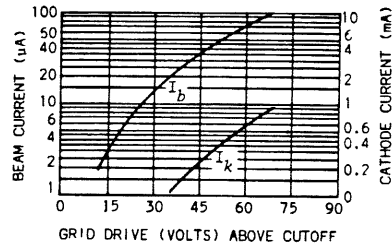
Figure 2-2

Notice that the shape of the equipotential lines in each case is different and therefore the lens effect is different in each case. The factors affecting V_{co} are the same as those affecting the equipotential lines: grid-cathode spacing, grid material thickness, and anode and grid aperture diameter. If the field increases near the cathode so does the cutoff voltage. The field can be increased by: (1) decreasing the grid-cathode spacing, (3) decreasing the grid material thickness, or (4) increasing the grid aperture diameter.

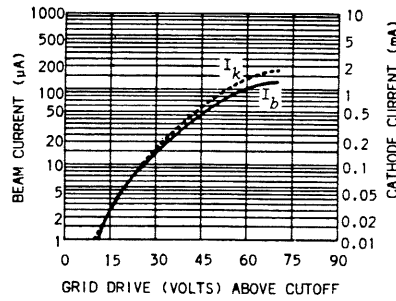
When the grid-aperture diameter is reduced, the cutoff voltage is decreased. A reduction in anode voltage causes the field to decrease, and the cutoff decreases.

These graphs show the change in beam current and cathode current with respect to grid-drive voltage which is shown in volts above cutoff. The grid voltage in normal operation is the result of the setting of the intensity control and the unblanking pulse. Notice that on the left the vertical is calibrated in μA of beam current (I_b) while on the right in mA of cathode current (I_k). The horizontal is in volts above cutoff of the tube with the actual cutoff voltage (V_{co}) and the voltage on the acceleration anode (V_A) given. The curves are valid only for the given first anode acceleration voltage and are average for a group of tubes.

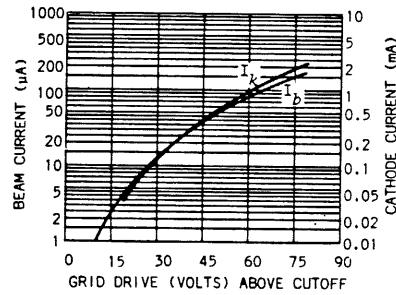
T5030
 $V_{co} = -57\text{V}$
 $V_A = 3000\text{V}$



T5470
 $V_{co} = -76\text{V}$
 $V_A = 2000\text{V}$



T6470
 $V_{co} = -92\text{V}$
 $V_A = 2250\text{V}$



From these graphs the beam current for any reasonable grid drive may be found. If the amount of beam current is known then trace width, light output, and relative writing speed may be approximated. These approximations will be shown later.

As the emitting diameter changes, the cathode loading (current/unit area drawn from the cathode surface) changes. The cathode loading is not uniform across the emitting area but peaked as shown in Figure 2-3.

Figure 2-3 shows a high current density or loading present in the center of the emitting area and tapering off toward the edges. It also shows that the peak current density has a different value for different values of grid voltage. Curves showing the distribution of electrons within the beam would have the same shape as those shown in Figure 2-3.

Grid-cathode spacing will also affect cathode loading. A decrease in spacing will cause an increase in cathode loading and therefore more current for a given grid voltage. As mentioned previously, this decrease in grid-cathode spacing causes a higher V_{co} .

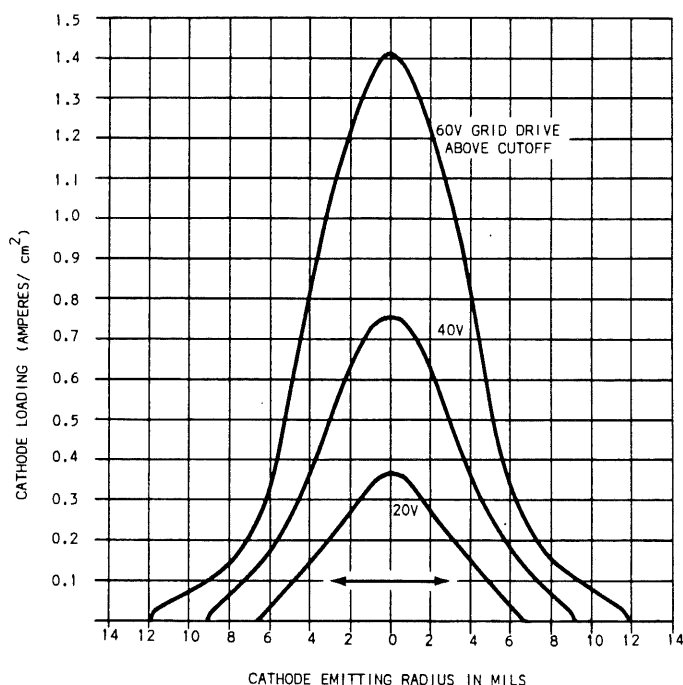


Figure 2-3

UNBLANKING

Some means of controlling the number of electrons is needed in the triode section of a CRT. In any triode the current may be controlled by changing the voltage on the grid with respect to the cathode. Similarly, a front panel control (Intensity) varies the grid voltage of the CRT and allows the operator to adjust the beam current.

In normal operation of the CRT the beam appears on the screen only after the sweep has been triggered. In most CRTs a positive pulse is applied to the control grid for the duration of the sweep. This method is called grid unblanking. The grid voltage is set by the intensity control below V_{co} . As the sweep starts, the gun is turned on by a positive unblanking pulse applied to the grid. The gun is cutoff in the absence of an unblanking pulse (Figure 3-1) when the intensity control is properly set.

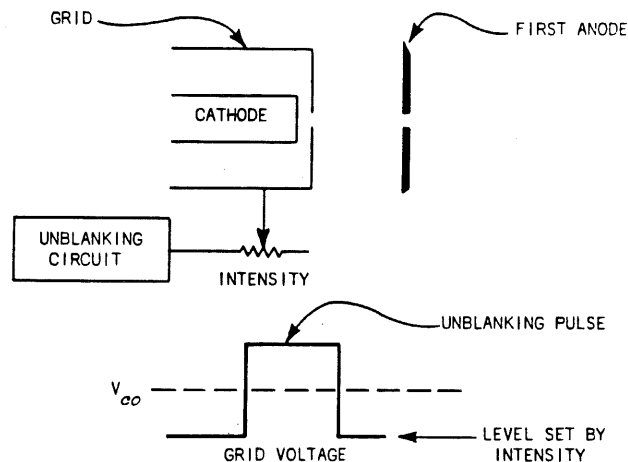


Figure 3-1

Another method of controlling the beam is called deflection plate unblanking. This requires a set of plates immediately following the first anode which in this case is a plate rather than a barrel type anode. The deflection plates are positioned horizontally. A top view of this type of unblanking is shown in Figure 3-2.

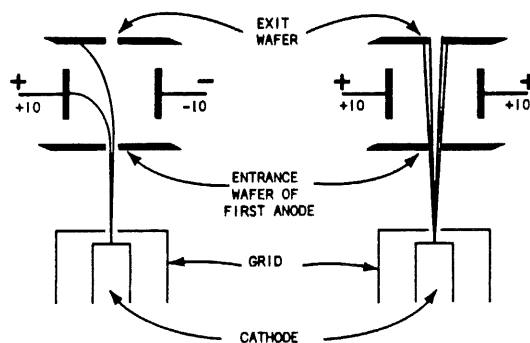


Figure 3-2

The left plate, for example, may be connected to a fixed positive voltage such as 10 V. The right plate is connected to the unblanking circuit in the oscilloscope. When the sweep is not operating, the right plate is at a negative potential with respect to the left plate. The beam is deflected to the left and absorbed by the plate and exit wafer of the first anode. The beam is still turned on but is being deflected off axis and does not reach the screen of the CRT.

When the sweep is triggered, a positive pulse is applied to the right plate. This brings it to approximately the same potential as the left plate and the beam is allowed to pass through the exit aperture.

When grid unblanking is used in a CRT, a spot may be obtained on the screen in the absence of an unblanking pulse by adjusting the intensity control. The grid voltage is raised above cutoff voltage V_{co} and beam current is present. The beam current is increased if an unblanking pulse is then applied to the grid, with the distinct possibility of burning the phosphor. The capability of overriding the unblanking and obtaining a spot may, however be of great aid in trouble shooting or in setting up the measurements.

Grid unblanking requires more power and stiffer power supply regulation. It is therefore used most often in oscilloscopes where power supply regulation and power conservation are not limiting factors.

The intensity control sets the voltage on the grid of the CRT even when deflection plate unblanking is used. The gun is usually turned on and beam current is present at all times with deflection plate unblanking. When the tube is blanked, the beam is deflected and not allowed to reach the screen. In the absence of an unblanking pulse the spot is not seen on the screen even with maximum beam current. The beam is deflected and collected prior to reaching the screen.

In some single-event photography applications it is necessary to monitor the screen for a long period with the shutter of the camera open before the occurrence of the event. Deflection plate unblanking may cause spotting or fogging of the film due to the failure of the deflection unblanking system to collect all of the beam electrons.

The life of a CRT is dependent on, among other things, the life of the cathode, which can be expressed as a function of beam current and the time this current is drawn from the cathode. When an unblanking pulse is absent in a tube using grid unblanking, beam current is usually not present. In a tube with deflection unblanking, the unblanking pulse controls beam deflection and not beam current. Unless the intensity control is turned down, the cathode is being consumed when unblanking is not present. This may reduce the useful life of the tube. Consequently, tubes with high cathode loading do not use deflection unblanking.

Figure 3-3 shows a typical deflection plate unblanking system. Notice that two sets of plates are used and they are cross-connected in the drawing. (The lower left plate is at the same voltage as the upper right plate). The need for this configuration is shown in Figure 3-4 and 3-5. The electrons entering the first anode aperture are subjected to a slight divergent action due to the penetration of the equipotential lines through the aperture. Assuming that one plate is slightly negative with respect to the other plate, the electrons would have a path as shown in Figure 3-4. Some of the electrons would be collected by the positive plate and others by the exit wafer. Some of the electrons, however, would pass through the aperture in the exit wafer and strike the screen. This causes a problem. These electrons have an apparent source off the axis of the tube. This is shown in Figure 3-4 by drawing tangents to the different electron trajectories.

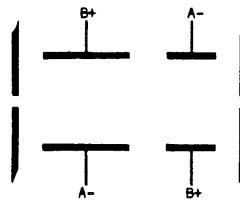


Figure 3-3

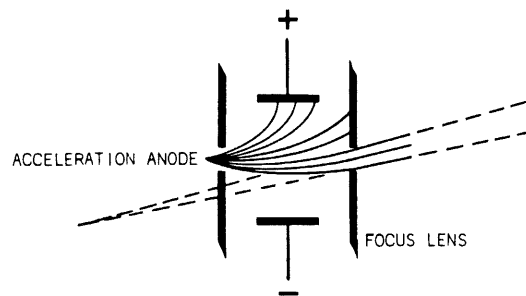


Figure 3-4

Figure 3-5 shows that the apparently off-axis electrons will strike the screen at a different point than electrons from a source on the axis. When the tube is blanked, one plate is much more negative than the other and none of the electrons pass through the aperture. But when the unblanking pulse is applied to one plate, it drives the plate positive and during this change from blanked to unblanked the situation in Figure 3-5 exists. The voltage on the driven plate will be slightly negative with respect to the undriven plate and will be changing until it reaches the same voltage. During the period of change the beam will move on the screen from Point A to Point B (Figure 3-5). The same situation in reverse will occur when the unblanking pulse drives the one plate negative in order to blank the tube. Beam movement on the screen during blanking and unblanking is undesirable.

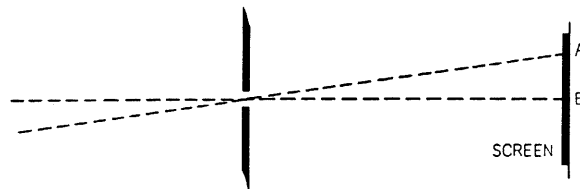


Figure 3-5

The problem can be solved by adding a second set of plates that will bend the beam back toward the axis as shown in Figure 3-6. The tangents to the trajectories with the double plate system show the apparent source to be on axis at all times during blanking or unblanking. With this system there is no movement of the beam on the screen due to unblanking pulse action.

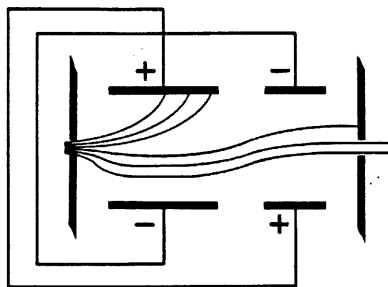


Figure 3-6

Another problem common to deflection plate unblanking is that the beam current may be less than optimum due to normal variations in plate to plate spacing or aperture alignment. An example is shown in Figure 3-7 (only two plates are shown to simplify the drawing).

Case A shows both plates at the same potential. It would be expected that the beam would be centered, allowing the maximum amount of current to pass through the aperture because the maximum concentration of electrons is near the center of the beam. Toward the edge of the beam the density falls off.

Case B shows what might happen if the alignment is slightly off. The beam is slightly offset and beam current is not maximum. This situation might also arise if the peak amplitude of the unblanking pulse was not exactly equal to the voltage on the opposite plate, as shown in Case C.

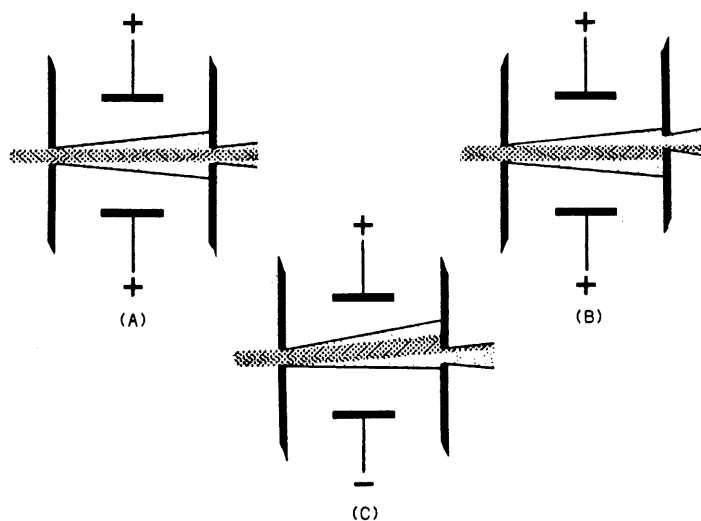


Figure 3-7

The loss in beam current may be unimportant and thus no effort made to correct the situation. Where loss is important, an internal adjustment allows the voltage on one deflection plate to be adjusted for maximum beam current. This control is called the Blank Balance control or the Unblanking Center control. These controls are not front panel controls but are located inside the oscilloscope. Once they have been adjusted they need be checked only during the calibration of an instrument.

It should be said that the use of deflection plate unblanking is no longer done in Tektronix instruments. Grid blanking is now used nearly universally by Tektronix.

FOCUS AND ASTIGMATISM LENS

When the electrons pass through the first anode exit aperture they are slightly divergent. The function of the focus lens is to converge these electrons and cause them to focus or cross the axis at the face plate or screen of the CRT. The focus lens consists of the first anode, the focus ring, and the second anode.

The size and shape of the spot seen on the screen of a CRT is controlled by two controls, Focus and Astigmatism. These controls adjust the voltages on the elements comprising the focus lens.

The equipotential line plot for this lens is shown in Figure 4-1 and the electron trajectory is shown in Figure 4-2. Notice that the lens is divergent at first, then the electrons move parallel to the axis, then the lens is convergent. Note that in the first section of the lens the electrons are passing through a decreasing field and are, therefore, decelerated. They are accelerated in the second half of the lens and exit with the same velocity as they had on entrance.

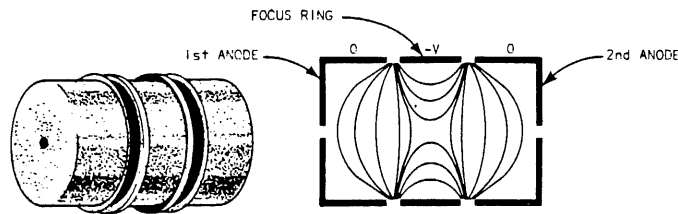


Figure 4-1

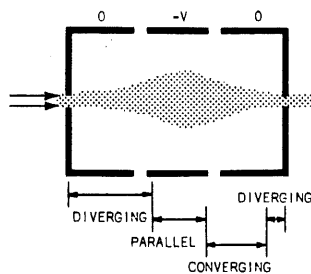


Figure 4-2

The Focus control on the oscilloscope front panel sets the voltage on the focus ring. The lens effect will become stronger as the voltage on the focus ring is made more negative with respect to the two outside electrodes. The increase in the lens strength will shorten the focal length or distance from the lens at which the electrons will cross the axis. The beam is to be focused on the face of the CRT. By changing the focus voltage and thereby the focal length of the lens, the size of the spot on the screen can be adjusted for minimum size (Figure 4-3).

The Astigmatism control sets the voltage on the second anode. Between the second anode and the deflection plates which follow, a cylindrical lens is formed. The astigmatism voltage is adjusted for the roundest spot on the screen which indicates the lens is correcting for any defocusing that might be present.

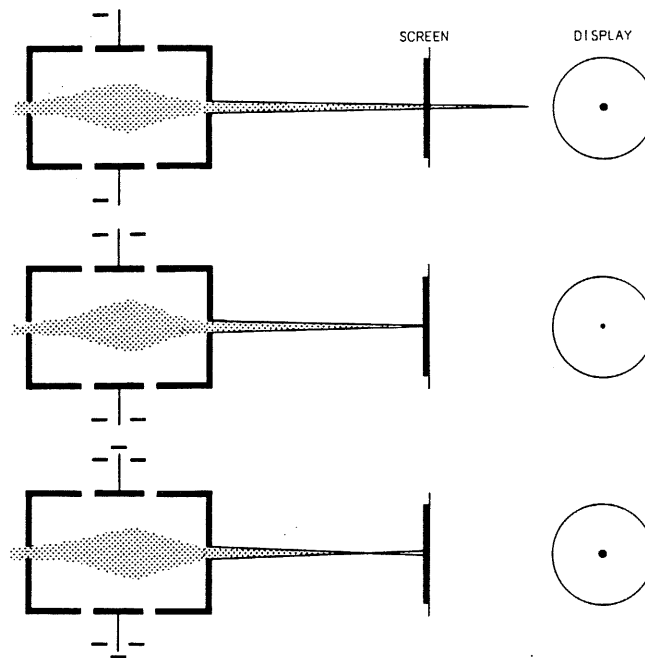


Figure 4-3

THE DEFLECTION SYSTEM

The purpose of the CRT deflection system is to deflect the electron beam vertically and horizontally with minimum deflection factor and minimum distortion. (Minimum deflection factor is the same as maximum deflection sensitivity.) The system must be mechanically and electrically compatible with the other parts of the instrument.

Figure 5-1 shows the second anode of the focus lens and a set of vertical deflection plates. (Several assumptions will be made in the following presentation to simplify the subject.) Notice that the potential on the two plates is equal and that they are approximately equal to the second anode potential. An electron's path is shown. After passing the deflection plates no other forces affect the direction or acceleration of the electron. The electron travels in a straight line and strikes the screen near the center.

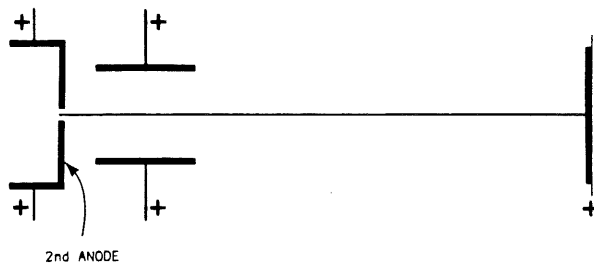


Figure 5-1

The electrical center of a CRT is the point that the beam strikes on the screen when the two deflection plates are at the same potential. The plates are operated at some DC potential near the second anode voltage. When checking a CRT for its electrical center, the plates should be shorted together (NOT TO GROUND) with a well insulated tool.

The deflection above the axis (Y) is directly proportional to the deflection voltage (V_d), the plate length (l), and the distance from the plates to the screen or throw (L). Y is inversely proportional to the distance between the plates (D) and the average deflection plate voltage (V). The formula is:

$$V \approx \frac{Y_d l L}{2 D V}$$

This relationship is shown in Figure 5-2.

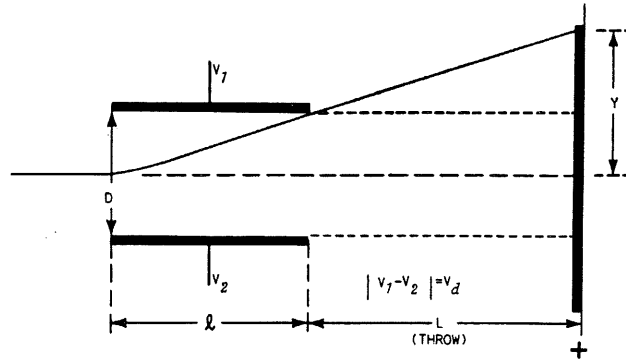


Figure 5-2

The deflection factor (DF) of a CRT is the voltage required for one division of deflection. Volts/cm usually expresses deflection factor. The deflection sensitivity (DS) is the number of divisions of deflection per volt difference between deflection plates. The ratio cm's/volt commonly expresses deflection sensitivity.

$$DF \approx \frac{1}{DS}$$

Both terms are in general use. However, Tektronix has standardized on the term deflection factor. A high deflection sensitivity and a low deflection factor is desired.

Taking the formula $Y \approx \frac{V_d IL}{2DV}$

we see that the deflection sensitivity is equal to

$$\frac{Y}{V_d} \approx \frac{IL}{2DV}$$

and the deflection factor is equal to $\frac{V_d}{Y} \approx \frac{2DV}{IL}$

Figure 5-3 shows a deflection system with parallel plates. The maximum deflection or scan before the beam strikes the plate for a given plate length is shown. The scan could be increased by decreasing the plate length but this would increase the deflection factor or the number of volts per cm of deflecting voltage. The scan could also be increased by increasing the plate spacing but this would also increase the deflection factor. Scan could also be increased by increasing the distance between the end of the deflection plates and the screen, but this would require a longer tube.

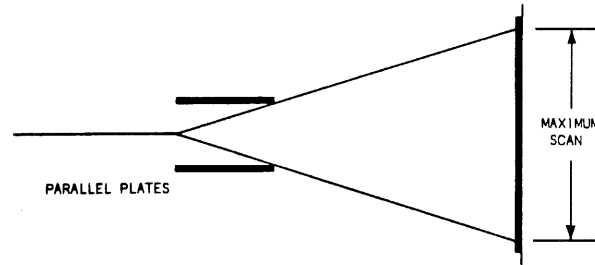


Figure 5-3

Bent plates as shown in Figure 5-4 would increase the scan while holding most other factors constant. The actual section of the plates act in the same way as has been previously described. The bent section acts like sections of parallel plates with increasing plate spacing and therefore increasing deflection factor. The increased deflection factor can be overcome by an increase in plate length. In actual construction the plates may be segmented for ease of construction. (Figure 5-5).

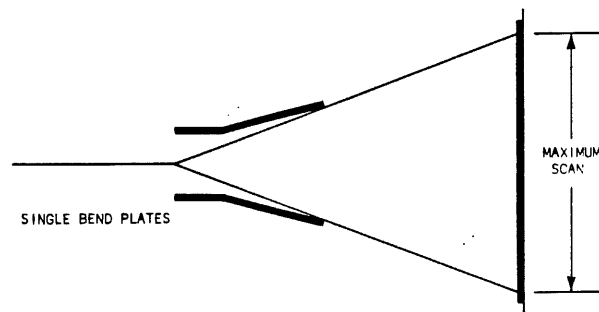


Figure 5-4

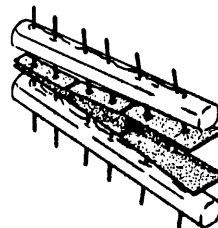


Figure 5-5

The first set of deflection plates after the focus lens is denoted D3-D4 and usually deflects the beam vertically. The next set of plates is denoted D1-D2 and usually deflects the beam horizontally. In some tubes horizontal deflection is done prior to vertical deflection but the notation is the same. (D3-D4 near the focus lens, D1-D2 nearer the screen.)

The capacitive load on the amplifier driving a set of deflection plates may be reduced by using distributed deflection. A segmented plate configuration is used with the segments connected by small sections of delay line. The load is now the Z_o of the delay line and not the total capacitance of the plates. The load is now a constant of about 900 ohms as compared to a regular deflection system where the capacitance is typically 12-15 pf and the load varies with frequency. Distributed deflection may be used in a CRT when it is to be operated at 100 MHz and above.

When conventional deflection is used in a CRT, transit-time effect may reduce deflection at higher signal frequencies. If an electron beam is between a set of plates for 2 units of time and the signal on the plates during this time changes from zero volts to ten volts and back to zero volts, the net effect on the beam is less than the ten volts applied. Distributed deflection may be used to reduce this effect by matching the propagation velocity of the delay line to the velocity of the electron beam between the plates. This matching increases the deflection obtained at higher frequencies because an electron passing between the plates is affected by the same signal for the entire transit time.

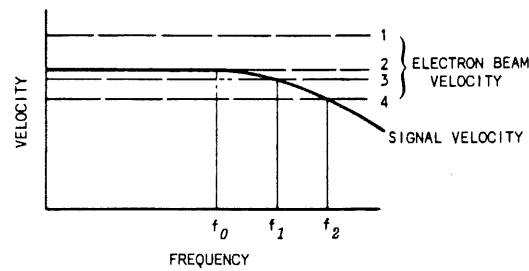
Consider both propagation velocity and electron beam velocity in a distributed deflection CRT. For optimum performance the electron velocity (V_e) and the signal velocity (V_s) match. The difference in potential between the vertical deflection assembly and the cathode determines electron velocity independent of frequency considerations. Conversely, deflection assembly fixes signal propagation velocity as a function of frequency. Signal velocity diminishes with frequency.

Figure 5-6 charts the effects of electron beam velocity and signal velocity upon deflection. For both curves:

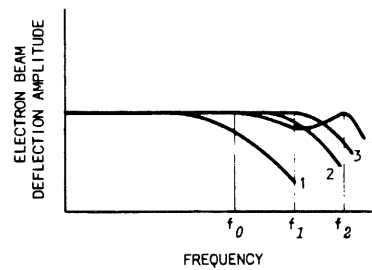
- (1) V_e greater than low-frequency V_s ;
- (2) V_e equal to low-frequency V_s ;
- (3) V_e slightly less than low-frequency V_s ;
- (4) V_e much less than low-frequency V_s .

Figure 5-6 A plots intercept points where electron beam velocity (V_e) and signal velocity (V_s) match. From these curves on plots Figure 5-6B.

- Curve 1: V_e exceeds V_s . A velocity mismatch occurs over the entire frequency spectrum. Electron beam deflection attenuation begins at a low frequency.
- Curve 2: V_e and V_s equal. The mismatch begins at f_0 as the signal velocity curve rolls off.
- Curve 3: V_e a little slower than V_s . Velocity match occurs at a higher frequency, f_1 . Consider electron beam deflection on this curve equal from DC to f_1 . Neglect the attenuation between f_0 and f_1 . (Figure 5-6A shows this attenuation more clearly than Figure 5-6B.)



(A) VELOCITY VS. FREQUENCY



(B) AMPLITUDE VS. FREQUENCY

Figure 5-6

Curve 4: V_e much slower than V_s . Velocities match at a much higher frequency, f_2 . However, beam deflection attenuates at frequencies both above and below f_2 .

Figure 5-7 schematically represents the distributed deflection assembly. Push-pull signal voltage, applied across $R1$ and $R2$, travels down the transmission line at a velocity determined by lumped L and C values. Signal energy dissipates in forward terminators $R3$ and $R4$. At some upper frequency limit, signal velocity becomes less than electron beam velocity, reducing deflection sensitivity.

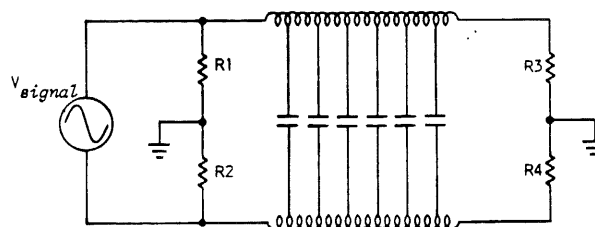


Figure 5-7

A CRT capable of vertical response in the gigahertz range (0.35 nanosecond risetime) connects directly to the signal source of interest. Further, CRT construction allows only single-ended deflection. The generally preferred push-pull deflection is preempted by the high frequency response required. Most circuit measurements are taken single-ended. Circuitry, such as a vertical amplifier, then converts the single-ended input signal into push-pull CRT drive. Current state-of-the-art amplifiers do not extend to fractional nanosecond risetime response.

Figure 5-8 schematically illustrates the single-ended distributed deflection system. Input signals transit the transmission line to dissipate in the forward termination, represented by R2. R1 and R2 must equal the characteristic impedance of the transmission line. The transmission line consists of a tapped inductance and parallel capacitance at each tap. Adjustable portions of C2 parallel the upper vertical deflection plate segments.

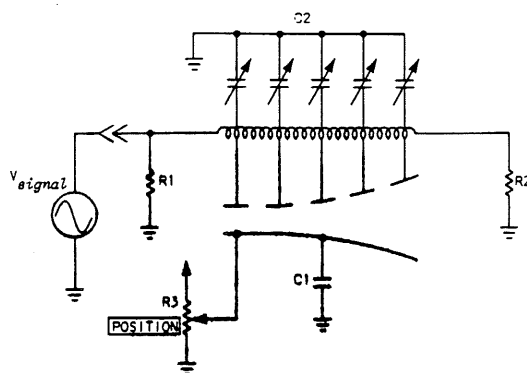


Figure 5-8

The lower deflection plate is a single plate. C1 bypasses the lower plate to ground, allowing application of positional voltages and the entire lower deflection plate surface to represent signal ground.

C2 provides the capability of calibrating the vertical deflection system. At the frequencies involved, stray reactances become an appreciable portion of the lumped-component transmission line, and capacitance between deflection plates changes from electron beam entrance and exit. At the point of beam entry the deflection plates are quite close. Deflection plate coupling then dominates transmission line capacitance. At the beam exit point, the widely separated plates constitute a minor capacitive component. Many upper deflection plate segments, more than shown, occur between electron beam entrance and exit. Each segment and associated inductance make up a short section of transmission line. Each line section must match all other sections. One adjusts C2 for optimum display of known input waveforms. In practice one tunes the deflection assembly then encloses it in the CRT envelope.

Figure 5-9 shows a cutaway drawing of this vertical deflection assembly. The upper vertical deflection plate and transmission line consists of a continuous, "S" shaped metal strip called a stripline (1). Stripline shape creates inductance and mechanical strength. Capacitive coupling occurs between the lower deflection plate and the stripline surface. The tuning screws also capacitively couple to the stripline surface, paralleling deflection plate capacitance.

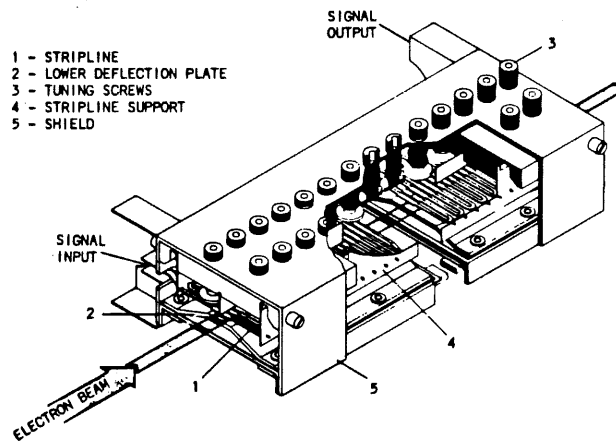


Figure 5-9

In Figure 5-10 single-ended drive is shown with 6 volts on one plate and 0 volts on the other plate. An electron passing through the second anode aperture is accelerated by the +3 volt equipotential line before entering the deflection region. The electrons axial velocity is increased and it gains some radial velocity as it passes through the deflection system and strikes the screen; for example, 2 divisions above center.

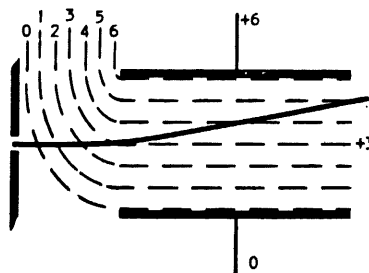


Figure 5-10

Figure 5-11 shows the top plate at -6 volts and the lower plate still at zero. An electron passing through the 2nd anode aperture is decelerated by the -3 volt equipotential line before it enters the deflection region and picks up some radial velocity striking the screen; for example 3 divisions below center. This nonlinearity is unacceptable in oscilloscopes and push-pull drive is used to insure linear deflection.

Most oscilloscopes have push-pull drive to both D1-D2 and D3-D4 because of the nonlinearity of single plate drive. Figure 5-12 shows a push-pull drive, the voltage between the plates being 6 volts. An electron passing through the second anode aperture sees an equipotential line about equal to the anode voltage. The electron is not accelerated before passing through the deflection system where it gains some amount of deflection (3 volts worth). The beam has been deflected up, say 3 divisions, above center. If the upper plate voltage is changed to -3 volts and the lower plate to $+3$ volts, the beam will be deflected down 3 divisions.

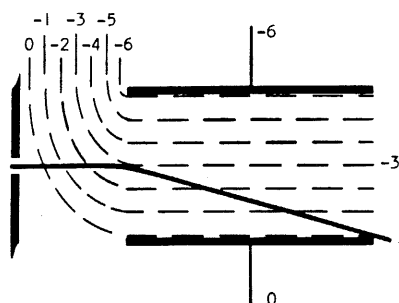


Figure 5-11

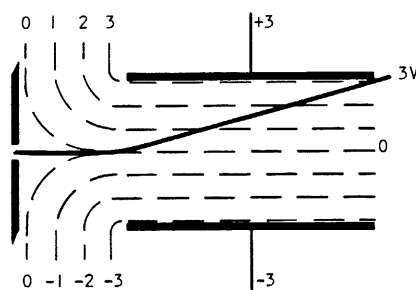


Figure 5-12

The graphs in Figure 5-13 show the deflection-linearity characteristics or change in deflection factor for three different CRT's with push-pull drive. The graphs show the percent difference in voltage required to deflect the beam one centimeter at any point on the screen, compared to that required to deflect the beam one centimeter at the axis. Notice that the T5470 has compression while the other two have expansion.

Figure 5-14 plots single-ended vertical deflection linearity of the T5470. Compare this graph to the T5470 plot of Figure 5-13. One sees the linearity contrast between push-pull and single-ended deflection.

When an electron beam is deflected near a deflection plate, some of the beam electrons are intercepted by the plate. This results in lower beam current reaching the screen and therefore a slight decrease in intensity. The percentage of beam current intercept is different for the vertical and horizontal so each axis must be measured.

$$\% \text{lb to screen} = (100\% - \% \text{ horizontal intercept}) (100\% - \% \text{ vertical intercept}) 0.01.$$

A T5030's beam located 4cm to the left and 3cm up from center for a Tektronix 503 would have 15% horizontal intercept and 5% vertical intercept or approximately 81% total beam current reaching the screen. Because of other factors, a 20% intercept does not yield a 20% decrease in visual intensity. The formula is less accurate as the percentage of both intercepts increases. The least accurate calculation would be for a beam located near the corner of the screen.

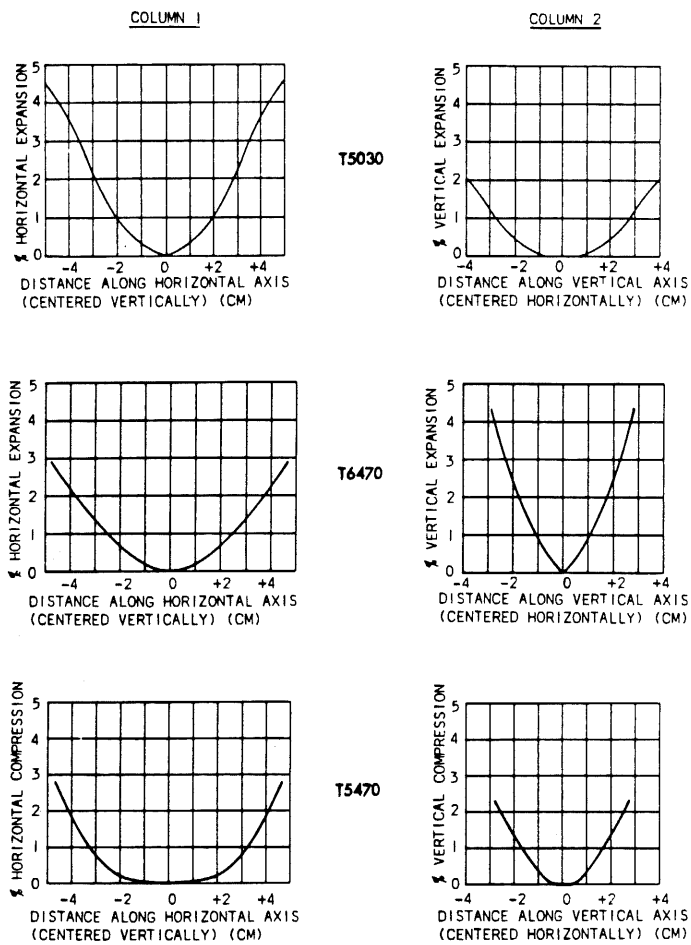


Figure 5-13

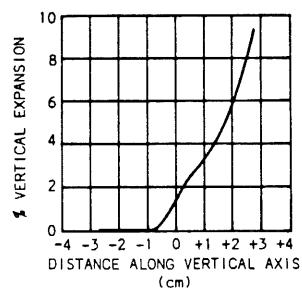


Figure 5-14

There are two causes of defocusing associated with the deflection plates. Geometric defocusing occurs when the beam is focused in the center of the screen. It is focused for some distance and when the beam is deflected the distance to the screen increases but focus distance remains the same. The result is a defocusing of the spot. The size of the spot is larger at the top, bottom, and on the sides of the screen than it is at the center of the screen (see Figure 5-15).

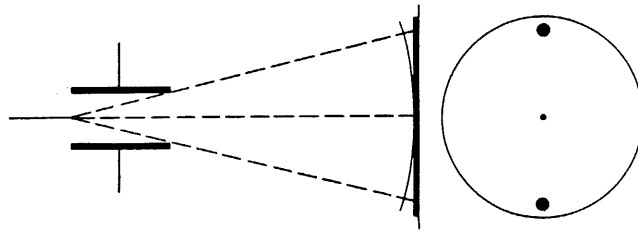


Figure 5-15

Deflection defocusing is greater (by a factor of about 10) than geometric defocusing. An electron beam has a finite thickness and when it passes close to a deflection plate the electrons nearer the plate are accelerated more than those further from the plate. The end product of this effect is defocusing of the beam when it is deflected off center (Figure 5-16). Deflection defocusing changes the shape of the spot making it oblong vertically when deflected close to a vertical plate and oblong horizontally when deflected close to a horizontal plate.

Consider the upper section of the beam. These electrons pass through an accelerating field, increase in velocity, and are then deflected. Their velocity is $V + V_d$. The electrons on the lower side of the beam pass through a decelerating field, decrease in velocity ($V - V_d$), and are then deflected. The slower electrons are between the deflection plates for a longer period of time and are therefore more affected by the deflecting field.

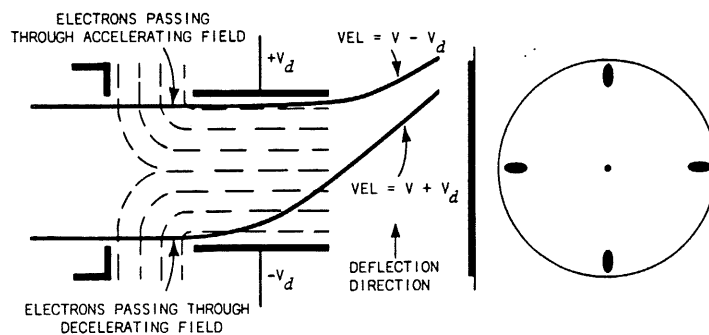


Figure 5-16

The pattern distortion shown in Figure 5-17 is caused by fringing fields between the deflection plates and the band of conducting Aquadag on the glass envelope of the tube in the region of the D1-D2 plates. The geometry control sets the voltage on this neck Aquadag and on the isolation shield. (In some tubes the geometry control also sets the voltage on the deflection plate shields which are indicated on the sides of the D1-D2 plates. See Figure 5-18.) The geometry control is adjusted for an unbowed display.

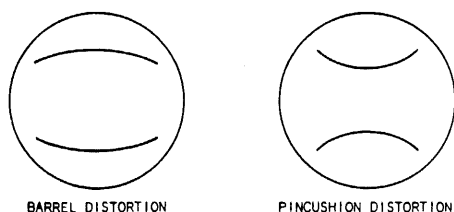


Figure 5-17

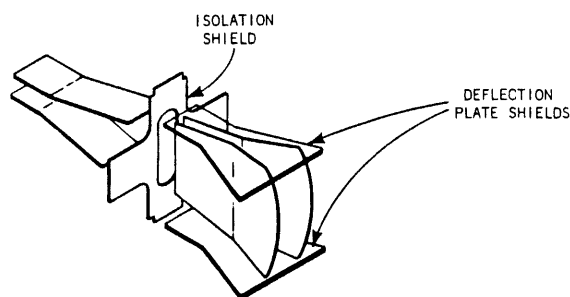


Figure 5-18

The beam may be deflected prior to passing between the D1-D2 plates. The path length within the plates for a deflected beam is different than for an undeflected beam and if the shape of the plate is not altered, a geometric distortion results. With correction, a deflected beam is affected the same as an undeflected beam.

Recall that the deflection of an electron beam above or below the axis is a function of, among other things, the distance from the deflection plates to the screen. If the tube length must be short, the angle of deflection must be larger to yield a given scan.

When an electron beam must be deflected through a wide angle, electrostatic deflection has limitations. These limitations are linearity and edge defocussing. These problems may be overcome by using magnetic deflection but the trade off of lower bandwidth is necessary.

Figure 5-19 shows the deflection yoke used in one of Tektronix's monitors. The horizontal deflection coils are wound around the core. The vertical deflection coils are fitted inside the core. Magnetic deflection is used in this instrument to give the maximum amount of deflection with the shortest tube in length.

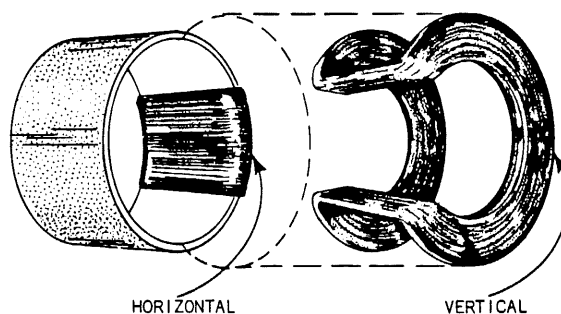


Figure 5-19

The yoke is positioned around the neck of the CRT as shown in Figure 5-20.

The magnetic fields created when current is passed through these deflection coils is shown in Figure 5-21.

If an electron is propelled through a magnetic field such as shown in Figure 5-21, the electron will feel a force that is normal to the direction of the field. This force causes the deflection. The direction of the field determines the direction of deflection and the strength of the field determines the amount of deflection. The strength of the field is a function of the amount of current in the deflection coils, the number of turns in the coil, and the physical dimensions and location of the yoke. The direction of the field is a function of the direction of the current through the coils.

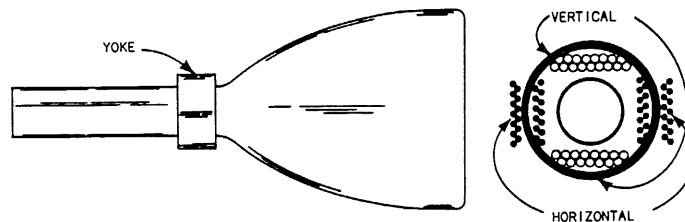


Figure 5-20

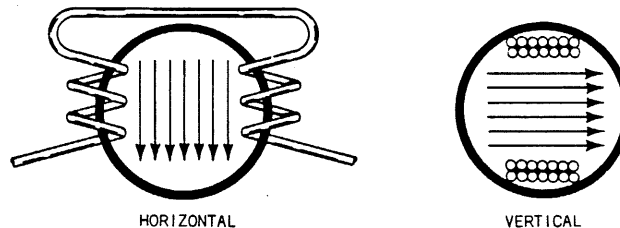


Figure 5-21

Occasionally an oscilloscope user monitors signals by connecting circuits of interest to vertical deflection plates through a simple coupling network. He does this to extend his frequency measurement capabilities. Tektronix CRT vertical frequency response curves follow the general shape of Figure 5-22.

The coupling network included allows predictable displays. Coupling capacitors C1 and C2 block DC since source voltage usually fails to match average deflection plate voltage.

Disturbing average deflection plate voltage creates geometry problems. Additionally, maximum voltage ratings between electrodes must be observed. Each type CRT has design maximum value ratings and the excerpt below is an example:

Average deflection plate voltage, 2000 volts DC maximum.

Astigmatism electrode voltage, 2000 volts DC maximum.

Peak voltage between astigmatism and/or any other deflection electrode, 500 volts DC maximum.

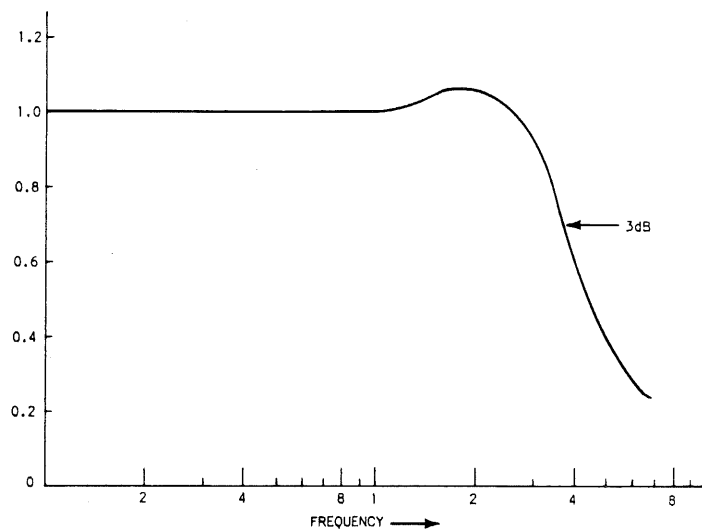


Figure 5-22

Notice the circuit of Figure 5-23 indicates push-pull drive. Many measurements are single-ended, therefore not related to the response curve shown.

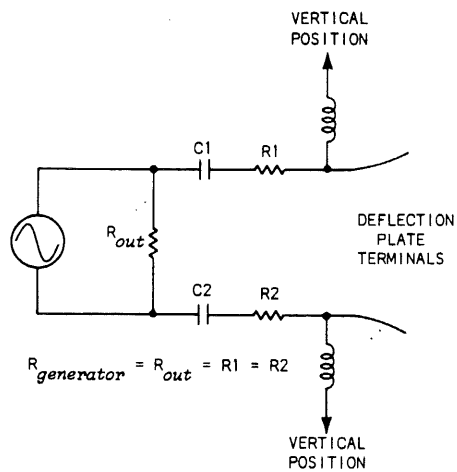


Figure 5-23

ACCELERATION SCHEMES

In a monoaccelerator tube the electrons are accelerated between the cathode and the first anode. The focus lens decelerates and then accelerates the electrons back to their entrance velocity and its overall effect on acceleration is zero. Once the electrons have passed the second anode of the focus lens in a monoaccelerator, no other force is applied to change their axial velocity.

The light output from a phosphor increases approximately as the voltage through which the beam electrons have been accelerated. In a monoaccelerator CRT this is the voltage difference between the cathode and the first anode, or approximately 3-4 kV. Frequently the light output from the CRT screen in a tube of this type is too low to produce a visible display of a fast risetime or high frequency signal. The specification sheet for a CRT may not state that the tube is a monoaccelerator. The exception would be a CRT using a low helix-voltage.

The light output could be increased by increasing the gun voltages, but this would increase the deflection factor. An increase in plate length would decrease the deflection factor but for a 6 to 1 increase in the acceleration potential, the plates would protrude beyond the screen of the CRT. Other than the bulky size of the plates, the capacitance between the plates would increase enormously and the use at high frequencies would be lost.

In order to overcome the problem of low light output, various schemes are used where the beam's electrons are kept at a relatively low voltage in the deflection region and then accelerated after deflection to a higher energy level. This concept of acceleration is called post deflection acceleration and is abbreviated PDA or just "post". Monoaccelerator tubes are referred to as just "mono". The main advantage of a post vs a mono is higher light output for viewing fast signals.

A monoaccelerator tube usually has a conductive coating or Aquadag on the inside of the tube from the deflection plates to the face plate. In some early PDA CRT's this coating was split into regions by an insulating gap (Figure 6-1). Each band had a different potential and accelerated the electrons in what had been the electron drift region. Because the acceleration occurs after deflection, the tube's deflection factor is not as adversely affected as in a monoaccelerator which has the same overall accelerating potential. The equipotential lines in Figure 6-1 show the lens action of this type tube. This type tube suffered from distortion and compression.

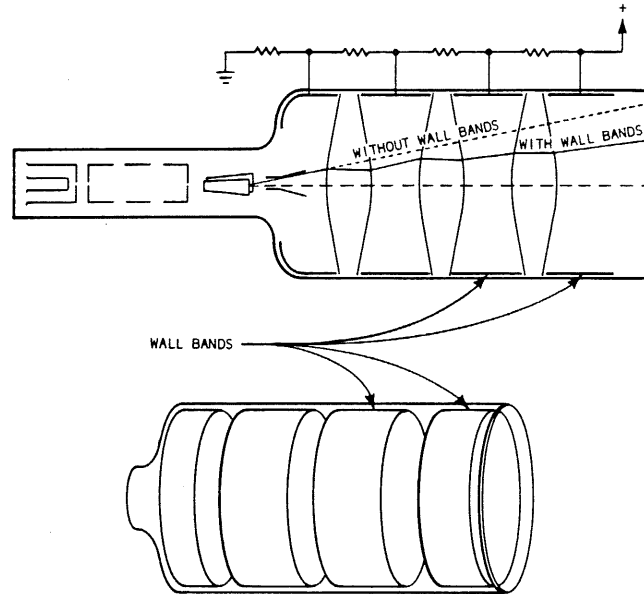


Figure 6-1

An innovation by Tektronix was to make a continuous electron lens over the entire funnel by using a helically wound resistive material in place of the Aquadag coated surface separated by insulated gaps. The type tube shown in Figure 6-2 is called a helix PDA tube. This type of tube has compression but not as severe as the wall-band Aquadag type.

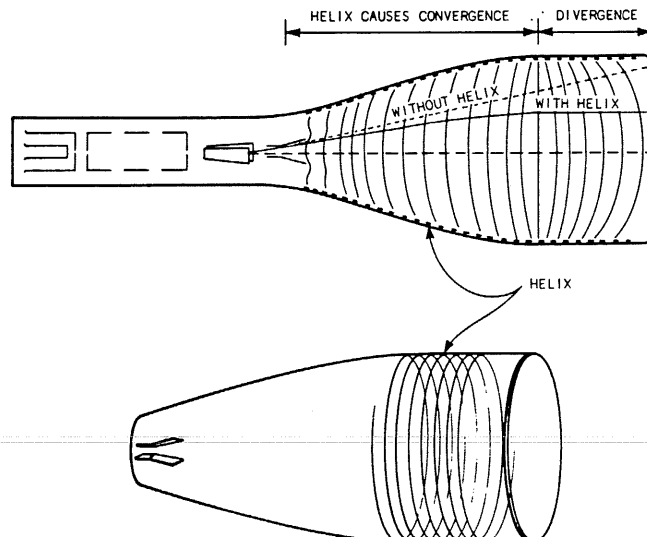


Figure 6-2

The helical post system allows the gun and deflection sections to be operated at lower voltages than a mono tube. The lower operating voltage reduces the velocity of the beam in the deflection region and is an aid to better deflection sensitivity. After the beam has been deflected it is then accelerated between the D1-D2 plates and the screen.

When a helix is used the electrons are accelerated after being deflected but compression reduces the scan and deflection sensitivity (Figure 6-2). Notice the equipotential lines are convex from the D1-D2 plates until over halfway to the screen. The electrons which do not enter perpendicular to the field lines, therefore, are bent toward the axis. Near the screen the electron velocity is such that the weak diverging field has little effect.

The overall acceleration potential using a helix PDA is usually 10 kV or greater. The increase in light output more than offsets the disadvantage of compression. A typical tube might have a scan compression factor of 1.7:1 for the vertical and 2.1:1 for the horizontal deflection.

Compression effects are not all bad. Since the beam passes through a convergent field, not only is scan reduced but also spot size.

A helix PDA tube has compression due to the convergent action of the field (Figure 6-3). This compression can be eliminated by a mesh located just past the D1-D2 deflection plates. This mesh forms a radial accelerating field (Figure 6-4). The combination of the mesh and the voltage distribution formed by the helix produce concentric spherical equipotential surfaces (Figure 6-4).

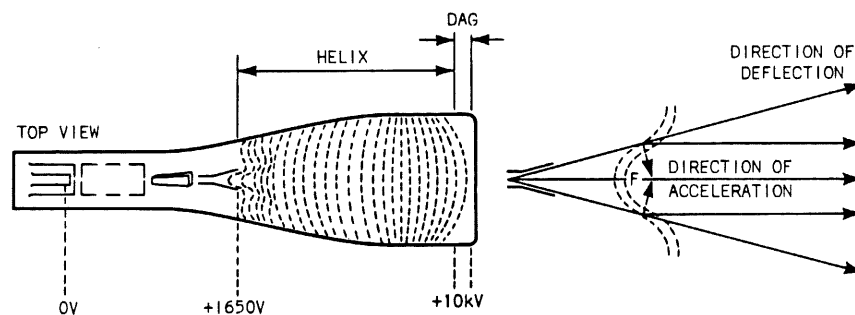


Figure 6-3

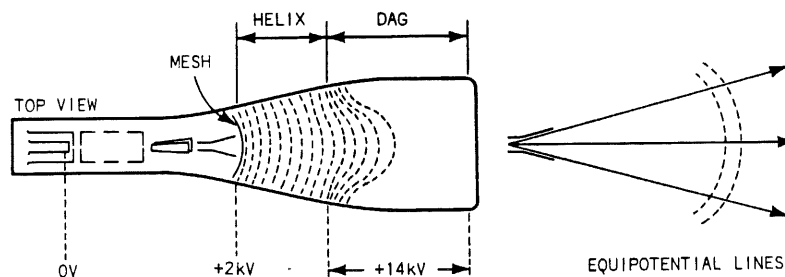


Figure 6-4

The mesh is a field-forming electrode. The electric field is then radial from the center of the deflection plates and little compression takes place. (The electrons pass normal to the equipotential surfaces and therefore increase in velocity. The path of the electrons continue in a straight line.) This system allows electrons to be accelerated without helix compression. Since the electrons travel in a straight line after deflection, the scan and deflection factor are about the same as the monoaccelerator tube.

This system suffers, however, from part of the beam current being intercepted by the mesh. The mesh is at a positive voltage and since it is a conductor it will collect electrons when struck by the beam. This reduction in beam current offsets somewhat the hoped for increase in light output. The mesh may intercept between 30-50% of the available beam current and since compression is no longer present, the spot size increases.

The advantage of lower deflection is traded for an increased spot size and decreased light output for the same accelerating potential. It is usual, though, to increase the accelerating voltage in a mesh tube to regain the light output lost to collection by the mesh, especially since little compression occurs as the voltage is increased.

The need for a shorter CRT with low deflection factor, motivated development of the magnifier or scan expansion tube. Reduced deflection factor (magnification) results from the effects of a mesh, or frame grid, on the force lines of a PDA CRT using a single, continuous, post deflection anode. The mesh distorts the normal force lines into a cone, creating a divergent lens (Figure 6-5). This lens action causes expansion. Controlled expansion produces a CRT with lower deflection factor.

In Figure 6-5A, conductive material surrounds the inner CRT wall, extending from the face plate to a point ahead of the deflection plates. The mesh appears in a plane between the deflection plates and conductive coating termination. Force lines emanate from the rear coating edges because the conductor completely surrounds the CRT bottle with equal voltage. Remove the mesh and this field develops approximately as the force lines nearest the deflection plates in Figure 6-3. In place, the mesh shapes the field into a divergent lens.

Figure 6-5B depicts the deflection magnification effect upon a electron beam. This technique reduces deflection factor to realize as much as 2 X deflection magnification.

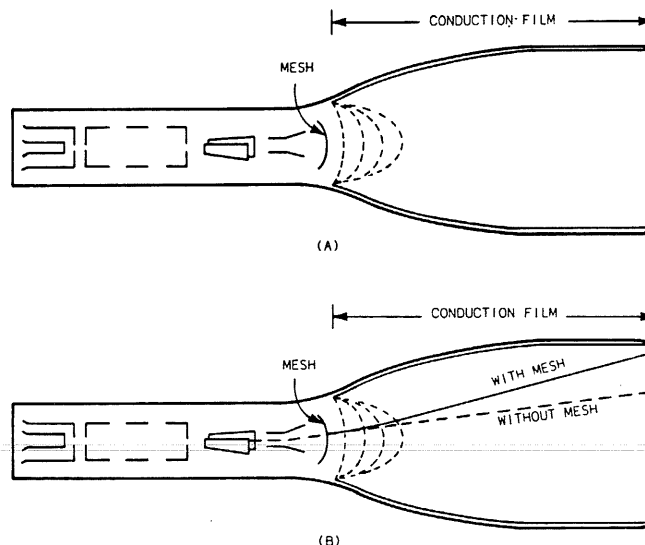


Figure 6-5

In any tube using a mesh, a shadow pattern can be seen on the screen when the spot is defocused. This shadow is not seen when the scope is operated in the normal mode.

The field-forming electrode configuration may be either mesh or frame-grid. The mesh tube has a structure with conductors running in both planes—similar to wire gauze. Its chief advantage is that it may be curved in both planes to obtain the desired field curvature. The major disadvantage is that it intercepts more of the beam current (30-50%) and defocuses the spot in both X and Y axis. The frame-grid has conductors running in only one direction and intercepts substantially less beam current (15-30%).

SPACE CHARGE REPULSION EFFECT AND TRACE WIDTH

Beam spot size on the CRT screen is affected by space charge repulsion in the beam. Electrons, being negative charges, tend to repel each other. When many electrons are formed into a beam, the higher charge density results in greater repulsion. As the current density increases, so does the repulsion effect.

Figure 7-1 shows a beam of electrons passing between two plates. From the cross section of the beam it may be seen that the electrons on the outer edges are being repelled by the electrons in the inner part of the beam. Figure 7-1 shows the expansion that would occur for a given potential difference between the plates. The potential determines the velocity and therefore the time the beam is between the plates. If the potential difference is increased, the time is reduced and the space charge repulsion has less time to affect the beam (Figure 7-2).

A monoaccelerator tube has a high space charge density in the drift region and the beam has a constant velocity. The spot size of the beam at the screen is large, due to space charge repulsion. In a PDA tube the beam electrons are accelerated after deflection. With the increase in electron velocity there is a reduction in the beam expansion due to space charge repulsion (Figure 7-2).

An increase in grid drive also increases beam current, space charge density, and the effects of space charge repulsion. A change in grid drive changes the size of the crossover (between grid and acceleration anode). The spot on the screen is the image of the crossover and an increase in the size of the object (the crossover) will yield an increase in size of the image (the spot on the screen).

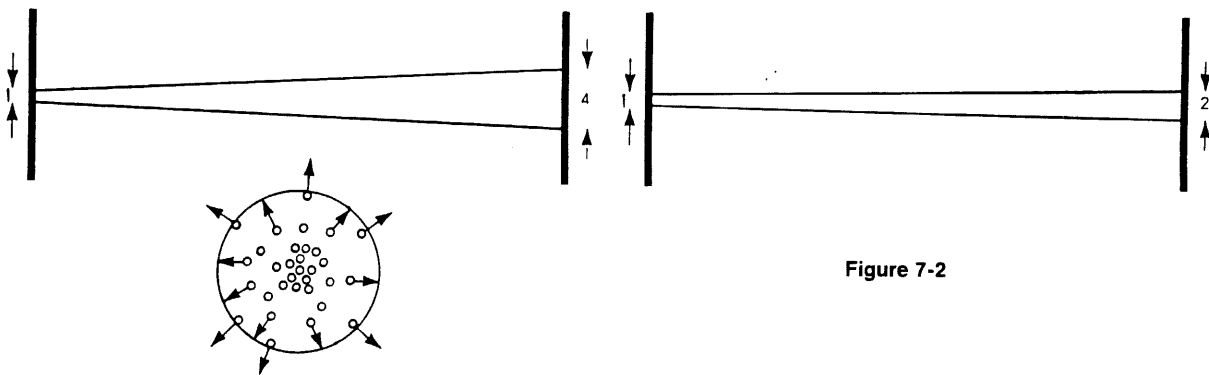


Figure 7-1

Figure 7-2

The graphs in Figure 7-3 shows the increase in trace width for increasing grid drive for three different tubes. The data used for these graphs is for a centered, best focused spot. At the low end, the increase in trace width for increasing grid drive is primarily due to the increase in crossover size. At higher grid drives, space charge repulsion within the beam between the gun and the screen is the prime cause.

The term "trace width" has been used in a general sense without definition. A line or spot on a CRT is not uniform in brightness but is brightest in the center and decreases in brightness toward the edges. The distribution of the electrons in the beam causing the trace or spot are concentrated in the center and the density decreases toward the edges. This variation in brightness presents a problem in answering the question, "how wide is the trace?"

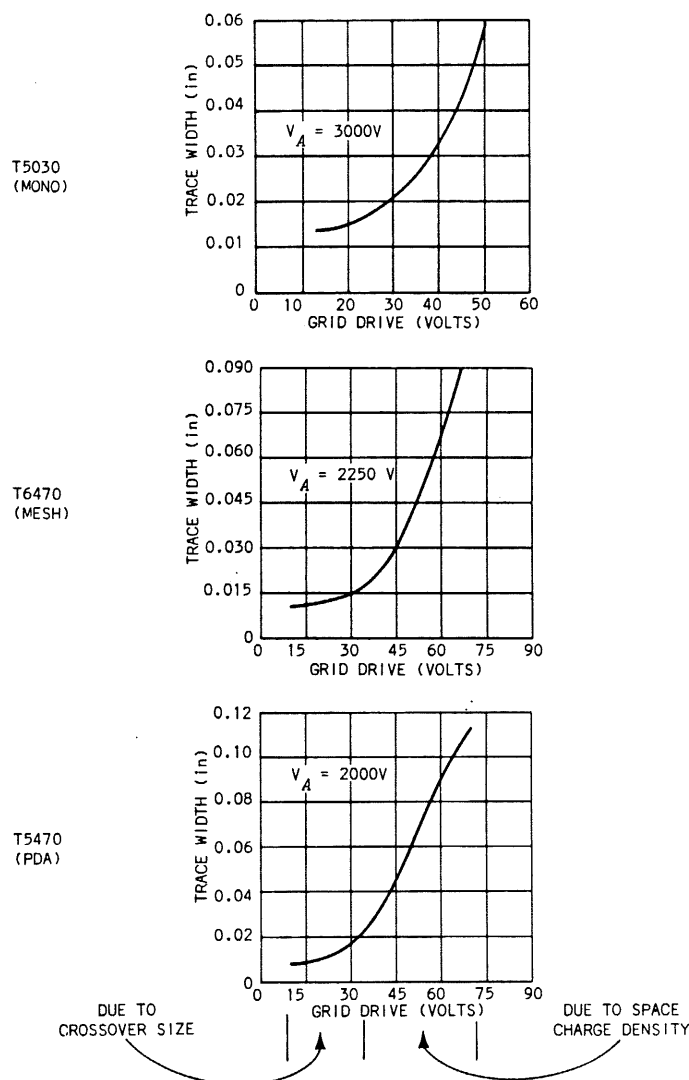


Figure 7-3

A solution (though not the only one) is to assume the distribution is Gaussian (Figure 7-4) and use a shrinking raster method of making the measurement. This method requires a raster (our example uses 11 lines—Figure 7-5). The measurement is made by shrinking the raster down until the 50% points of brightness on two adjacent lines merge. This 50% point is achieved when the dark line between the traces first disappears. The width of the raster is measured and the resultant trace width is 1/11 of the width. This yields a trace width measured between the 50% brightness points (Figure 7-6). All CRT design data is taken by this method.

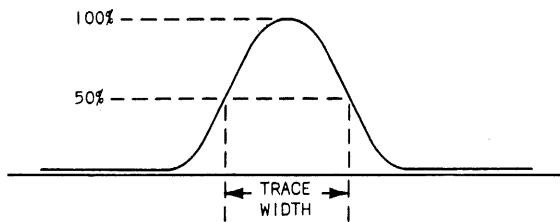


Figure 7-4

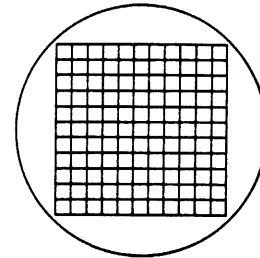


Figure 7-5

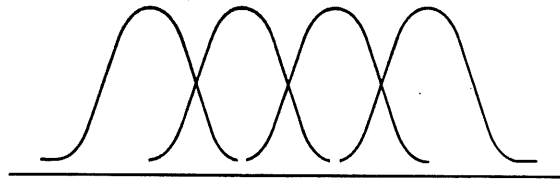


Figure 7-6

PHOSPHORS

The luminance or brightness of a phosphor is dependent upon the phosphor and the accelerating potential. When considering this characteristic, the measurement system's acceleration potential should be stated. All of the data presented here assumes a 10 kV acceleration potential, except where noted.

When the electron beam strikes the phosphor covered screen of a CRT, light and heat are emitted. The light is of primary interest, but the presence of heat and the possibility of burning the phosphor must also be considered.

The light output has several characteristics that should be considered. Luminance is the production of light when a material, such as phosphor, is excited with a source of energy. The luminescence of a phosphor or its total light output is usually divided into two parts. Figure 8-1 shows the waveform exciting a phosphor and the total light output. The light produced while the source of energy is applied is known as fluorescence. The light produced after the source of energy is removed is known as phosphorescence. A phosphor usually displays both fluorescence and phosphorescence. (The first 10 ns of phosphorescence is sometimes considered to be fluorescence.)

If a phosphor is suddenly excited by an electron beam, it requires some finite time for the light output to reach a constant level. The time required to reach 90% of that constant level under specified excitation conditions is called the build-up time of the phosphor. The build-up time of some phosphors is dependent upon the conditions of excitation. Build-up time will be appreciably shorter if the beam current density is increased.

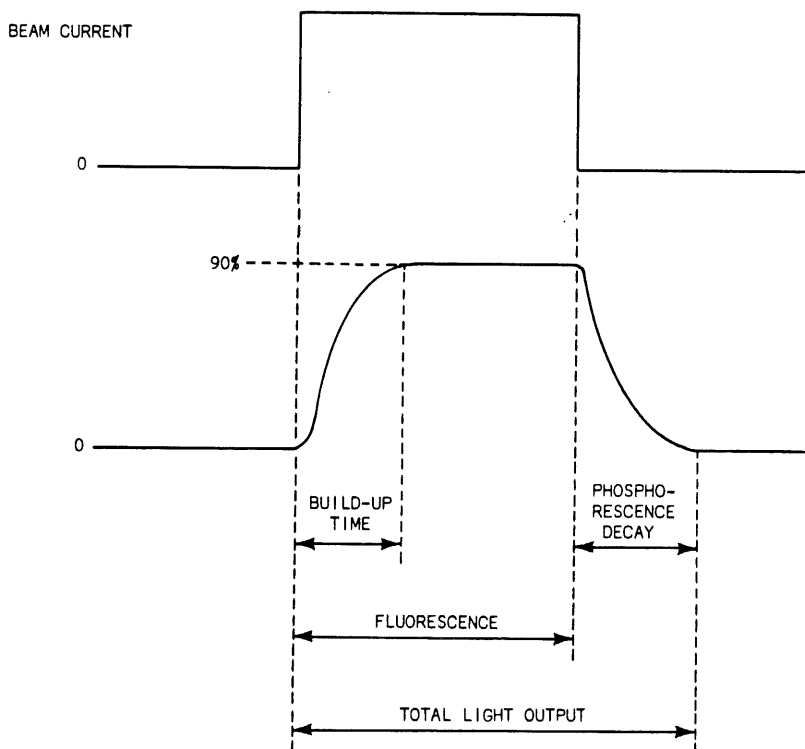


Figure 8-1

When the excitation is instantly removed from a phosphor, an interval of time is required for the light output to drop to a low level. This time is known as decay time and is usually expressed as the time required for the light output to drop to a certain percentage (usually 10%) of the original luminance level (Figure 8-2). The decay characteristic is sometimes termed persistence.

The decay time of some phosphors is linear with respect to time and some follow an exponential decay. For this reason decay curves are available for each phosphor.

The decay time of a phosphor must be considered for both visual and photographic applications. When visually viewing a slow sweep, a long decay phosphor with its "after glow" (phosphorescence) will allow the observer to see what has gone on even after the sweep has passed a given point. When a display is photographed, a long decay phosphor might fog the film, or the display from a previous sweep may still remain. For photographic use, a medium or medium-short decay phosphor is used for best results. For most applications a medium decay phosphor such as P31 is the best compromise. Oscilloscopes generally have P31 as a standard phosphor; however, many other phosphors are available on special order. See Appendix A.

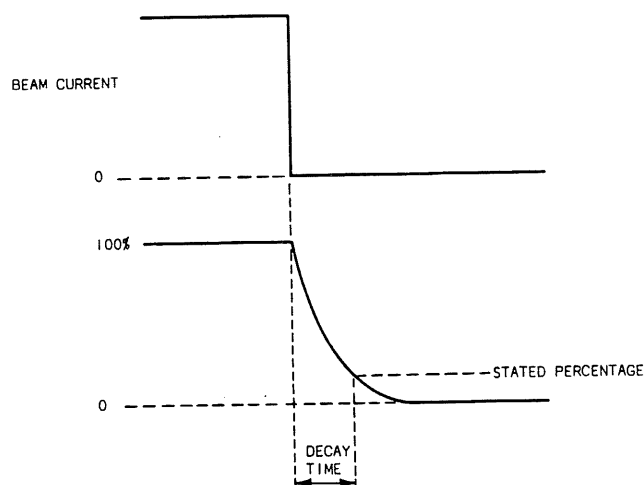


Figure 8-2

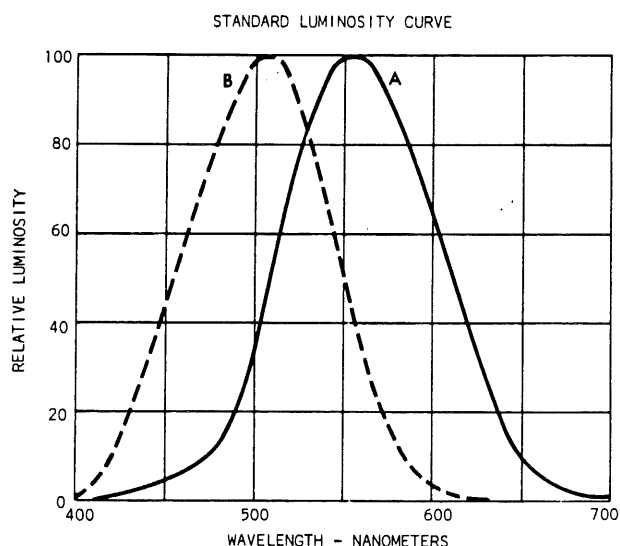
HUMAN EYE RESPONSE

An important factor in selecting a phosphor is the color or radiant energy distribution of the light output. The human eye responds in varying degrees to light wave length from about 400 to 650 nanometers or from deep red (650 nanometers) to violet (400 nanometers). The human eye is peaked in its response in the yellow-green region at about 555 nanometers and falls off on either side in the orange-yellow area to the right and the blue-violet region to the left (Figure 9-1). The eye is not receptive to deep blue or red.

If the quantity of light falling on the eye is doubled, the brightness "seen" by the eye does not double. The brightness of a color tone as seen is approximately proportional to the log of energy of the stimulus.

The response of the eye to various colors is believed to be due to the construction of the eye. One theory is that the cones of the retina respond to color stimuli and that each cone consists of three receptors. Each receptor is believed to respond to a different wave length of visible light; a yellow-blue, a red-green and a black-white receptor. An average can be taken of the color response of many people and a "standard" response curve for an average person, as shown in Figure 9-1, can be compiled.

The term luminance is the photometric equivalent of brightness and is based upon measurements made with a sensor having a spectral sensitivity curve corrected to that of the average human eye. The unit commonly used for luminance measurements is the foot lambert. The term luminance implies that data has been measured in a manner, or has been so corrected, to incorporate the CIE standard eye response curve for the human eye. CIE is an abbreviation for "Commission Internationals de l'Eclairage" (Interntional Commission on Illumination). The luminance graphs and tables are therefore useful only when the phosphor is being viewed visually.



Curve A: 1924 CIE Photopic Luminosity function. Represents relative sensitivity of the average human eye to various wavelengths of radiant energy under good lighting conditions.

Curve B: 1951 CIE Scotopic luminosity function for young eyes (under 30 years of age). Represents relative sensitivity of the average young dark-adapted eye near the threshold of extrafoveal vision.

Optical Society of America, Committee on Colorimetry, "The Science of Color", Thomas Y. Crowell Company, 1953, p. 225.

Figure 9-1

The color of a phosphor or any visible color may also be described by a standard chromaticity chart as shown in Figure 9-2. The bounded area includes all real colors perceptible to the average human eye. The numbers indicated along the periphery are the wavelengths in nanometers of the spectral colors. The center area is white, with color purity (saturation) increasing toward the periphery. The point marked CIE Illuminant "C" is the standard representation of average daylight.

The transition from one color to the next is gradual rather than sharply defined as shown. The divisions used on the chart have been standardized to aid in designation of colors by name. Any visible color can be specified by an X and Y coordinate.

P7	P11	P15	P31
X = 0.191	X = 0.151	X = 0.205	X = 0.248
Y = 0.159	Y = 0.083	Y = 0.380	Y = 0.556

The terms brightness, hue, and saturation are often used when referring to light or color. Hue indicates the wavelength of a color or its position in the color spectrum. Hue does not change with luminance, for no matter how dim or bright the light its hue remains the same. A saturated color or pure color is one that does not contain any white light. When white light is present the color is said to be desaturated (as a pastel color).

On the standard chromaticity chart, the colors around the border are pure or saturated (contain no white light). The saturation decreases towards the center of the chart.

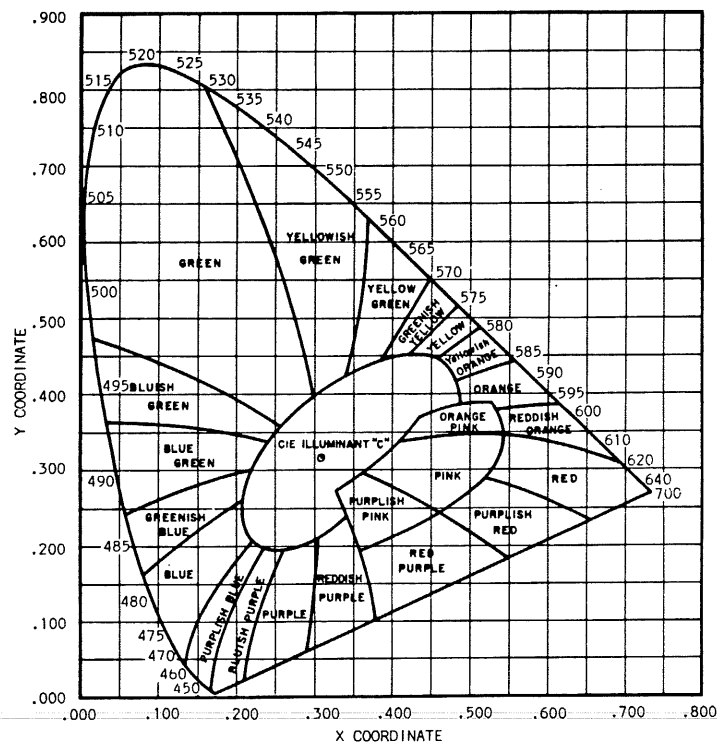


Figure 9-2

LUMINANCE CHARACTERISTICS OF PHOSPHORS

The luminance of a phosphor is dependent on several variable factors. If beam current is increased or the same amount of beam current is concentrated in less area by reducing the spot size, there will be an increase in luminance. An increase in accelerating potential will yield an increase in luminance. The luminance is also a function of the time the beam strikes a particle of phosphor; therefore, sweep speed and repetition rate will affect this characteristic.

The graphs in Figure 10-1 are compiled from measurements taken with a Spectra Brightness Spot Meter observing a 0.250 inch diameter area of a 2 X 2 cm, 135 line, focused raster. Notice that the horizontal scale of the graph is in average current density ($\mu\text{A}/\text{cm}^2$) and the vertical is in luminance (foot-lamberts). These graphs may be used for comparing the luminance of one phosphor with another when all other factors are equal.

Average beam current density can be found using the formula:

$$\frac{\text{average beam current display}}{\text{trace length X spot size}} = \frac{\text{beam current X duty cycle}}{\text{trace length X spot size}}$$

When someone asks "how bright is the display on my oscilloscope?", the question can have two meaningful answers. The first answer is a relative one and is in terms of how much brightness there is as compared to another phosphor. P31, for example, is about 5 times as bright as P11 to the eye. But just how bright in quantitative terms requires an absolute answer which is difficult to arrive at due to the variables listed above. For this reason most luminance data is in relative terms.

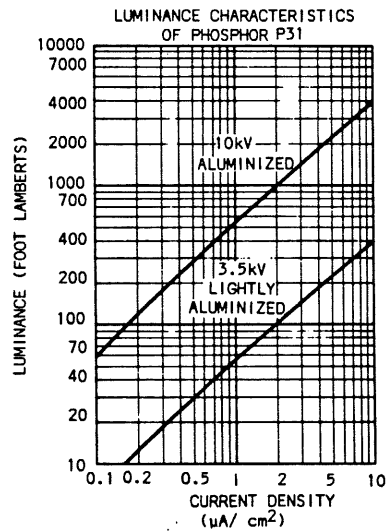
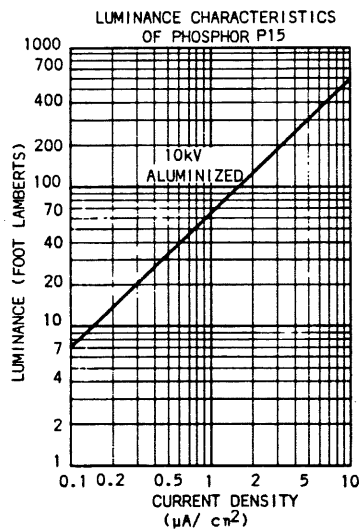
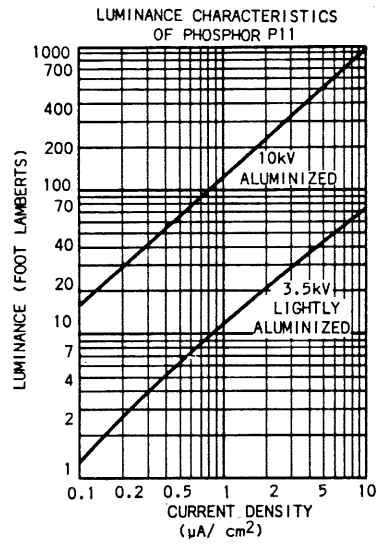
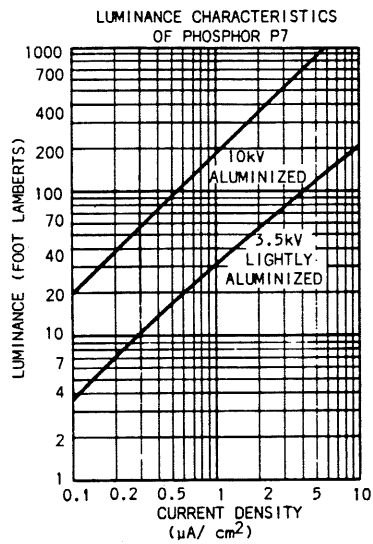
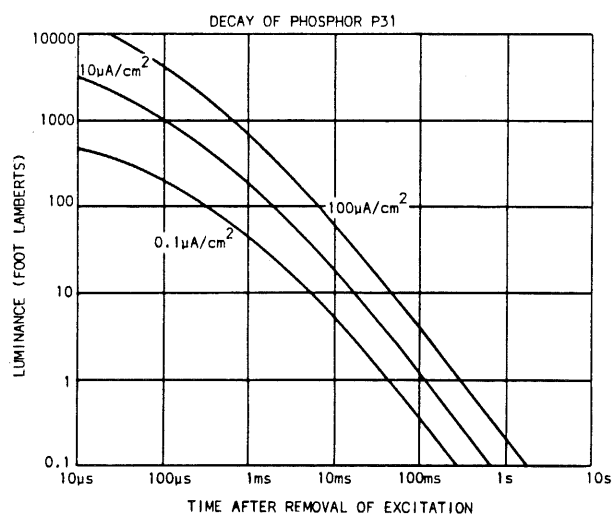


Figure 10-1

The decay chart in Figure 10-2 can be used to find the time required for a phosphor to decay to an absolute luminance level for a given beam current density. Notice that higher beam current density results in higher original luminance and longer decay times.



BUILD UP: Approximately 500 microseconds to 90% at $10\mu\text{A}/\text{cm}^2$.

DECAY: Essentially power law, somewhat dependent upon excitation conditions.
Measured using tube type T5470 at 10kV and 5ms excitation pulse.

Figure 10-2

SPECTRAL RESPONSE

The color of the light output or radiant energy emission characteristics of several phosphors is shown in Figure 11-1. Notice that P7 phosphor peaks in the blue-violet region along with P11 while P15 and P31 peak more in the green region. Since the eye is more responsive to yellow-green, P15 and P31 are better phosphors for visual observations. These graphs are NOT corrected for the color response of the human eye. They show the relative radiant energy as seen by a device with a flat response.

In some applications the display on a CRT will not be viewed with the human eye but with other light sensitive devices such as photographic film or photocells. Each of these devices have their own spectral response and the selection of the phosphor will therefore be dependent upon the device used.

Photographic film, for example, is more responsive to blue light and a phosphor peaked in this region, such as P7 or P11, will give better results than most others. (Decay time may cause problems when P7 is used.)

The radiant energy distribution of some phosphors will change for different beam-current densities. At $100 \mu\text{A}/\text{cm}^2$, P31 has more blue energy than when the beam current is 1 and $10 \mu\text{A}/\text{cm}^2$ (Figure 11-1).

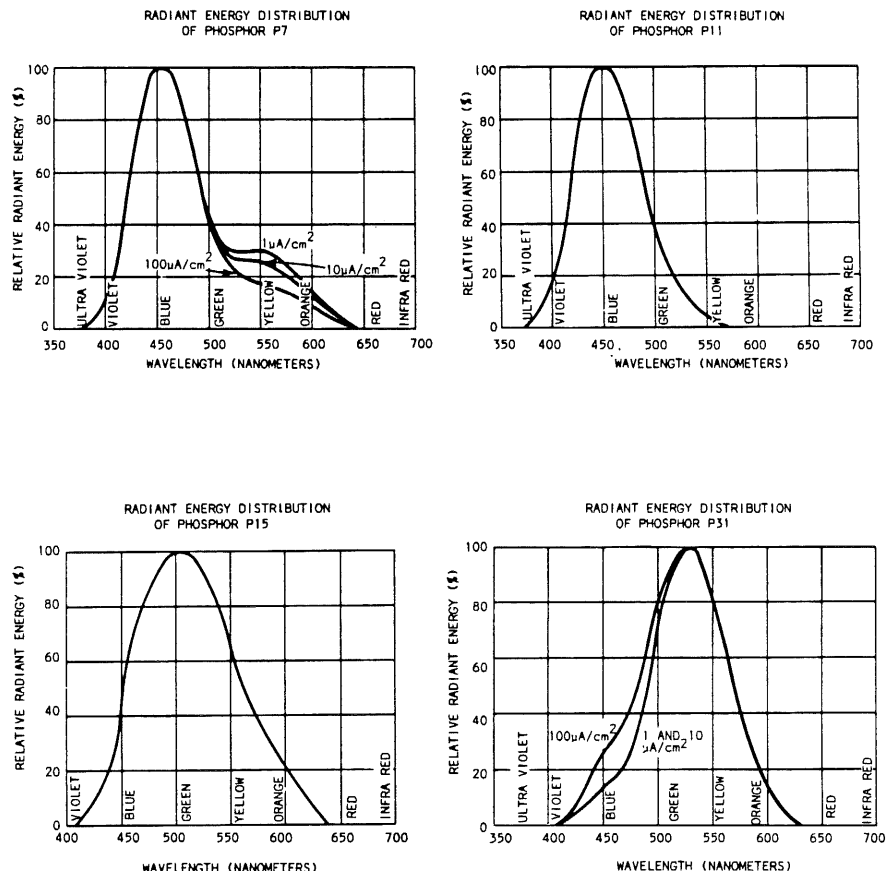


Figure 11-1

PHOTOGRAPHIC WRITING SPEED

The writing speed figure expresses the maximum single-shot velocity (in cm/ μ s) which may be recorded on film as a just-visible trace. Where the highest possible photographic writing rate is required, a phosphor having blue fluorescence such as P11 is generally used since most types of film are more sensitive to blue light. Because of the difference in spectral sensitivity of the human eye and film, a phosphor having high luminance will not necessarily have high photographic writing speed. Sometimes a trace may be visible to the eye in a darkened room but difficulty may be encountered in trying to photograph the display.

The factors which influence writing speed may be divided into three groups: those attributed to the CRT, the instrument, and the camera (including film). The table below shows the groups and some of the factors involved. Table 12-1.

CRT	INSTRUMENT	CAMERA
Spot size	Intensity setting	Beam-splitter transmission
Edge defocus	Unblanking pulse amplitude	Film fog level
Plate intercept	Heater regulation	Lens transmission
Phosphor efficiency	Graticule transmission	Film sensitivity
Uniformity	Accelerating potential	Film response
Decay		Film age
Spectral emission		Lens speed
Beam current		

Table 12-1

A relative writing speed figure may be used when comparing writing speeds of two different phosphors to be used in the same oscilloscope. The table in Figure 12-1 shows the relative writing speed of the many phosphors along with relative luminance. (Remember, luminance is CIE-eye-response corrected.)

Notice that P11 has a relative writing speed of 100. This says that all other factors being the same, a CRT with P11 phosphor will have a higher writing speed than any other phosphor. How fast is that? That depends on all those factors previously listed.

Note that P31 has a relative luminance of 100 and a relative writing speed of 75. P31 is bright and has excellent (second only to P11 and P7) relative writing speed and is therefore the standard phosphors of most CRTs.

TYPE	FLUORESCENCE	PHOSPHORESCENCE ¹	RELATIVE ² LUMINANCE	RELATIVE ³ WRITING SPEED	
P1	Yellowish-green	Green	45	35	
P2*	Bluish-green		60	70	
P3	Greenish-yellow		45	15	
P4	White		50	75	
P5	Blue		3	15	
P6	White	Yellow-green	70	25	
P7*	Blue-white		45	95	
P8*	Obsolete -- Replaced by P7				
P9	JEDEC registration withdrawn				
P10	Dark trace storage - Not luminescent				
P11	Purplish-blue	Orange	25	100	
P12*	Orange		18	3	
P13	Reddish-orange		4	1	
P14*	Purplish-blue		40	60	
P15	Bluish-green		15	25	
P16	Bluish-purple		0.1	25	
P17*	Yellowish-green		30	15	
P18	White		18	35	
P19*	Orange		25	3	
P20	Yellowish-green		85	70	
P21*	Orange		25	8	
P22	Three-color dot pattern for color television				
P23	White		80	35	
P24	Greenish-blue		8	6	
P25*	Yellowish-orange		12	4	
P26*	Orange		17	3	
P27	Reddish-orange		20	7	
P28*	Yellowish-green		50	50	
P29	Two-color stripe pattern				
P30	Not registered with JEDEC				
P31	Green	Yellowish-green	100	75	
P32*	Blue-green		25	15	
P33*	Orange		20	7	
P34	Blue-green		17	15	
P35	Blue-white		55	45	

¹Where different than fluorescence.

²Taken with Spectra Brightness Spot Meter which incorporates a CIE standard eye filter. Representative of 10 kV aluminized screens.

³Taken with 10,000 ASA Polaroid film for 10 kV aluminized screens.

*Phosphors having low level decay lasting over one minute under conditions of low ambient illumination.

NOTE: Tektronix supplies CRT's with only those phosphors listed in the catalog.

Figure 12-1

An absolute writing speed number requires a detailed statement of all the factors affecting the measurement and how the measurement was made. Such a statement is made in Figure 12-2.

The speed of the film used is 10,000. If the film were faster then the writing speed would be faster. Without changing any other factors an improvement by the film makers gives oscilloscopes a faster writing speed.

Writing speed approximations result from measurement and computation of specific components. Usually one uses the damped sinewave technique. This results in a changing spot speed in which high amplitudes in the first part of the signal deflect the spot faster than those at the low amplitude end.

Horizontal velocity is negligible compared to vertical velocity. So one computes writing speed by comparing the amplitude where the first discernable trace crosses the X-axis—the region of maximum velocity.

PHOSPHOR	PHOTOS	CRT's	Photo Writing Speed cm/us		
			High	Low	Average
P1	30	6	333	258	290
P2	15	3	835	660	737
P7	60	12	1310	943	1160
P11	60	12	1260	1020	1120
P31	55	11	903	675	760

MEASUREMENT NOTES

OSCILLOSCOPE: Type 547
 CRT: T5470 (with phosphors listed)

1. Accelerating potential: 10kV overall
2. Unblanking pulse amplitude: 60V peak
3. INTENSITY: In the absence of ambient light, the INTENSITY control was adjusted to the point of visual extinction of an undeflected spot. Photos do not show an undeflected spot.
4. FOCUS & ASTIGMATISM: Adjusted to produce a sharp trace on both vertical and horizontal axes during low repetition-rate displays of the test signal.
5. SCALE ILLUMINATION: Zero, to avoid prefogging of film.
6. Phosphor was dormant; maintained in total darkness for about five minutes before each test photo.

SIGNAL: Exponentially-decaying sinewave.

CAMERA: Frame: C-27
 Lens: f/1.3, 1:0.5
 Exposure: Single-shot. Shutter was left open for five seconds to make use of available decay.
 Film: Polaroid 410, 10,000 ASA; five exposures were made of each CRT.
 Prefogging: None.

INTERPRETATION: Prints are backlit with fluorescent light. Peaks of sinewaves are masked to avoid illusion of complete cycle.

CALCULATION: Writing speed (cm/us) = $\pi f A$
 f = frequency (megahertz/second)
 A = peak-to-peak amplitude (centimeters) of the sinewave cycle whose center is just visible to the eye.

Figure 12-2

Figure 12-3 shows the display used to measure writing speed. Apply the following formula:

$$WS = \pi f A$$

Where:

WS = writing speed (cm/ μ s)

f = frequency of damped sinewave (mHz)

A = vertical distance between peaks of first discernable sinewave (cm)

Starting from the left, find the first rising or falling portion of the damped signal visible in its entirety. A is the distance between peaks connected by this portion. Ignore horizontal distance if A exceeds the horizontal dimension by three or more.

Consider this method as a close approximation only. Absolute writing speed depends upon variables not accounted for here.

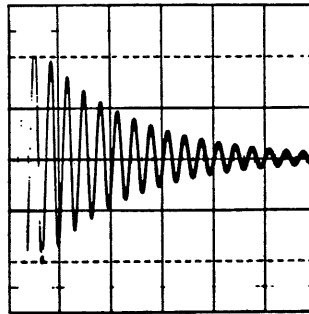


Figure 12-3

PHOSPHOR BURNING

When phosphor is excited by an electron beam having an excessively high current density, a permanent loss of phosphor efficiency may occur. The light output of the damaged phosphor will be reduced and in extreme cases complete destruction of the phosphor may result. Darkening or burning occurs when the heat developed by electron bombardment cannot be dissipated rapidly enough by the phosphor.

The two most important and controllable factors affecting the occurrence of burning are beam-current density (controllable with the Intensity, Focus and Astigmatism controls) and the length of time the beam excites a given section of the phosphor (controllable with the Time/Div control). Under normal conditions in CRTs with grid unblanking, the ambient voltage on the control grid will hold the tube in cutoff and no spot will be present on the screen.

When the sweep is triggered, the unblanking pulse turns on the gun and if everything else is working properly the beam can be seen as it moves across the screen. But what if the horizontal amplifier is inoperative? The horizontal plates will not receive a signal under that condition and the beam will not be deflected but it will be turned on by the unblanking pulse. Result?-possibly a burn mark on the screen!

The Intensity control can be adjusted to override the normal cutoff condition of the gun in the absence of an unblanking pulse in a CRT using grid unblanking. If this is done, a spot of reasonable intensity will be seen on the face of the CRT. If the sweep is now triggered, an unreasonably bright spot will occur. Result?-you guessed it-a burn mark.

Remember, burning is a function of intensity and time. Keeping intensity down or the time short will save the screen.

Any phosphor can be burned but some more easily than others. Phosphors may be divided into three groups when considering their burn resistance:

Group 1	Low (easily burned)	P12, P19, P26, P33
Group 2	Medium (moderate)	P2, P4, P1, P7, P11
Group 3	high (hard to burn)	P31, P15

Group 1 phosphors are easily burned and should be used with great care. Group 2 phosphors are about 10-100 times more difficult to burn than those in Group 1. A P31 phosphor is quite difficult to burn. In fact, you really have to want to damage the phosphor even with a 10 kV tube.

The typical phosphor is about 10% efficient. This means that of the total energy from the beam, 90% is converted to heat and 10% to light. A phosphor must radiate the light and dissipate the heat; or as any other substance, it will burn.

ALUMINIZED TUBES

When an electron beam excites a particle of phosphor, light is emitted in all directions. Therefore, only part of the light emitted is seen when viewing the CRT (Figure 14-1). Some of the light is lost as it is emitted back into the tube. The lost light can be saved by coating the back of the phosphor with a thin coating of aluminum to act as a mirror. The electron beam will penetrate the aluminum coating and the emitted light that would usually be lost is reflected forward. Figure 14-2.

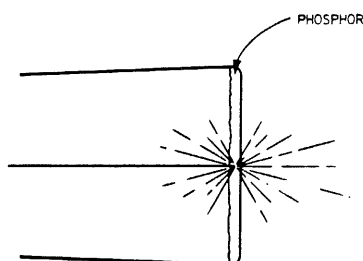


Figure 14-1

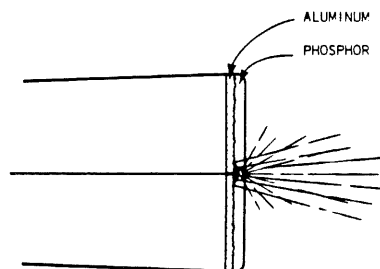


Figure 14-2

Some of the effective energy of the beam is used to penetrate the aluminum coating, reducing the effective acceleration potential. The effective deceleration of the beam depends on the thickness of the aluminum and may range from 1 kV to 3 kV or more. The overall result is, however, a brighter trace in an aluminized tube when accelerating potentials are well above the potential required to penetrate the aluminum.

The aluminum coating also forms a heat sink for the phosphor, removing some of the heat which might otherwise cause burning. The effective reduction in acceleration potential also helps prevent burning.

Filters also may be used to separate the long-decay component from the short-decay component of a phosphor which has a different color for each. P7, for example, is blue-white for its short-decay component and yellow-green for its long-decay component. An amber filter would enhance the slow component and a blue filter would enhance the fast component.

Filters are usually not used in photographic applications since they absorb light even at their spectral peak. However, color filters may be used for the purpose of blocking long or short persistent components as discussed above or to prevent cathode glow fogging of film when making long time exposures. The cathode glows red when heated and this light will fog film in a long time exposure, if the tube is not aluminized or a blue filter is not used to attenuate most of the red glow. In an aluminized tube the light from the cathode is reflected and causes little problem.

A polarizing filter also increases contrast ratio but uses a different principle than the color filters. This filter has the effect of a light trap for outside light. Incidental light entering the filter and reflecting from the face of the tube is phase changed in such a way that it cannot re-emit from the filter and is thus trapped and dissipated inside. Light emitting from the phosphor passes through the filter with attenuation of about 70-75%. The contrast ratio however is about 20:1, a vast improvement.

The mesh filter also improves the contrast under higher ambient light conditions. This filter is a metal screen of subvisible mesh, with the surface treated for low reflectance. This filter works on the same principle as the colored filter. The screen is tautly mounted on a metal frame which can be placed over the CRT faceplate. The light transmission is approximately 28%.

The mesh is grounded to the metal frame and effectively carries a large part of the CRT emitted RF spectrum to chassis ground. The actual quantitative filtering ability depends upon the characteristics of the radiation, which varies between scope types.

GRATICULES

The display on the face of a CRT would be less meaningful if there were no markings to indicate divisions. The various time and amplitude characteristics of the display may be found by counting the number of divisions and multiplying by the appropriate switch setting. There are three types of graticules that can provide these division marks.

An external graticule consists of a piece of scribed plexiglass mounted in front of the CRT. Two or more graticule lamps illuminate the scribed lines and are controlled by the Scale Illumination Control on the front panel of the scope. This type of graticule has the advantage of being easily changed. Graticules marked in degrees for color-TV vector analysis, special risetime markings, or many other patterns may be quickly mounted on the scope.

The external graticule has the major disadvantage of having parallax (Figure 15-1). The scribed lines on the graticule are on a different plane than the trace. Therefore, the alignment of the trace and the graticule will vary with the viewing position.

Visual observation of parallax can be overcome by always viewing the trace at one point at a 90° angle. Observing a second point requires moving the head and viewing the trace at the second point at a 90° angle. This will correct for parallax. A camera has a similar parallax problem and cannot be shifted.

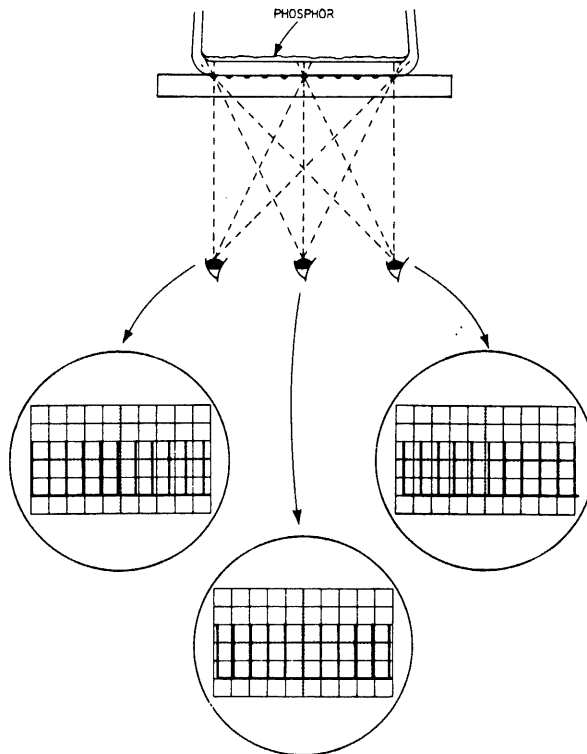


Figure 15-1

A graticule on the inside surface of the faceplates of the CRT is called an internal graticule. The trace and the graticule are in the same plane and there is no parallax (Figure 15-2). This absence of parallax is a major advantage. This type of graticule is more costly to manufacture and cannot be changed without changing CRTs. Edge lighting the graticule lines is more difficult and illumination is not as bright as an external graticule. This type of graticule requires some means of trace alignment, which adds cost.

The third graticule type is the projected graticule. It is limited to camera system applications. The projected graticule is diagrammed in Figure 15-3. A light splitting mirror is mounted in the camera housing. Light from the screen is split, part being reflected for visual observation and part passing through the mirror to the film. Below the mirror is a graticule of a transparency, much like a film slide.

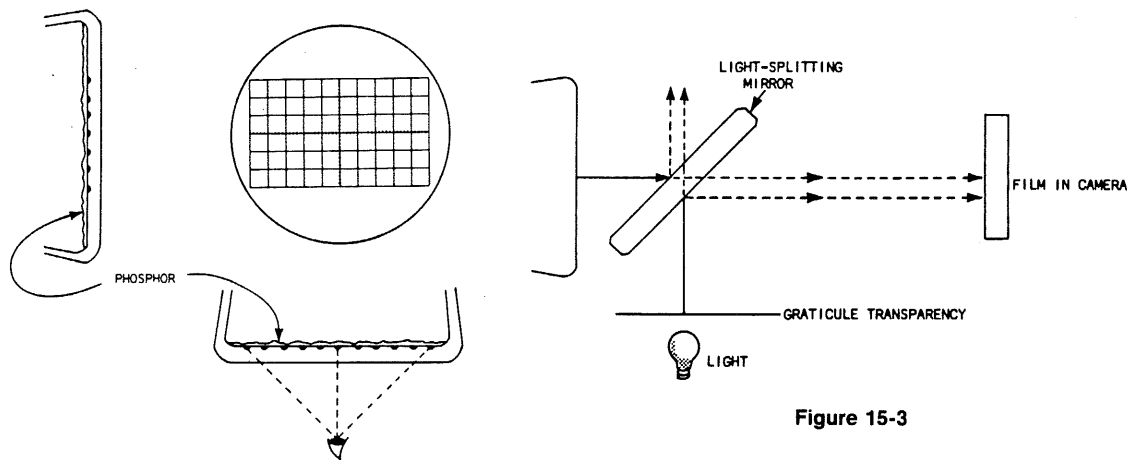


Figure 15-2

Figure 15-3

The light from below the graticule is split by the mirror, part going through for visual observation and part being reflected to the film. With proper adjustment of the distance between the mirror and the graticule transparency, the face of the CRT and the graticule will appear to be in the same plane when viewed by the observer or the film in the camera and therefore parallax will not exist.

The projected graticule system is limited to camera system applications. It has the advantage of graticule versatility. Any transparency can be used. Clear blank areas on the graticule transparency allow notes to be written which will show up on the photograph.

TRACE ALIGNMENT

When an external graticule is used, the trace and the graticule may be aligned by removing the side panel of the scope and adjusting the bracket which holds the neck of the CRT. This will turn the CRT until the trace and the graticule are aligned (Figure 16-1). When an internal graticule is used or the CRT envelope is rectangular a trace alignment control on the front panel of the scope is used (Figure 16-2). The control sets the current through a coil around the outside of the front section of the CRT. The coil's electromagnetic field interacts with the electron beam to rotate the trace about the CRT axis. The forces acting on the electron beam are shown in Figure 16-2.

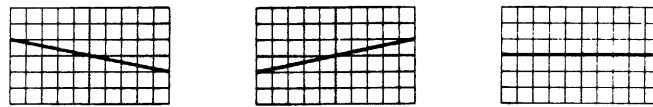


Figure 16-1

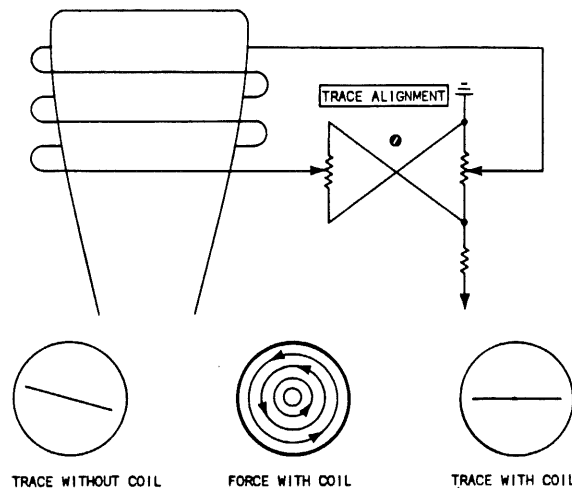


Figure 16-2

When a beam is deflected vertically the deflection should be perpendicular to the horizontal deflection. The orthogonality (perpendicularity) of the trace deflection may be affected by the trace rotation control. A vertically deflected beam may be more affected than a horizontally deflected beam in which case some correction is needed.

The Y-axis alignment control is shown in Figure 16-3. This control is a second rotation coil located around the outside of the tube in the region of the vertical deflection plates. The trace rotation control is adjusted for the alignment of a horizontal trace and the Y-axis alignment control is adjusted for the alignment of a vertical trace.

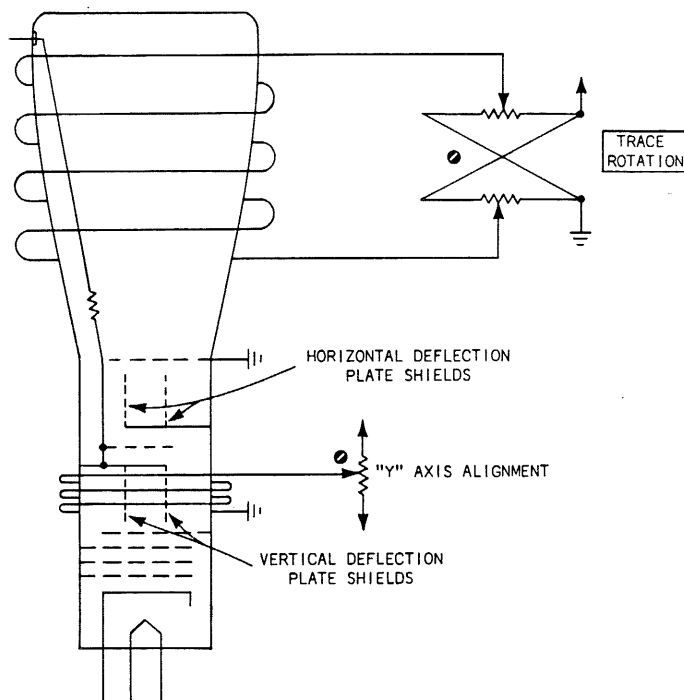


Figure 16-3

SPECIAL CRT TYPES — DUAL BEAM

An application which requires the viewing of two singularly occurring, simultaneous events would require a dual-beam scope. The dual-beam CRT has two independent beams.

The block diagram of a dual-beam, single horizontal scope is shown in Figure 17-1. This type of CRT has two guns, two sets of vertical deflection plates, but only one set of horizontal deflection plates. The two beams may be deflected vertically by two different signals but both beams are deflected horizontally by one set of horizontal plates.

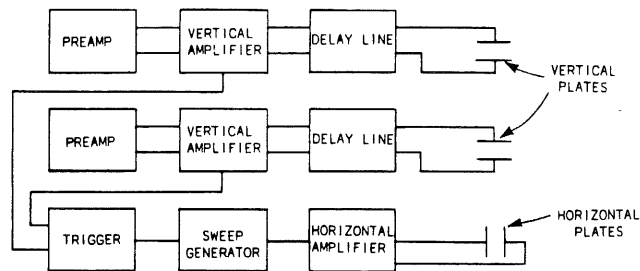


Figure 17-1

SPECIAL CRT TYPES — DUAL GUN

Figure 18-1 shows the block diagram of a dual-beam, dual horizontal scope. Notice that each beam has an independent vertical and an independent horizontal. Each beam in this type CRT can be deflected horizontally at an independent sweep speed and vertically by an independent vertical signal. This type CRT is called a dual-gun CRT since each gun is complete by itself. In a dual-beam, single horizontal oscilloscope there is usually only one front panel intensity control. This control sets the voltage on both CRT grids. Because of slight differences in the two gun structures some means of balancing the intensity of the two beams is needed. The Intensity Balance control or the Intensity Adjust perform this function (Figure 18-2).

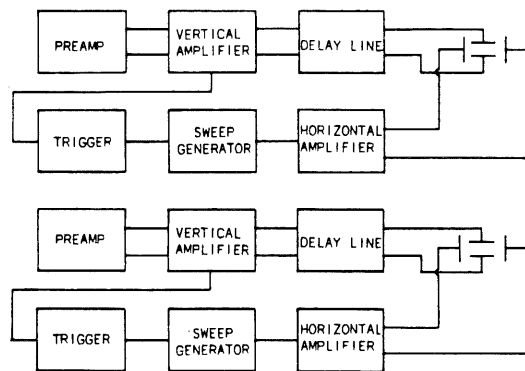


Figure 18-1

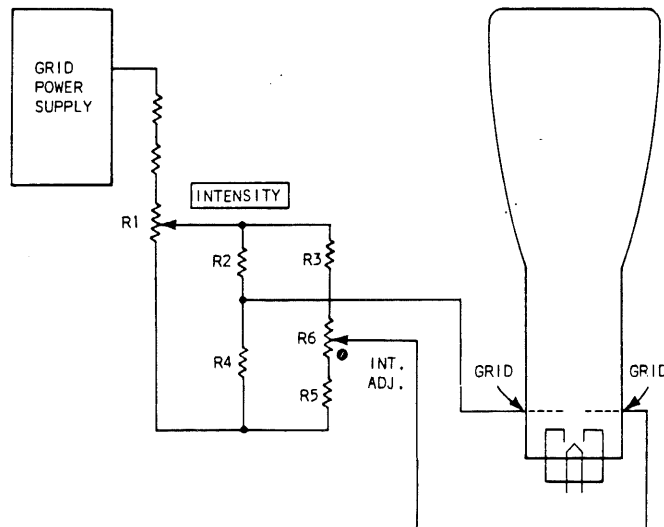


Figure 18-2

The Intensity control R1 sets the voltage at the top of R2 and R3. R2 and R4 form a fixed divider that sets the voltage on the grid of the bottom gun. R3, R5, and R6 form a similar adjustable divider for the grid of the top gun. By adjusting R6 the intensity of the two beams can be balanced. Once they are balanced the front panel Intensity can set the intensity of both beam.

A dual-beam, dual horizontal oscilloscope has an intensity and focus control for each beam on the front panel of the scope and each beam can be positioned horizontally with its own horizontal positioning control.

Dual-gun oscilloscopes have independent horizontals. The horizontal position of each beam is adjustable from the front panel. A dual-beam oscilloscope with but one horizontal system requires another means to adjust the horizontal alignment of the beams. This is done by splitting the first anode of these guns. The horizontal beam registration control sets the voltage on the second section of this anode (Figure 18-3).

In the section on deflection-plate unblanking it was noted that the horizontal position of the beam would be affected if the apparent source of the electrons was off axis. By adjusting the beam registration control, the apparent source of the beam electrons is adjusted until the horizontal position of the beams are aligned.

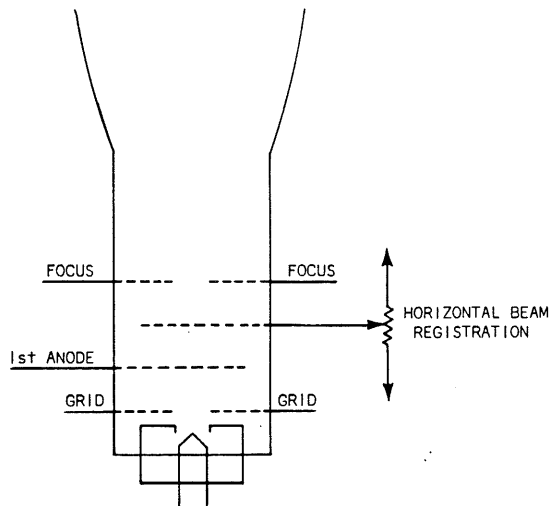


Figure 18-3

SPECIAL CRTS

7612D ELECTRON BOMBARDED SEMICONDUCTOR TUBE FOR HIGH-SPEED ANALOG-DIGITAL CONVERSION

The basic concept of the device is illustrated in Figure 19-1. An electron gun produces a ribbon beam which bombards a semiconductor target. The beam is focused by a cylindrical lens to form a flat ribbon-like beam which can be deflected over the target area. The target consists of a silicon chip containing a number of long diodes overlayed by a pattern of thick and thin metal in the form of a digital Gray code. A simplified version of the target is shown in Figure 19-2. The diodes are reverse biased and normally non-conducting. When the beam bombards a thin metal (window) area, it penetrates to the diode junction region and generates an output current. Due to the large number of electron hole pairs excited in the semiconductor, a considerable electron gain occurs in the target, on the order of 2000 for a 10-kV beam. In the thick metal regions of the target there is no beam penetration and no output signal.

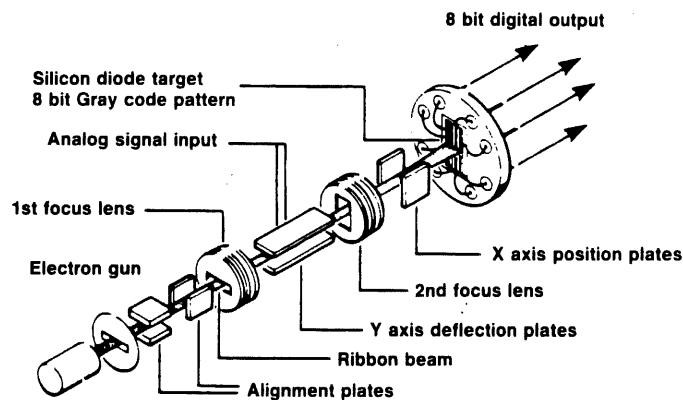


Figure 19-1

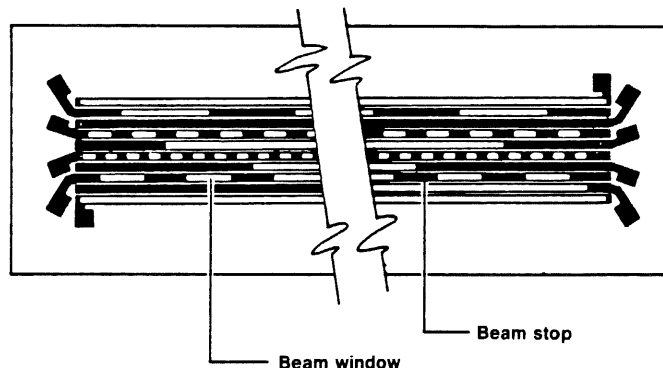


Figure 19-2

In operation the input analog signal is applied to the signal deflection plates and moves the beam up and down the target. In any position, some diodes will be on and others off. At the target, a parallel digital output code is thus generated which uniquely defines the beam position and hence the amplitude of the input signal. Since electron beams can be readily deflected at high speeds and diodes can be designed to give a fast response, the device is capable of giving high-speed conversions with good accuracy.

Electron-beam A/D converters were used in early pulse code modulation systems. The first tubes used a round beam which was scanned over a coded aperture plate. A single collector electrode behind the plate provided an output signal when the beam was positioned over an aperture. The signal to be coded was applied to vertical deflection plates while the beam was scanned horizontally. This provided an output in serial form. The speed was limited but sufficient for audio signals. A later version of the tube employed a ribbon beam with separate electrodes for each bit of the code. This gave a parallel output word and enabled operation at conversion rates to 10 MHz, which is suitable for handling video data.

The use of a semiconductor target fabricated with planar technology, as described in this section, allows the coding pattern to be integrated with the beam collector. In addition, the high electron gain possible with electron-bombarded silicon diodes increases the sensitivity of the device considerably and enables operation at much higher conversion rates.

Semiconductor targets have been used successfully in a variety of amplifier tubes and in a scan converter. An electron-beam sampling device which uses a semiconducting target as a detector has also been described.

ELECTRON GUN DESIGN

The electron gun was designed to produce a ribbon-like beam which could be focused to a fine line image on the target. This beam shape is necessary to address all diodes simultaneously and give a parallel read-out signal. The beam potential was chosen to give the best compromise between target gain (which increases with beam voltage) and deflection sensitivity (which decreases). Previous studies have shown that 10 kV is an optimum choice for a monoaccelerator gun of this type. This beam voltage results in a net gain of about 2000. For an output signal of 5 mA from each diode, the beam current per diode is then $2.5 \mu\text{A}$. Since only a portion of the beam lands on an active area of the target, the total beam current required is about $50 \mu\text{A}$. In order to obtain 8-bit resolution with a practical target size, the focused beam linewidth was designed to be 0.0012 in. ($30 \mu\text{m}$) full width at half maximum (FWHM). This size enabled the required beam current to be obtained with a reasonable gun length.

A ribbon beam is formed in the gun by using beam apertures which are slots rather than round holes as in most guns. The lenses formed by these apertures produce a focusing action in only one axis, the axis which is perpendicular to the slots. Theoretically, this is true only if the slots are of infinite length, but an aspect ratio of length to width of at least 6:1 gives an adequate approximation. The triode section of the gun forms a line crossover which is subsequently focused into a line image at the target. A second slot lens perpendicular to this first focus lens confines the spread of the beam in the other axis and improves gun efficiency. The potential on this second lens is set below that required for a fully focused condition, to obtain the required beam profile as shown in Figure 19-3.

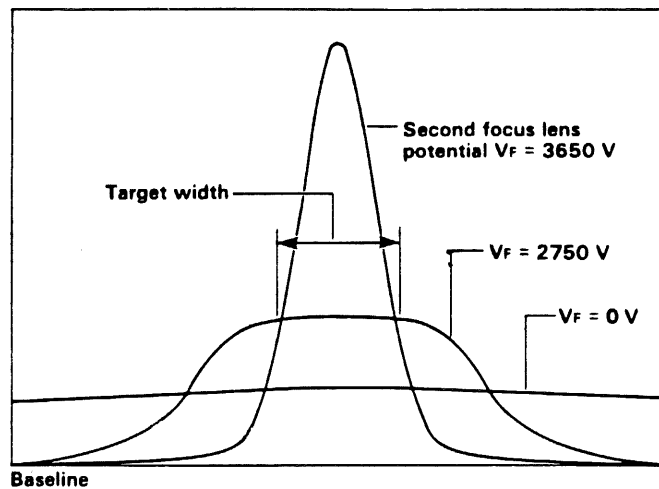


Figure 19-3

The gun contains four sets of deflection plates. They are the x and y axis alignment plates, the x axis position plates, and y axis signal plates. The x and y axis alignment plates correct for triode misalignment by centering the emitted current distribution on the respective beam limiting apertures at the focus lens entrances, thus maximizing beam current. The x position plates are used to center this distribution on the target. The signal plates, of course, carry the analog signal which is to be digitized.

The sensitivity of the signal deflection plates is nominally 23.5 V/scan. To achieve this value with a 10 kV beam required fairly long plates (2.75 in. or 7 cm) which limits the frequency response due to electron transit time. However, for a 100 MHz signal bandwidth, solid deflection plates gave an adequate response, and it was not necessary to use a traveling-wave deflection system.

The ribbon beam was found to be more susceptible to distortion from fringing fields in the deflection system than is the case with a round beam. To avoid these distortions, an adequate plate width and good shielding was necessary. The extra plate area increased the plate capacitance, but it was within acceptable limits for the signal amplifier.

An external magnetic coil is mounted in the entrance region of the deflection plates. It rotates the ribbon beam into precise alignment with the target. This location allows the ribbon beam to be rotated without producing an unacceptable amount of scan rotation. The scan alignment is maintained with the aid of alignment pins which align the target assembly to the electron gun.

The mechanical stability of the gun is an important consideration in a digitizing tube since small movements of the gun with respect to the target upset the calibration. Microphonic effects cannot be tolerated as these produce oscillations in the output signal. To avoid these problems, additional supports were provided for the gun to ensure that it was rigidly mounted in the envelope.

TARGET DESIGN

The target was required to supply an output signal of 5-10 mA per diode into a 50 Ω load. To keep the capacitance low for a fast response time, the target was made as small as possible, the limit being determined by the electron beam width. The smallest window opening, i.e., that on the diode providing the least significant bit (LSB) of the output code, needs to be large enough to allow most of the beam to penetrate the diode, otherwise the LSB output will be smaller than that of the other diodes. Since the beam size in the y axis is on the order of 0.0011 to 0.0013 in. (28 to 33 μm) (FWHM), the window opening in the LSB diode was made 0.0018 in. (46 μm) which will pass about 90% of the beam.

The target pattern is in the form of a Gray code since this gives more accurate output than straight binary in the device configuration. With the Gray code only one transition occurs at a time and each transition is equivalent to a change of one LSB.

An 8-bit Gray code requires 8 diodes with 64 cycles in the LSB diode. This sets the diode length or vertical scan at 230 mils. An additional continuous diode is located on each side of the coded area for alignment purposes, making a total of 10 diodes per die. The size of the target die is 0.25 x 0.04 in. (0.635 x 0.102 cm).

The target is fabricated using silicon planar technology. A cross section of a target die is shown in Figure 19-4. An n-type epitaxial layer is grown on a (100) oriented n+ silicon substrate.

The wafer is oxidized and openings for the diode are cut in the oxide by photolithography. Diodes are then formed by a boron diffusion. The junction depth is very shallow, about 0.25 μm , to minimize the loss of beam energy in the p region. An aluminum film approximately 1- μm thick is deposited over the target and photoetched to form the Gray code pattern. Finally, a thin (500Å) aluminum film is deposited over the diode to provide a low resistance contact for the diode current. Each diode is surrounded by n+ channel. The purpose of this is to isolate the diode thus improving stability, reducing leakage currents, and minimizing crosstalk between diodes.

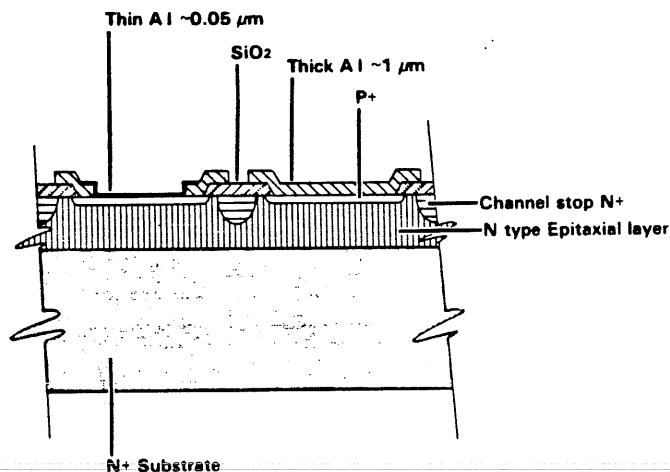


Figure 19-4

The width and resistivity of the epitaxial region was chosen for the best compromise between a low diode capacitance and high level of current saturation. Output limitations on EBS diodes have been discussed in the literature. In general, limitations occur when the electric field in the depletion region of the diode falls below the minimum value required to maintain electron drift velocity (approximately 1.6×10^4 V/cm. Modifications to the electric field can occur due to space charge associated with the carriers that produce the diode current or to a reduction of the diode voltage through large signal swings. In the digitizer device, the output signal of 250 mV has negligible effect on the diode bias (11.5 V). The main restriction is thus due to space charge which limits the current density that can be generated in the diode before the response speed is affected.

In Figure 19-5 the epitaxial thickness to maintain a minimum electric field of 10^4 V/cm is plotted against the epitaxial layer resistivity. Also shown are the corresponding values for the maximum current density and the diode capacitance. The value of epitaxial resistivity used for the design is $15 \Omega/\text{cm}$ giving an epitaxial thickness of $4.5 \mu\text{m}$, a target capacitance of 2.32×10^3 pF/cm², and a maximum current density of 750 A/cm.

There were two main points to consider during the target mounting design. First, it was important to have the silicon chip containing the diodes accurately positioned with respect to the beam, particularly in regard to rotational alignment. If the ribbon beam is not orthogonal to the diodes, errors in the output code can occur. The second concern was to have an adequate thermal path to dissipate the power generated in the target.

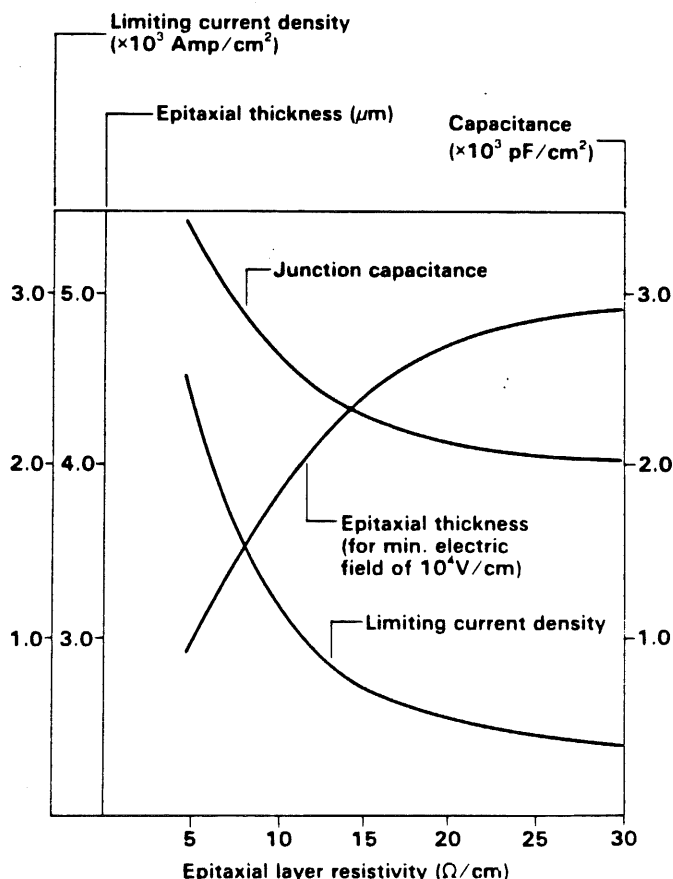


Figure 19-5

In most applications the exact position of the die is not critical, consequently, the equipment available for die attach is not capable of accurately aligning the die on the substrate. To overcome this problem, the die is attached to a separate carrier consisting of a ceramic substrate brazed to a kovar platform. This carrier is then welded to the target header in a special fixture which enables the diodes to be accurately positioned with respect to indexing pins on the header. These pins align the header with the gun during final assembly.

Another advantage of the ceramic substrate is that it allows thin-film coplaner transmission lines to be used for connecting the diodes to the header feed-through pins, thus avoiding the extra inductance incurred when using long bonding leads. The feed-throughs and transmission lines were designed to have a characteristic impedance of $50\ \Omega$ to match the input impedance of external comparator circuits.

Since the beam occupies less than 2% of the target area, power is dissipated in only a small part of the target at any instant. The worst case is when the beam is stationary on the target in a position where all the diodes are turned on. In this case power is concentrated in a small area and can reach power densities of $760\ \text{W/mm}^2$. Under normal operation about 1.1 W are dissipated in the target due to the beam and induced current in the diodes. In addition, an external comparator circuit which is attached directly to the header dissipates 4.8 W and further compounds the cooling problem.

Both alumina and BeO ceramic were tried as substrates. Measurements of the temperature rise at the diode surface were made using an IR microscope. For these measurements special die were used in which a small area could be forward biased to simulate the power dissipation effects of the beam. Tests were carried out with both internal and external power applied. With and without forced air cooling, to determine the temperature rise expected on the device when mounted in an instrument. The maximum temperature difference between the hottest spot on the diode surface and the outer edge of the header was $57^\circ\ \text{C/W}$ for an alumina substrate and $44^\circ\ \text{C/}$ for BeO.

Although BeO had the best thermal results, it gave poor parts yield due to shorts on the coplaner transmission lines which occurred during the brazing cycle. Since the alumina gave adequate results and was easier to work, it was decided to use this material. The maximum temperature on the outside of the target header in an instrument environment is expected to be about $70^\circ\ \text{C}$ which would result in a maximum diode junction temperature of $127^\circ\ \text{C}$.

PERFORMANCE

The performance of the digitizer determines how accurately the output code represents the input signal. It is convenient to consider this in two parts: (a) the static or low-speed capability and dynamic or high-speed limitation. The various factors which determine the performance of the device are considered in the following sections.

A. Static Characteristics

The dc linearity of the device is determined by the signal deflection plate linearity and the accuracy of the code pattern on the target. Since the electron gun is a 10-KV monoaccelerator with a maximum deflection angle of less than 1.6° , non-linearity in the deflection is expected to be very small, of the order of 0.03%. This is confirmed by the linearity measurement described below.

The pattern in the Al film on the target is produced using photolithographic techniques and can be made quite precise. Small variation can be expected from run to run, but these are carefully controlled and checked on each run. Measurements are made on the length of the window opening in the thick metal of the LSB diode. A tolerance of $\pm 2\%$ is specified for the window which ensures that the transition in the code pattern are in the correct position within ± 0.09 LSB. Generally targets are well within this tolerance.

To verify the linearity of the device, measurements of the deflection voltage at each LSB transition were taken on several tubes. A typical result is shown in Figure 19-6, which indicates the voltage required to deflect the beam between adjacent transitions as a function of the position on the target. Note that there is a difference of 10 mV between the average positive and the average of the negative going transition. This indicates that the length of the windows on the LSB diode in this target is 5% smaller than the space between windows. Ideally these would be equal. The difference is equivalent to $2.4 \mu\text{m}$ which is within the tolerance of $4 \mu\text{m}$ specified for target processing, and represents a displacement of the code transition points of 0.05 LSB. Non-linearity due to deflection would result in a reduction of the voltage between transitions at each end of the target. This effect is masked by the other variation in our measurements.

A more serious problem with the EBS digitizer is non-alignment of the sheet beam with the target and changes in the beam shape. Some of the problems that can occur are shown in Figure 19-7.

Static beam rotation is shown in Figure 19-7(a). This occurs when the target is not aligned with the vertical axis of the gun. Since the target pattern is designed for a ribbon beam which is perpendicular to the diodes, a significant rotation of the beam (2° or larger) with respect to the target can result in errors in the output code. Care is taken to ensure that this alignment is as close as possible during assembly and small errors are corrected with an external beam rotation coil.

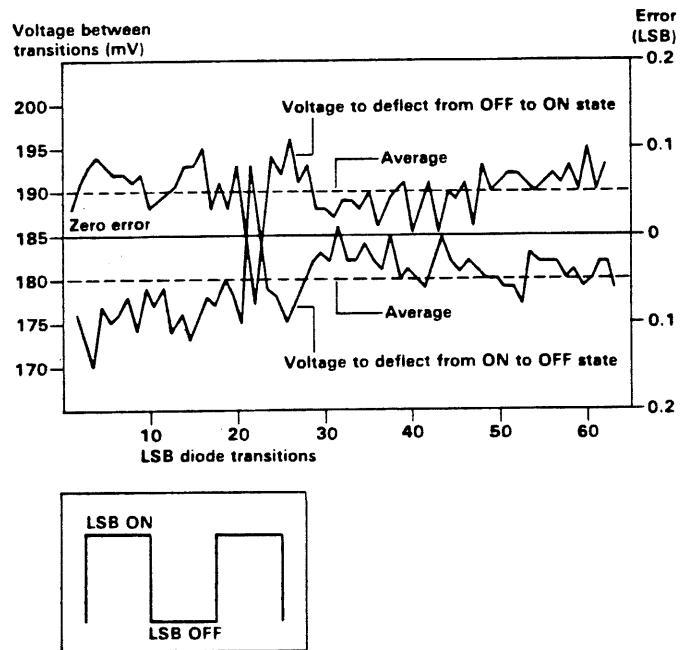


Figure 19-6

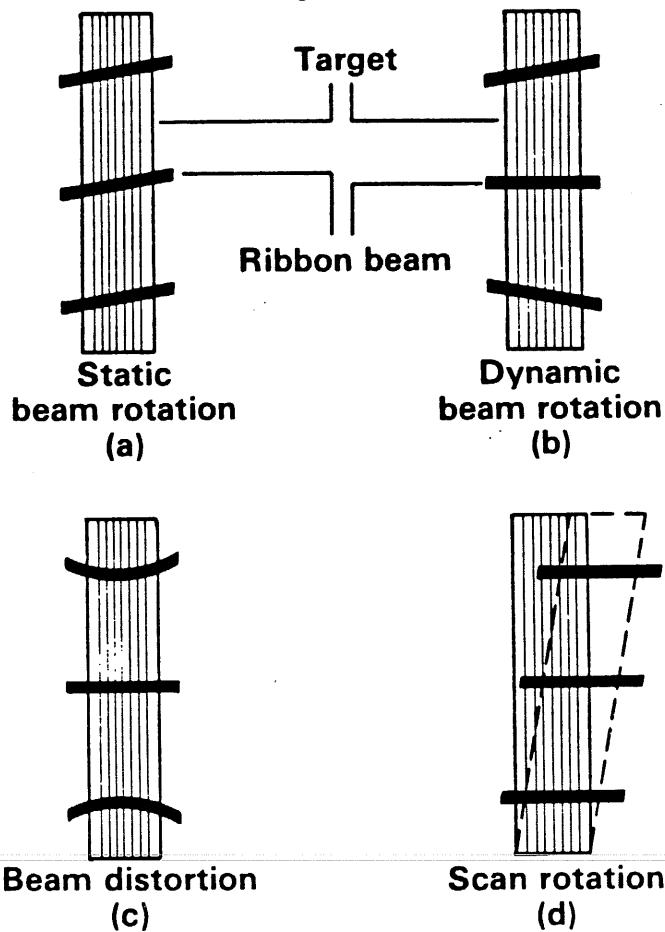


Figure 19-7

Dynamic rotation occurs when the angle between the beam and the target changes with deflection as shown in Figure 19-7(b). This effect can occur when the deflection plates are not parallel. The deflection sensitivity then varies across the plates resulting in a rotation of the beam. This rotation is increased by the second slot lens since the long axis of this lens is perpendicular to that of the beam. In this case, the slot lens magnifies the angular error in the alignment of the ribbon beam axis to a line perpendicular to the long axis of the lens. The rotation coil used to correct static rotation is not suitable for correcting dynamic rotation. However, hexapole fields will correct this defect. The action of an electrostatic hexapole field is illustrated in Figure 19-8 which shows the magnetic fields acting on the ribbon beam for three positions of the deflected ribbon beam.

Both electromagnetic and electrostatic hexapoles were tried. The electrostatic one worked particularly well. These systems were not used in the final version of the gun because dynamic rotation was held to less than 1° by maintaining a close tolerance on deflection-plate spacings and strength of the second slot lens.

Curvature of the beam, Figure 19-7(c), can be caused by fringe fields along the signal deflection plates. This effect is minimized by making the signal deflection plates sufficiently wide.

Scan rotation results in a horizontal shift in the beam with vertical deflection as shown in Figure 19-7(d). Small amounts of scan rotation are generally not a problem provided the horizontal profile of the beam has a constant amplitude for a distance somewhat greater than the target width. If the profile is not flat the amplitude of the signal from the diode can vary with vertical position. Scan rotation is kept to a minimum by careful alignment during assembly as explained above.

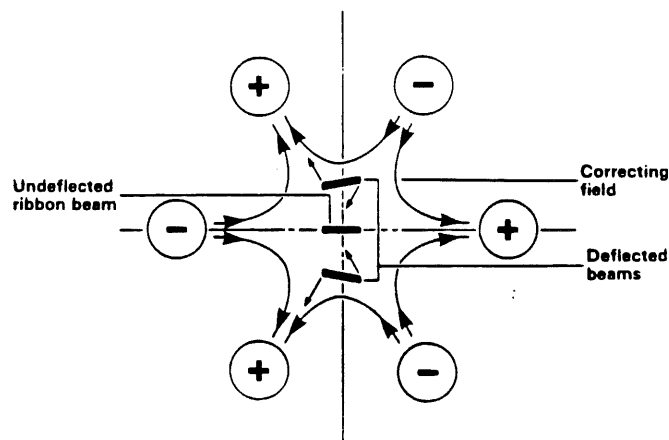


Figure 19-8

If the beam is free from curvature [Figure 19-7(c)], beam rotation can be determined from the transition point of the various diode signal as the beam is scanned across the target. Figure 19-9 shows that LSB signal and the signal from the 2nd and 3rd bit diodes. Transition points of the higher order bits should occur at the peaks of the LSB signal. Shifts from the true position can be measured on an oscilloscope and used to determine the rotation angle. The standard measurement on the device is made on the 2nd and 3rd bit signal. For the particular geometry used in the target, the rotation angle ϕ is given by

$$\phi = \tan^{-1}[(2/3)(S/B)]$$

Where S is the shift from the true position and B is a reference equal to 2 cycles of the LSB signal.

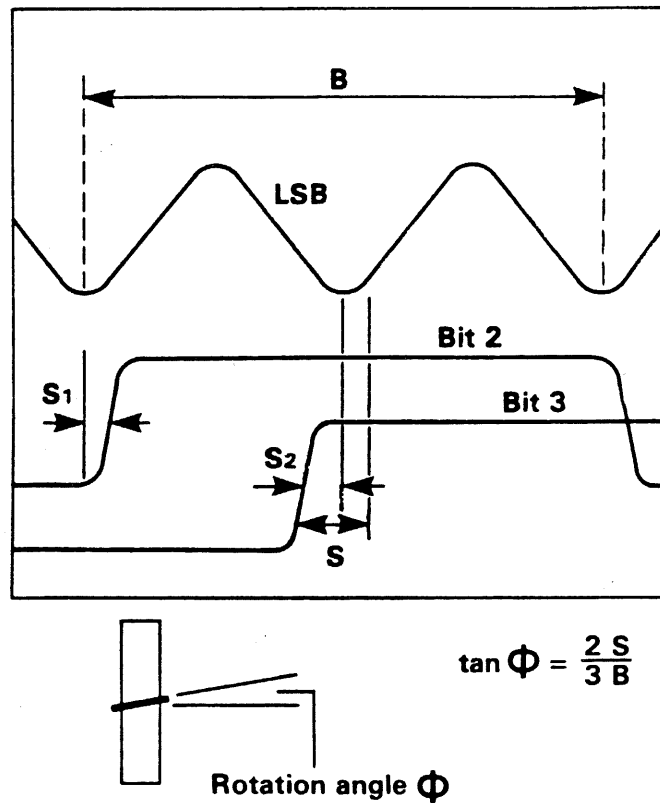


Figure 19-9

In the above discussion, the main types of beam distortion have been described. In practice, additional perturbation in the beam shape are sometimes present which do not fit these categories. Extending the method used for measuring beam rotation, an estimation of the beam shape at various points on the target can be made from the position of the transition of the higher order bits compared to the LSB signal. This measurement assumes that the target pattern is accurate and errors are due to the beam alone. In Figure 19-10, the beam shape in a sample tube is plotted at several places on the target using this method, the vertical scale in the vicinity of each plot is enlarged for clarity.

It can be seen that the beam has a static rotation (of about 1.6°) which is fairly constant over the length of the target. This can be corrected with a rotation field. In addition, there are small perturbation in the beam giving a maximum error with respect to an average straight line of 0.1 LSB.

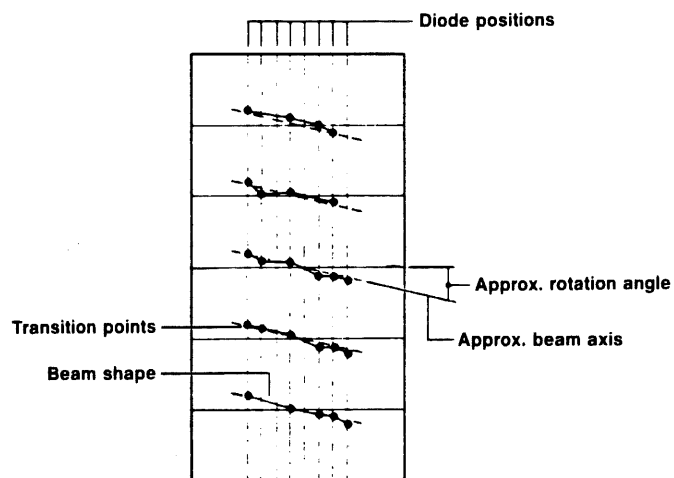


Figure 19-10

The effects of dynamic beam rotation on the output code were investigated using a computer simulation program which was designed to estimate the performance of the digitizer in an operating system. The model used for the program assumed that the beam remained straight, had zero rotation at the target center and the rotation increased linearly with deflection towards the target ends as shown in Figure 19-7(b). The results indicated that a maximum rotation of 2° could be tolerated before errors in excess of $1/2$ LSB appeared in the output code.

The overall performance of an A/D converter is determined by the accuracy of the output code. This is generally done by comparing the output against a standard reference code. To check the performance of the EBS digitizer, a digital test circuit was built which is shown in a simplified block diagram in Figure 19-11.

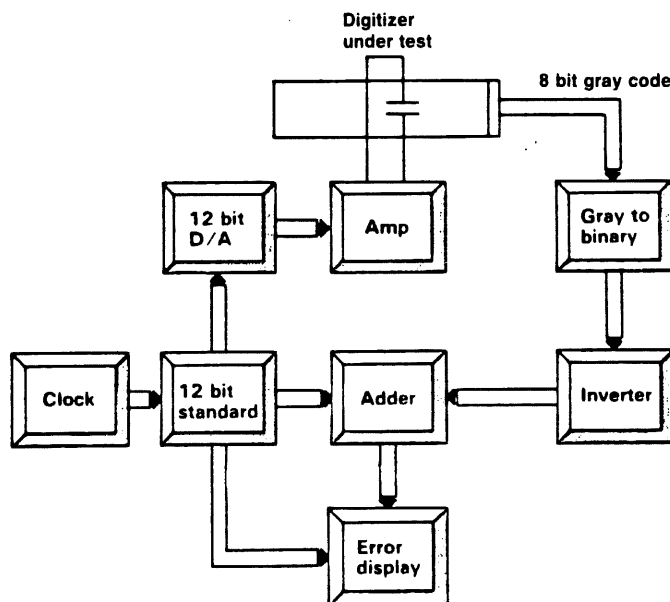


Figure 19-11

The test circuit is built around a standard 12-bit binary code generator which can be cycled from 0 to 4096. This standard generator is used to drive a 12-bit D/A converter to provide a ramp for applying to the deflection amplifier of the digitizer. The output Gray code is converted to binary, inverted, and added to the standard binary to produce an error signal. A comparison is made at each transition of the output code. The error signal is then a measure of the difference between the actual output transition point and the ideal transition as represented by the standard. Since the 12-bit standard has 16 transition between successive points on the 8-bit code, the actual output transition points can be located to 1/16 of an 8-bit LSB. An error plot can be obtained by using the error signal as an ordinate and the standard 12-bit binary as an abscissa. These signals can be applied to an oscilloscope to give a continuous display. A clock rate of about 100 KHz is sufficient for a flicker-free display but slow enough to avoid settling time errors in the circuit.

The error display has proved useful in setting up the digitizer. Adjustment in signal gain and dc position have a marked effect on the error signal and can be readily optimized with the aid of an error display.

B. Dynamic Characteristics

The frequency response of the device is dependent of the rise time of the diodes and output circuit at the target and the bandwidth of the deflection system.

The main factor which limits the accuracy of the device at high speed is the response of the LSB diode. This is because the LSB output signal contain much higher frequency components than the applied signal. For the case where the input is a full amplitude sine wave, the maximum frequency component in the output from the Nth-bit diode $(\int N)$ max will occur at the zero crossings of the sine wave where the beam deflection velocity is greatest. For the Gray code pattern, which has 2^{N-2} windows, it is related to the input signal by

$$(\int N) \text{ max} = 2^{N-2} \pi \int \text{sig}$$

where N is the number of resolution bits and $\int \text{sig}$ is the input signal frequency. For the LSB diode on the present device where $N = 8$, the maximum frequency in the LSB signal is approximately 200 times that of the applied signal.

As the input frequency is increased, the amplitude of the LSB output signal is reduced when the diode response is exceeded, until a point is reached where the output code is effectively decreased from 8-bit to 7-bit accuracy. At still higher frequencies the next higher bit drops out giving a 6-bit code. Thus, accuracy is progressively lost as the signal frequency is increased.

The basic response of the target is determined by the diode capacitance C and the output impedance R. The rise time is approximately 2.2 CR which for typical device values of $C=5$ pF and $R=50$ ohms gives a value of 550 ps. For the situation in which the beam is continuously deflected over the target (e.g., for a sine wave input) the amplitude of the signal from the Nth-bit diode, V_N , at high speed is given by

$$V_N = V_N \sqrt{\frac{[1 - \exp(-t_N/CR)]}{2[1 - 1/2[1 - \exp(-t_N/CR)]]}}$$

in which V_N is the maximum (low speed) value and $t_N = \left(1/2 \int N\right)$ the dwell time of the beam in each open window of the diode. The signal will have a dc component equal to $V_{N/2}$. Using this expression, the decrease in the LSB signal at higher frequencies was calculated and is shown in curve A of Figure 19-12.

A more complete model of the output circuit takes into account the inductance of the lead bond wires, the impedance of the coplanar waveguide on the target substrate and the capacitance of the output feed-through. An equivalent circuit is shown in Figure 19-13.

The frequency response of this model was estimated using a computer simulation of the circuit and is shown in curve B of Figure 19-12. Measurements of the frequency response of the target and output circuit were made by observing the signal from the LSB diode on a sampling oscilloscope as the beam was swept along the target. By varying the beam deflection speed the relationship between frequency and amplitude of the signal can be determined directly from the scope display. A typical result is shown in Figure 19-12.

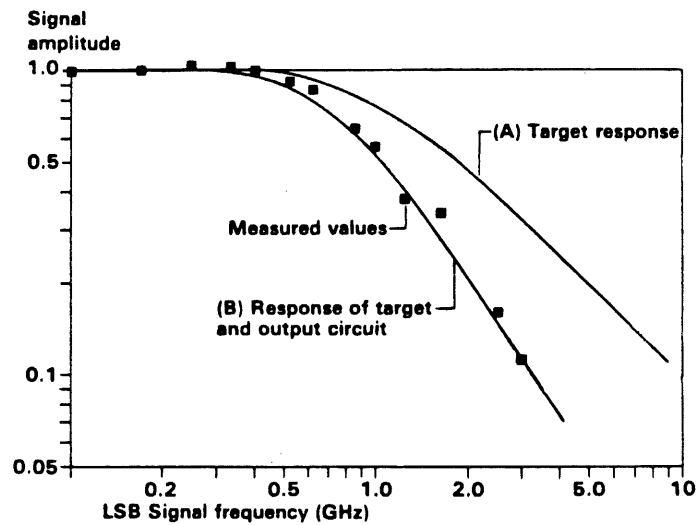


Figure 19-12

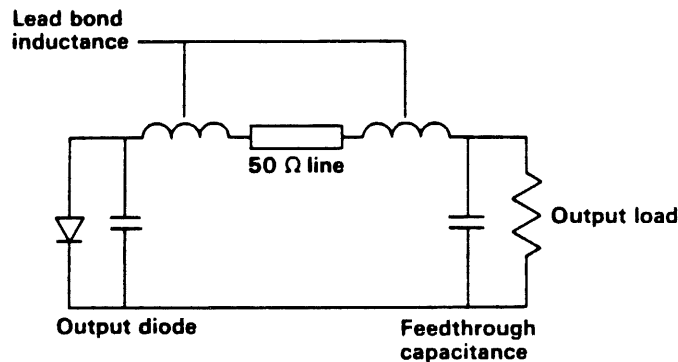


Figure 19-13

The minimum useful output signal depends on the value required for reliable operation of the comparator circuits which detect the target output. The comparator reference is normally set at a voltage which is the value about which the LSB output oscillates. Error in comparator circuits can be of the order of a few mV, so that 10 mV changes about the reference value can be easily detected. To estimate the performance of the digitizer, a minimum LSB signal of 25 mV peak to peak will be used, which is 1/10 that of a typical low-speed signal amplitude of 250 mV. The dc component is assumed to be at the comparator reference of 125 mV. From Figure 19-12, the frequency at which the LSB signal falls at 1/10 maximum is 3 GHz. The equivalent maximum full-scale sine wave at the input is obtained from Eq (2) and is 15 MHz for 8 bit, 20 MHz for 7 bit, and 60 MHz for 6-bit resolution.

If the beam is at rest on the target, the dc value of the LSB output can vary from 0 to V_N . When the beam is deflected, the dc value changes to $V_N/2$ within a few LSB cycles. Since the beam cannot be deflected to maximum speed instantaneously, the dc value of the LSB signal is normally at the $V_N/2$ value by the time the maximum speed is reached.

Exceeding the frequency response of the deflection system results in a decrease in amplitude of the high frequency components of the signal being digitized at the target. Since the deflection plates form part of the output circuit of the signal amplifier, the total system needs to be taken into account when considering the bandwidth limitations due to deflection. One parameter that can be considered separately is the limitation due to electron transit time within the deflection plates. The plates are 2.75 in. long which gives a transit time of 1.18 ns for a 10-KV beam. This results in a reduction of deflecting power for signals above 100 MHz. The 3-db point in the rolloff due to transit time occurs at 450 MHz. At 100 MHz, deflection sensitivity has decreased by 2.1%.

RELIABILITY

Life tests lasting several thousand hours have been carried out on a number of devices. The results indicate that the main aging process is an increase in the reverse leakage current in the target diodes due to bombardment by the electron beam. Prior to operation diode leakage is normally less than 5 nA. During the first few hours of operation, the leakage increases to several hundred nanoamps. It then remains at this level for the remainder of the life test. The reverse breakdown voltage remains fairly steady throughout the operation.

The increase in leakage is believed to result from charge created in the oxide and at the silicon-oxide interface by electrons and X ray from the electron beam. This charge alters the electric field at the junction edge leading to increased leakage. By providing additional shielding for the junction edge, it should be possible to reduce the radiation effects of the beam. However, the leakage levels normally observed are several orders of magnitude below the signal level and do not interfere with the normal operation of the device.

High voltage arcs either in the tube or the external circuits produce high-level transients which can damage the diodes in the target. The result is usually a decrease in the diodes reverse breakdown voltage and a considerable increase in leakage current which causes a shift in the baseline of the output signal. Damage can be avoided by isolating the target bias circuit from potential transients, by providing safe return paths for arc currents, and by limiting the energy that can be dissipated in an arc. If adequate precautions are taken, arcing can occur without damaging the target.

SPECIAL CRTS

7912 SCAN CONVERTER CRT

The 7912 tube is a double-ended scan converter, with the read gun facing the diode array and the write gun on the opposite side of the target, pointing at the back of the array (Figure 20-1). The input signal is applied to the vertical deflection plate of the writing gun as its beam sweeps across the target. The charge pattern this makes on the diode array is scanned by a low-velocity reading beam, modulating the read current to create the output signal.

The target is an array of pn junctions formed on an n-type silicon wafer by means of standard integrated-circuit techniques (Figure 20-2). During fabrication the wafer is overlaid by a thermal oxide, in which an array of holes is etched by photolithography. Boron diffused through the holes forms the diodes. A density of 2,000 diodes per inch yields sufficient resolution for the 1/2 by 3/8 in. scan employed. A central area, 0.75 in. diameter is thinned to about 10 micrometer.

Reverse-biased silicon diodes do, however, have a small leakage current that results in a target dark current of about 15 nanoamperes at 30° C and doubles for every 10° C increase in target temperature. While some dark current is desirable to help bias the p region of the diode positive for reduced lag, (induced conductivity) high dark currents will reduce the dynamic range of the target, limiting the maximum obtainable signal current. For the diode-array scan converter, the read beam's current saturation is 300 nA, so that dark currents much in excess of 100 nA cannot be tolerated. This limits the target's maximum temperature to about 60° C.

Increasing the applied target voltage does not increase the silicon array's gain-unlike in a photoconductive vidicon target-but it will reduce lag. On the other hand, dark current increases about 10% per volt in the range of 8 to 16 v, so a compromise must be obtained between dark current and lag. This translates into a compromise between maximum digitizable writing speed and maximum signal dynamic range, usually attained by setting the target voltage to obtain the required dark current (15 nA at 30° C).

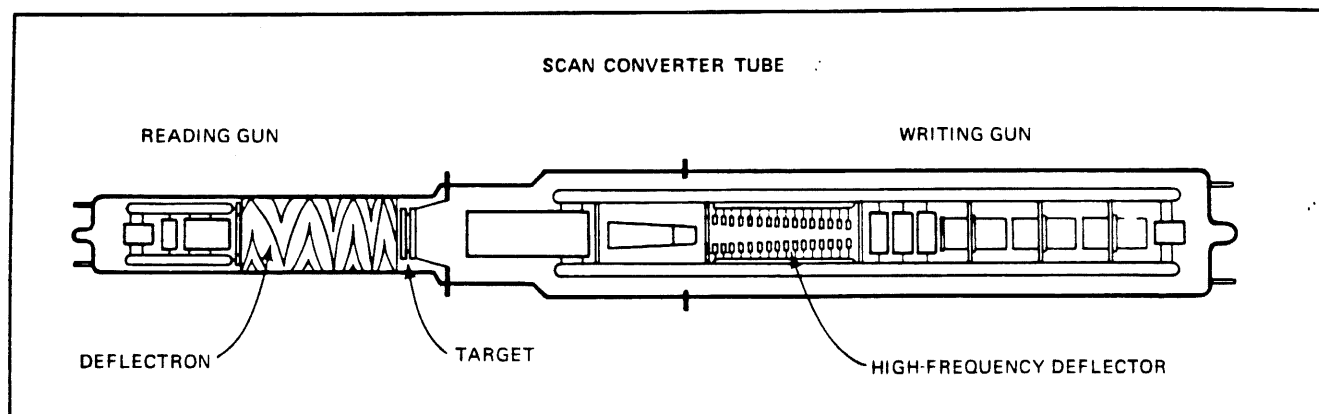


Figure 20-1

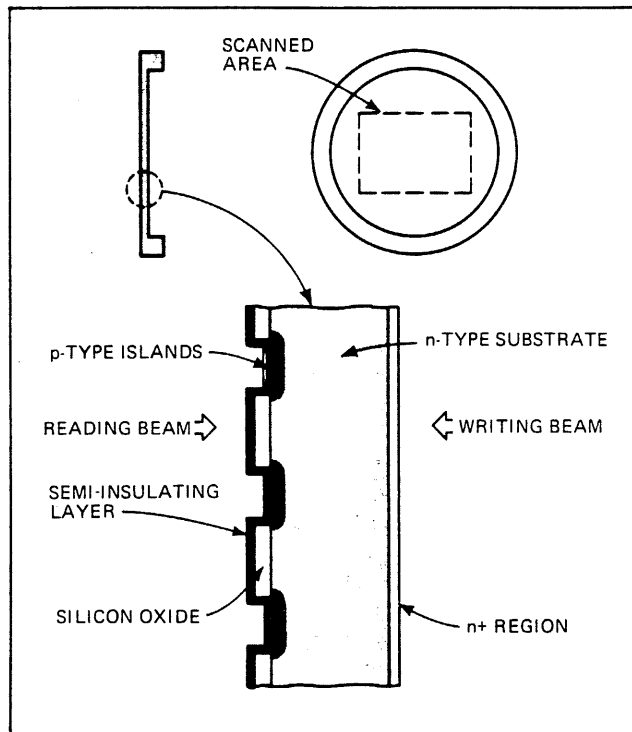


Figure 20-2

In operation, the reading section functions like a vidicon camera's tube. The target substrate potential is held a few volts positive with respect to the reading gun's cathode. On being scanned by the reading beam, the target is charged negatively to the cathode potential, in which condition the diodes are reverse-biased.

During writing, 10-Kilovolt electrons bombard the side of the target opposite the diodes and create many electron-hole pairs near the surface. The holes diffuse through the target and drift across the depletion region formed by the reverse-biased diodes, causing the diodes to conduct and discharge in the written area. When the reading beam next scans this area, the diodes are recharged and a signal current is obtained in the target lead. This provides the output signal, which can be amplified for further processing.

Since the average energy required for the creation of an electron-hole pair in silicon is 3.6 electronvolts, roughly 2,780 electron-hole pairs are created by each incident 10-KV electron. Certain losses occur from the recombination of charge carriers and from the back scattering of some incident electrons, so that the effective charge gain of the target is about 2,000. This gain mechanism is responsible for the sensitivity of the target and the high-speed performance of the scan converter.

Because the penetration of the 10-KV writing-beam electron is small, about $1\ \mu\text{m}$, and the carriers they generate must diffuse through the wafer, causing losses in collection efficiency and deterioration in resolution, target thickness should be kept to a minimum. This is the reason the target is thinned in the center working region to about $10\ \mu\text{m}$, a practical thickness.

To further assist collection efficiency, a thin n layer is diffused in this thinned region, to create an internal field and repel carriers away from the surface, where they would recombine.

In the targets used for the scan converter, a semiconducting layer is formed over the diode side of the target in order to prevent charging of the oxide web surrounding the diodes and consequent interference with the operation of the reading beam.

To achieve a large target gain, a high-energy writing beam is required, but for good deflection sensitivity the beam voltage at the deflector should be low. A post-deflection acceleration scheme would do, except that it would require a high voltage at either the beam deflectors or the reading section. Since the vertical deflector has a bandwidth of more than 2 GHz, it is important to keep the average potential near ground to facilitate connection to the vertical amplifier or signal source. The reading section handles signals as low as a few nanoamperes, and maintaining good signal-to-noise characteristics at an elevated voltage presents formidable practical problems. These considerations led to the adoption of a monoacceleration writing gun, with both deflectors and reading section near ground potential.

The writing gun was designed to achieve the best compromise between deflection sensitivity, resolution, accelerator voltage, and beam current. It was important to design for high deflection sensitivity so that the tube could be used with available wideband amplifiers, which have only limited output voltage swing at frequencies above a few hundred megahertz. (Alternatively, such a tube could be used with direct access of the signal to the deflection plates). But only a modest beam current is necessary when a high-gain target provides writing speed; the advantage is that the triode section of the gun can then be designed to maintain a small beam spot size at all grid drives, and tube resolution will not deteriorate at fast writing speeds.

Tradeoffs between the four parameters were optimized by means of a computer program. The best design consisted of a 10-KV mono-accelerator writing gun having a vertical deflection sensitivity of 24v per scan, a beam spot size of 0.001 in., and a scan at the target of 3/8 by 1/2 in. The maximum beam current is in the range of 3 to 10 microamperes.

At high frequencies, the transit time of the electron beam through the deflection plates becomes comparable to the period of the deflecting signal, and the deflection efficiency is decreased. To avoid this, the deflectors of high-frequency scan converters and cathode-ray tubes are usually made in the form of a delay line. For optimum performance, the delay line should have minimum dispersion and the phase velocity of signals on the line should match the electron velocity in the beam.

The vertical deflector used in the scan converter's writing gun consists of two helical delay lines assembled into a balanced deflection system. The deflecting field appears in the gap between the helices, which are contoured to provide the required sensitivity and scan. The final design has a deflection sensitivity of 24 v per scan and a bandwidth of 2.5 GHz as determined from risetime measurements. The delay line's impedance was set to 864 ohms line to line, to match the wideband deflection amplifier available.

The reading section requires a low-velocity beam with minimum shading and good resolution. To accommodate variable scan rates, electrostatic deflection was preferred to the electromagnetic deflection common in vidicons. Generally, however, electron guns which use electrostatic fields for focusing of the beam have poor shading characteristics.

Shading is caused by off-normal landing of the beam on the target and results in a variation in the level of the readout signal's base line. It is particularly objectionable in a measuring instrument, especially when the readout signal is to be digitized by a Schmitt trigger circuit. With appreciable shading, the Schmitt trigger level must be set high to avoid triggering off the uneven base line, which means that small signals cannot be detected and high-speed performance suffers.

To avoid this, a hybrid design was developed having an electrostatic deflection yoke immersed in an axial magnetic focusing field. The yoke consists of a cylindrical electrode pattern continuing a 90° twist about the axis between each end. This deflection pattern is photoetched on the interior wall of the tube, the axial magnetic field being provided by an external solenoid.

For high-speed oscilloscope instrumentation, the parameters of most interest in a scan converter are writing speed, bandwidth, and resolution. For measurement purposes, good linearity and minimal distortion are also important.

The performance of the scan converter is probably easiest to appreciate when it is compared with that of a conventional high-speed CRT (Figures 20-3 and 20-4). The leading edge of a single-shot pulse recorded by the scan converter and displayed on a Tektronix 630 TV monitor is Figure 20-3a and c, which are reductions from a 20 by 25 cm. monitor display. Similar pulses photographed with a 10,000 ASA speed film from the screen of a Tektronix 7904 oscilloscope are shown in Figure 20-3b and d; in them, the CRT approaches its limit in writing speed, even though a small scan (4×5 cm) increases brightness.

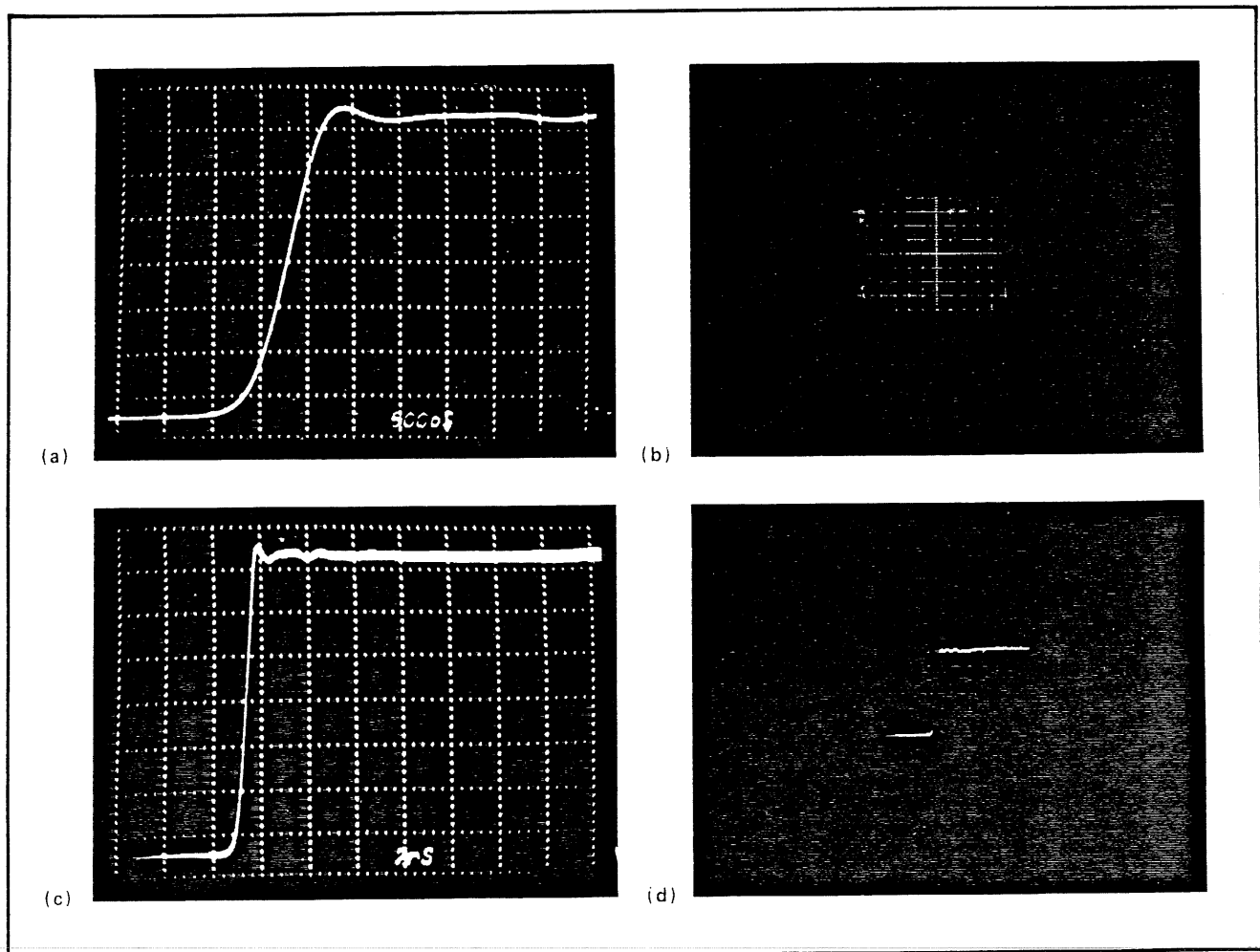
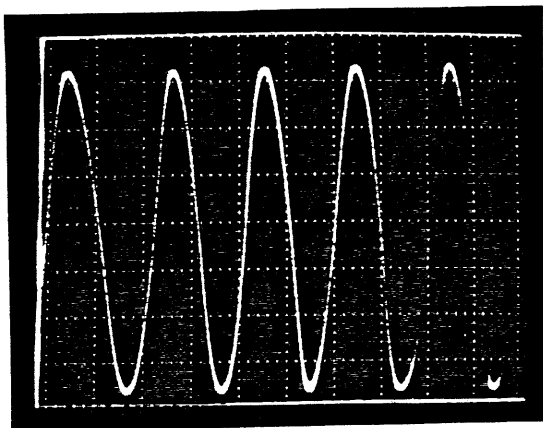
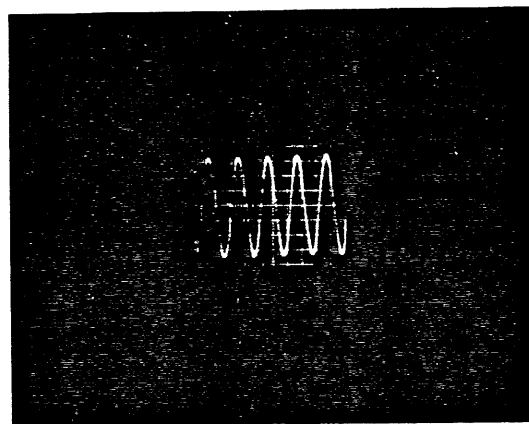


Figure 20-3

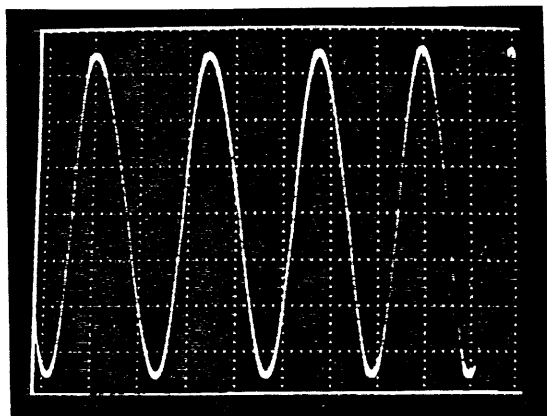
Figure 20-4 illustrates the effect observed as the limiting writing speed is approached. The photographs were taken from single-shot sweeps at various signal frequencies. With a 100-MHz signal, both devices have sufficient brightness for adequate film recording. At 500 MHz, the center portion of the sine wave is too fast to record on the CRT, and only the peaks of the waveform can be seen. The scan converter, however, gives a clear signal at 2.4 GHz, a figure that is at five times better than the writing speed of the 7904 CRT.



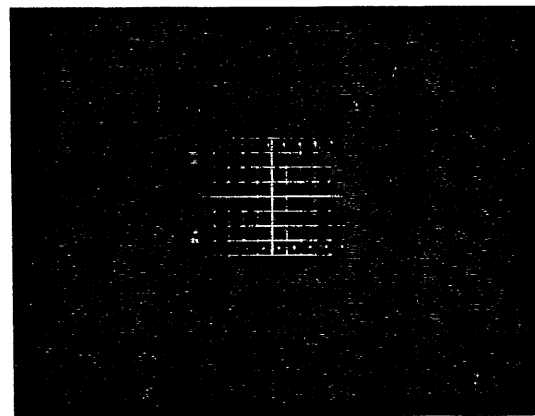
(a)



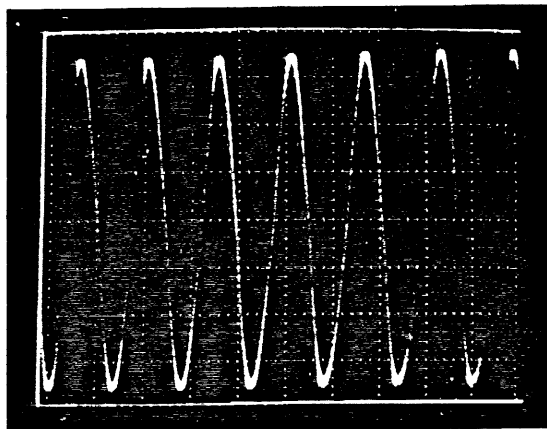
(b)



(c)



(d)



(e)

Figure 20-4

SPECIAL CRTS

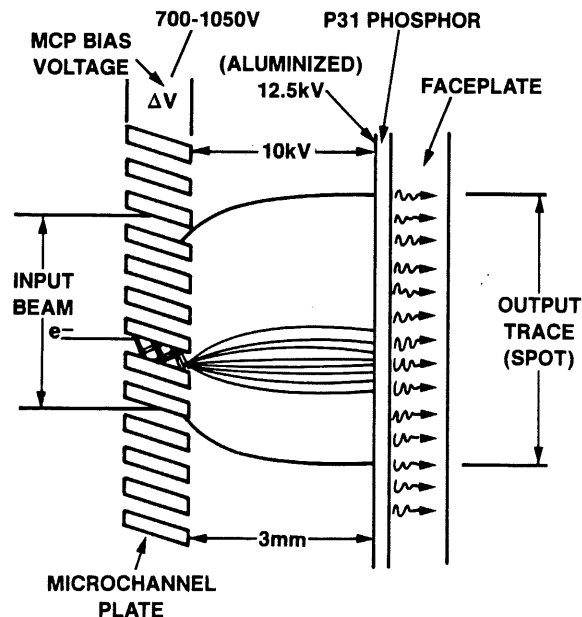
7104 MICRO CHANNEL PLATE

The CRT continues to be the dominant display for high frequency, realtime waveforms. Tektronix' contribution to this field is the 7104 general purpose oscilloscope employing a high resolution, high frequency, microchannel plate (MCP) based CRT, the T7100. While the MCP, which multiplies a single electron entering a channel tens of thousands of times, is the heart of these CRTs, they also employ many novel electron features.

MICROCHANNEL PLATE (MCP)

The microchannel plate is an assembled structure of microscopic conductive glass channels. The channels are parallel to one another with the entrance to each channel on one side of the plate and the exits on the other side. See Figure 21-1.

An electron entering a channel will produce secondary electrons as it strikes the channel wall. When a voltage potential is applied across the two main plate surfaces, that is, across the length of the channels, the secondary electrons will accelerate and themselves collide with the channel walls. This dislodges additional secondary electrons. The process cascades down each channel struck by the CRT electron beam and results in a multiplication of electrons.



2. A microchannel-plate.

Figure 21-1

MCPs have had short lifetimes as one of their drawbacks in use as oscilloscope display. The MCPs in Tektronix T7100 CRTs are made using a proprietary process that reduces this drawback. Rather than decreasing rapidly with useage, the gain of the MCP in these tubes remains relatively constant. These same manufacturing processes also result in a fifty percent gain increase. The T7100 CRT employs the MCP in the proximity focus mode. The MCP is located about 0.3cm from an aluminized screen, and with 10 KV applied across this gap, the spreading of the beam from the MCP is minimized. On the 7104' scope, the INTENSITY control adjusts the MCP gain and beam current simultaneously in order to keep a solid trace at all settings. Without this precaution, the trace could take on a granular appearance when beam current was reduced or pushed toward its writing speed limit (3-5 Ghz) in direct access mode. The graininess results from individual input electron and individual channel gain statistics. That is, at any instant, electrons are not deposited into every channel covered by the beam, and a channel previously excited by an electron will have a considerable gain variation from event to event. In designing a CRT, writing speed is but one of the parameters that must be considered. The very large gain in writing speed provided by the MCP is useful in that part of it can be traded off in return for increases in resolution, bandwidth, and deflection sensitivity, and a reduction in unblanking requirements. The writing speed that remains after these tradeoffs is still good for use at several Gigahertz.

SCAN EXPANSION LENS (SEL)

The first CRT element behind the MCP is a variation on a classic quadripole design. The new design offers advantages in terms of both performance and manufacturing costs. The constraint of high bandwidth implies very low sensitivity deflection structures. However, the higher the bandpass of a CRT, the more sensitive the deflectors have to be. To achieve this, the CRT is generally made quite long and the scan relatively small. For the desired scan size and sensitivity of the T7100, the CRT, if made this way, would be over seven feet long. Of course this is not acceptable in a benchtop scope. Some novel techniques were used to shorten the actual CRT. One was the use of a scan expansion lens. Classic quadripole lenses have been used for scan expansion in several CRTs, including the Tektronix T7830. They are particularly advantageous when placed between the deflectors. The chief appeal of this lens can easily be analyzed mathematically. Its liabilities are the need for exacting alignment and dimensional tolerances and the small aberration free aperture to focal length (A/f) ratio off the axes of focus. In the T7100 the scan expansion lens is functionally a quadripole lens. Yet by deviating from the classic quadripole architecture, considerable improvements were made. This lens is far less critical with respect to dimensional and alignment tolerances. It has about triple the off-axis aberration A/f ratio, and allows one to correct a number of gain related geometry defects and to tailor the display linearity to very close specifications (typically one percent for most other CRTs). The deflection sensitivity in the negative axis of the lens can be adjusted over a range of about 20 percent. Another benefit of the scan expansion lens CRT compared to a long CRT is that the lens minimizes certain high frequency deflection artifacts stemming from the vertical deflector acting as a linear accelerator at very high frequencies.

The price of this improved capability and versatility is complexity. Whereas in its simplest form the classic quadripole requires only two potentials, this lens requires up to seven. In operation the SEL is a strong positive lens in the vertical axis and causes the beam to cross over or invert the vertical deflection. The vertical scan is expanded four and a half times. In the horizontal axis, the SEL is a negative lens, which merely enhances the deflection of the beam. The horizontal scan is expanded four times.

DEFLECTORS

The T7100 CRT employs traveling wave (slow wave or delay line) deflectors in both axes. These are helical transmission line deflectors where the velocity of the input signals along the helical conductors is equal to the speed of light, but the phase velocity along the length of the helix is nearly matched to the electron beam velocity as it propagates along the helix. The reason for a slight mismatch of velocities is a slight dispersion of the signal in the helix. That is, not all frequencies propagate down the helix at the same speed. To obtain the best compromise in both the time and frequency domain, the beam velocity must be slightly mismatched to the theoretical helix phase velocity (the velocity at which the power frequencies propagate). The dispersion of these deflectors is small, resulting in only a two percent mismatch of velocities. The phase velocity and thus the beam velocity is about $0.1c$ for these deflectors. The helix crosses the beam, not at right angles, but at an angle with a tangent of $1/10$. Thus, in the vertical deflector, each side of the beam is deflected by the same potential. As the signal propagates across the beam and in the horizontal deflector, all portions of the vertical scan are deflected equally. If the horizontal helix were not so inclined, there would be a twelve picosecond timing error between the bottom and top of the display, yielding a sweep speed dependent orthogonality error. The inclination of the helix in the vertical deflector eliminates beam defocus which otherwise occurs under high dv/dt conditions. Some high dv/dt defocus remains which is dependent upon the displacement of the beam from the horizontal center screen. This is the result of linear accelerator action upon portions of the beam by the deflectors. The effect is scarcely evident up to the 1 Ghz bandpass of the 7104 oscilloscope, but due to the outstanding triggering of the scope, one can observe the effect above 1.5 Ghz.

The horizontal deflector employs much the same construction and impedance compensating techniques as the vertical deflectors of the T7100 CRT. It also has the same impedance, 365 ohms. The horizontal deflection sensitivity is less than 2V/div (compared to 3V/div vertically and 7V/div horizontally in the 7904), and the bandpass is greater than 1.5 Ghz, allowing 350 Mhz response in the X-Y mode of the 7104. The vertical deflector is a novel modification of the internal groundplane structure. This is an extremely rugged, low mass high-percussion design that requires no impedance compensation. The structure can be mounted into an otherwise finished electron gun and is easily salvaged from rejected CRTs. The impedance is 200 ohms, line to line. deflection factor is less than 1V/div, and bandpass is about 3 Ghz. The vertical deflector and its groundplane are silver-plated to minimize skin losses. Connections to the vertical and horizontal deflectors are made through carefully spaced neckpins. The vertical deflector also employs strip-line leads between the deflector and the in/out neckpins. Both deflectors use external terminations.

ELECTRON GUN

While the gun design may appear complex, it is composed of simple parts. First, and immediately upstream from the vertical deflector is the beam limiting aperture. This contains the cross-sectional profile of the beam in a field free region, to provide maximum current while minimizing the acceleration effect of the vertical deflector on the beam. Ahead of the aperture, there is a dedicated astigmatism lens. Usually, the astigmatism lens is created by a potential difference between the focus exit (second anode) element and the adjacent deflection plates. But because of the exacting requirements of the intermediate spot images, and because the vertical deflector with its internal groundplanes is not the last of the astigmatic lenses, a special low aberration astigmatism lens was developed. This lens is designed to act as a positive lens in the vertical axis with no effect in the horizontal axis. This condition of vertical overconvergence results from the

requirements of the scan expansion lens. As noted earlier, the SEL is a strong positive lens in the vertical axis and a negative lens in the horizontal. If the beam is to be focused upon the MCP in the vertical axis a real line image of the cross-over must be formed before the SEL. In the horizontal axis, a vertical line image of the cross-over is required after the SEL. Thus the beam is always more convergent in the vertical axis and requires only vertical astigmatism control. In spite of considerably different optics the vertical and horizontal axis, the design maintains the same magnification of the cross-over in each axis to maintain a round spot on the screen.

The primary focus lens is of the classic Einzel configuration, but considerable effort was made to minimize aberrations of the lens in this application. Preceding the focus lens is a stigmator lens, which is an extremely weak lens used to make slight adjustments to the axis of astigmatism. Rotational alignment errors between the deflection axes and the scan expansion lens produces a slight orthogonality error, which is easily corrected by the rotator coil (wound on a form on the CRT neck) at the exit of the vertical deflector. Rotator coil correction disturbs the alignment of the axes of spot focus to the SEL, so the stigmator makes correctional rotational adjustments of the axes of focus.

Another device used to shorten the CRT is a crossover demagnification lens. This lens produces a real image of the crossover about halfway between the diode and the primary focus lens. The demagnification factor for the T7100 is 5 times, and the focus element for each operates at cathode potential. Since this lens operates in a demagnification mode, its aberrations are insignificant but it has the effect of increasing the magnification of the primary focus lens with the result of roughly doubling the aberration of that lens.

ION TRAP/VACUUM PUMP

The final innovative feature of this CRT is an ion trap/vacuum pump. This pump is incorporated into the structure of the first anode barrel. Gas ions which might normally damage the cathode are drawn out of the anode and deposited upon a gathering or gas adsorbing surface on the grid wafer. Since no change of operating voltages is required, this technique can easily be incorporated into other CRT types.

CATHODE

The cathode is a conventional oxide structure with a somewhat smaller than normal grid aperture. This is a proven design which provides more than adequate writing speed with 50 volts of unblanking. For further writing speed enhancement, the grid may be unblanked to over 70 volts. For easy reclaim of the gun or rebuilding of the entire CRT, the grid, cathode, and heater assembly can easily be removed or replaced intact.

Finally, in addition to the orthogonality coil wound on the neck of the CRT, a graticule alignment coil is wound on the envelope at the glass-ceramic interface. This permits the beam of the CRT to be aligned exactly with the horizontal graticule lines.

STORAGE TUBE BASICS

All storage tubes rely on the mechanism of secondary emission from a dielectric surface. In this chapter we shall study the principles of this mechanism.

The purpose of storage tubes is to record the movement (and in some cases the intensity) of an electron beam over a target area. In order to make the various parts of the target separately addressable, the target must be made of a dielectric material of such composition and construction that lateral leakage is kept to a minimum. The target should therefore be thought of as a collection of separate insulated points, and since it is insulated it can be described as "floating".

When a beam hits such a dielectric target, secondary emission can occur, due to the landing energy of the electrons, other electrons are knocked out of the target surface and collected by a nearby collector element. In order to do its job as a collector, its voltage has to be more positive than that of the target itself, but not so positive as to appreciably attract the primary beam electrons.

It stands to reason that when the electron beam lands with very little energy on the target it will knock out few, if any, secondary electrons. As the landing energy is increased, secondary emission will increase until, beyond a certain limit, the landing electrons hit the surface with such force and penetrate the material so deeply that more and more of the secondary electrons produced by the impact are trapped within the material instead of escaping. The landing energy of the electrons is determined solely by the potential difference between the cathode from which they originate and the target on which they land; it is not affected by intermediate accelerating and decelerating potentials.

If the landing speed is varied and the amount of secondary emission plotted, a curve with the general appearance shown in Figure 22-1 results. This is true of all dielectric materials, but the exact voltages at which the crossovers and peak occur depend on the characteristics of the dielectric material. The figures shown are typical for the dielectrics used in the tubes discussed in this text. (The slightly negative starting point of the curve is due to the thermal energy with which electrons are leaving the cathode.)

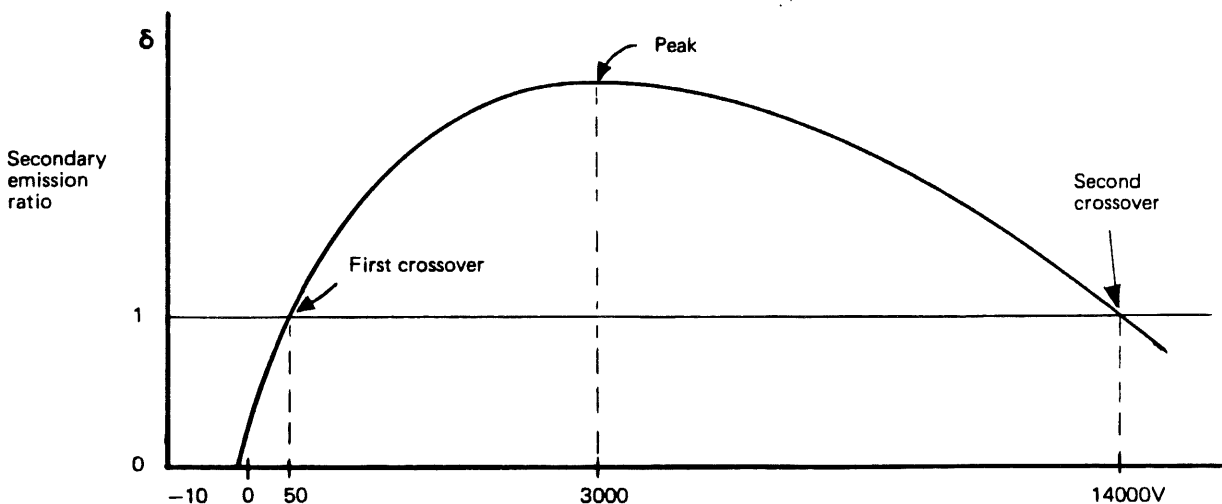


Figure 22-1

Secondary emission curves are generally shown in terms of the ratio δ of secondary emission to primary (or incident) beam. Such a presentation is valid and useful because, for a given target material and construction, the ratio does not change with the intensity of the primary beam, and plotting the curve in these terms brings out the essential points about secondary emission.

The line on the graph representing $\delta = 1$ is of great significance. Portions of the curve above it represent conditions under which the target loses more electrons by way of secondary emission than it gains, and conversely at points below this line the target gains more electrons from the primary stream than it loses. Since the target is in fact a dielectric, which is electrically floating, its surface voltage will drift up or down whenever there is an imbalance between the number of electrons landing and leaving. But before we go to the trouble of studying the effect of this voltage drift in detail we must look at two factors which will lead us to modify the shape of this curve.

First, we assumed that the collector was always slightly more positive than the target, so that any electrons liberated from the target would be attracted by it. But since the target is in fact an array of insulated and independent points, what constitutes the target? How could we measure it? And how could we make the collector always sit at a level slightly higher than the target? As a practical solution the nearby collector is simply held at a reasonable fixed positive voltage, typically 150 V. This will be sufficient to collect secondary electrons as long as the target voltage does not exceed +150 V. But if, for any reason, a point on the target does exceed +150 V the liberated electrons will tend to return to the target at the most positive element in the neighborhood. This does not in any way affect the basic secondary emission curve shown in Figure 22-1, but if our interest centers not so much on the electrons knocked out of the surface but on the net gain or loss to the target, then we have to redraw the curve at and above 150 V to show that at such voltages the target does not in fact lose any electrons because of secondary emission. The curve drops to a secondary emission ratio of zero. This can be seen in Figure 22-2.

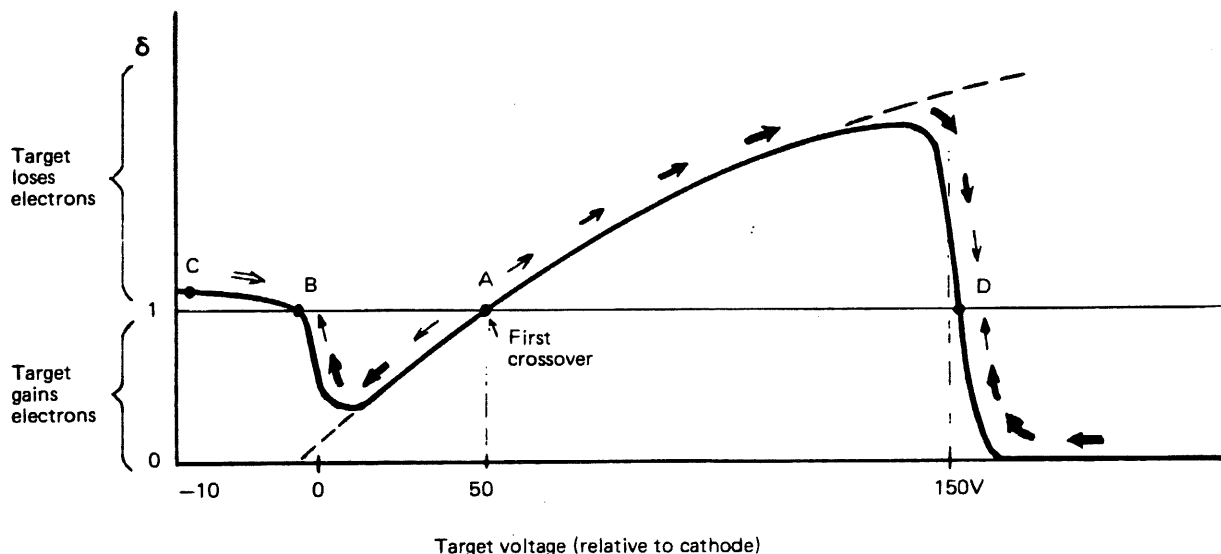


Figure 22-2

The second modification of Figure 22-1 occurs at the opposite end of the curve. Once the target voltage is below that of the cathode, the primary stream of electrons will not land on it any more but will go straight to the collector. Again this does not affect the validity of Figure 22-1. It is a fact that if any electrons did land they would land with zero energy and would be incapable of knocking off secondary electrons. But if we are concerned with the balance sheet of the target we will interpret the situation differently and say that since the target neither receives nor loses electrons and since therefore, in this trivial sense, the gains and losses exactly balance, we are dealing with a δ of 1. The way in which the new curve deviates from Figure 22-1 is again shown in Figure 22-2.

Figure 22-2, then, is not a curve representing the secondary emission ratio but one which plots the secondary emission yield (in other words the net gain or loss of the target) against the landing voltage of the primary beam. For simplicity, and to conform with literature, we will continue to label the ordinate δ .

A small point still remains to be explained: why the curve to the left of point B is shown slightly above the $\delta = 1$ line. If no electrons can land on the target because it is more negative than the cathode from which they originate, one would have expected the curve to remain at $\delta = 1$, representing neither gain or loss. In fact, within the stream of particles coming towards the target are occasional positive ions, and these will be attracted by the negative target and land on it. Since a gain of positive ions is equivalent to a loss of electrons, it must be shown on the balance sheet the same way as a loss of electrons—in other words, as if the secondary emission ratio were greater than one.

We can now return to the study of the voltage drift. The target is a collection of separate addressable points. As long as electrons arrive and leave in unequal numbers, these points will move up or down in voltage. A net loss of electrons, and therefore a drift in a positive direction, happens whenever the target voltage is in regions where the curve is above $\delta = 1$, and a net gain and negative drift in regions where it is below $\delta = 1$. This is shown by the arrows in Figure 22-2. Therefore, as long as the beam continues to hit a given target area, that area will charge in the direction of the arrows. If you study these directions for a moment, you will see that they converge on two points, B and D. These are the only two points at which the target can stabilize. (The target cannot rest at A since the unexpected gain or loss of a single electron due to noise will bring it under the influence of one or the other divergent trend.) B and D are called, appropriately enough, the lower and upper stable points.

The speed of the voltage drift is obviously a function of the amount of discrepancy between landing and leaving electrons.

Whenever the curve approaches $\delta = 1$, the movement will slow down, whereas in regions of large gains or losses the voltage will change more quickly. In Figure 22-2 we tried to make this point by varying the thickness of the arrows. The region between B and C is a special case. Drift in that part is due to the landing of positive ions rather than electrons, and since these are fewer in ratio of perhaps 1 to a million, the drift from C towards B is measured in minutes, compared with tens or hundreds of microseconds on other parts of the curve.

We said that this drift towards the stable states occurs in any part of the target, as long as that part has an electron beam directed towards it. Therefore, if the whole target were to be flooded with a defocused electron beam, all those portions of it whose surface voltage happened to set above A would move towards the upper stable point and the remainder towards the lower stable point, and under the influence of this floodbeam the target would be maintained at these points. This would give us a device capable of bistable storage of information in the form of a voltage pattern.

In order to be useful, we must of course have means of entering and deleting information-in other words, of writing and erasing-and we must make this voltage pattern visible. If the pattern becomes visible because of light emission from the storage tube itself, we speak of a direct-view storage tube. (The other method of making the pattern visible is by scan conversion: scanning the target with a reading beam which is then used to modulate some other light emitting device such as a TV picture monitor).

We will not discuss in this chapter how the pattern stored on the target is made visible in a direct-view storage tube. There are, as you know, two entirely different methods of doing this, which will be explained in later chapters. But with both methods it is convenient to use a higher target voltage for the written information and a lower one for the unwritten background. "Writing" therefore means lifting the target surface by means of a focused writing beam from a lower to a higher voltage-in the case of the bistable system, from the lower to the upper stable point.

How could this be done? Well, the target consists of a dielectric, and in order to increase the voltage of a given point on it we must cause that point to lose electrons. The only mechanism we have available is the one just studied: secondary emission. Writing beam electrons must arrive with enough energy to cause a secondary emission ratio of more than unity. The writing beam can only have so much energy if it originates from a cathode sitting at a considerably more negative voltage than the target. One could, in principle, stop the floodbeam, move its cathode sufficiently negative and focus it, then start writing on the target. Afterwards the flood condition could be re-established. (We shall see that in both types of storage tubes the floodbeam is the source of electrons which produce the visible stored display. In bistable tubes it also has the vital function of maintaining the written and unwritten parts of the target at their respective stable points as explained earlier.

In practice it is found simpler to use two separate guns in the same CRT envelope: a permanently defocussed floodgun, which maintains a floodbeam at all times, and a separate focussed writing gun, operating at a much more negative voltage, whose electron beam is controlled by a control grid in the normal manner.

When writing the target area, the writing beam action is initially opposed by the continuing floodbeam action. The target voltage will only move positive if the number of electrons lost due to greater-than-unity secondary emission of the writing beam exceeds the number of electrons gained from the lower velocity floodbeam. This will be considered in more detail. Once the target has moved above the first crossover point, the floodbeam will of course assist the writing beam in moving the target further positive.

Finally in this chapter, let us consider how this information could be erased after it is written. This involves moving all those areas of the target which are written back to the unwritten level. The target itself is, as we keep saying, floating. But the dielectric is in fact mounted on some kind of conducting surface, and if a negative pulse is applied to this surface, capacitive coupling will also move the target as a whole, negative by this amount. Once all points of it have been lowered below the first crossover, the continuing floodbeam will see to it that the target is then maintained at the lower stable point. This description of the erase process is only a preliminary one. The erase pulse is in fact more complex to take care of additional problems, and we shall look at these when discussing the two tube types in detail.

BISTABLE PHOSPHOR— TARGET TUBE CONSTRUCTION

We mentioned in the introduction that direct-view storage tubes fall neatly into two types, depending on the means adopted to make the stored pattern visible. These types are the phosphor-target tube and the transmission tube. In the first case the target dielectric is made of phosphor which will light up in the written areas and be looked at directly by the eye. In transmission tubes, on the other hand, the target forms a mesh which controls the flow of the CRT beam on its way to a conventional phosphor screen, acting much like the grid in an ordinary vacuum tube.

The earliest phosphor-target tubes had poor definition and an extremely dim display. This led designers to concentrate on transmission tubes. They on their part suffered from lack of reliability and were expensive to manufacture. Then Tektronix engineers returned to the phosphor-target idea and managed to refine it into a practical product. Their phosphor-target tubes represented a breakthrough in price and simplicity. They first entered the market in the type 564 oscilloscope in 1963 and are the subject of Tektronix patents.

The basic idea is simple enough: if phosphor is used as the dielectric in a bistable system such as we described, then the stream of flood electrons hitting the written areas with an impact speed equivalent to the 150 volts or so of the upper stable point will produce a light output, whereas the unwritten areas at the lower stable point receive no floodbeam electrons, or if they did the landing energy would be virtually zero, causing no light emission. This phosphor target will therefore continue to emit light from the written area as long as the floodbeam is present.

But there are of course problems. First, the phosphor must be suitable as a dielectric, which means it must offer a high secondary emission ratio and possess good insulating properties. The most efficient phosphor, P31, does not have these qualities; we generally use a modified form of P1 with about half the efficiency of P31, which means a dimmer trace. Furthermore, with the phosphor target at about 150 volts, compared with the more usual several kilovolts, the trace brightness is again appreciably reduced. Nevertheless, under subdued lighting conditions it is still a usable display.

Then there was the problem of poor definition in early tubes. This was traced to the lateral spreading of the written area after the passage of the writing beam, due probably to inadequate lateral insulating properties of the phosphor. Our solution was to deposit the phosphor either as a pattern of finely spaced dots or to lay it down as a layer of randomly arranged semicontinuous particles with the aim of preventing lateral leakage between areas.

The particles, whether regular dots or of random shape, must of course form a pattern so fine that the width of the focussed writing beam will cover several of these target elements. In this way the limits of definition are dictated by the fineness of the writing beam only.

You will remember that bistable target operation depends on a nearby collector to collect secondary electrons. This discontinuous nature of the phosphor deposition allows us to use the conducting film on which the target is deposited (Storage Target Backplate in Figure 23-1) as a collector. This film is so extremely thin that it appears to be transparent, so that light emitted from the phosphor can be seen through it by the observer. Secondary electrons knocked off the target will therefore be attracted through the gaps in the phosphor to the higher potential collector.

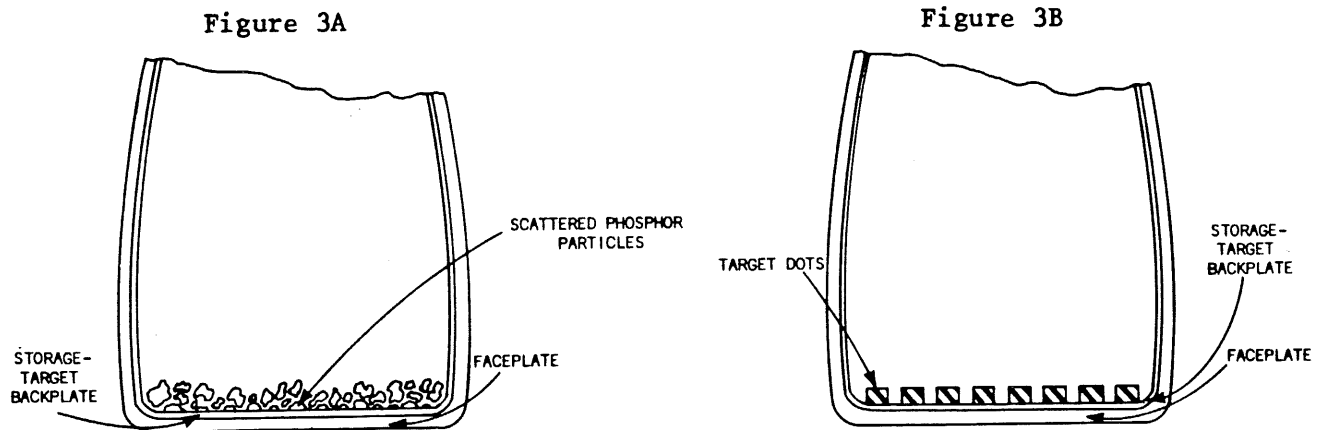


Figure 23-1

Perhaps we should consider briefly why the primary stream of flood electrons does not itself go directly through these gaps to the collector, thus defeating the whole purpose of the arrangement. The reason is that the flood electrons arrive with a fair amount of kinetic energy and are not easily diverted at the last moment to the minute gaps between phosphor particles. By contrast, secondary emission electrons have much lower energy and therefore move at much slower speed, which makes them more maneuverable. It is, incidentally, the difference between the high energy of the landing electrons and the lower energy of the secondaries which gets converted into heat and light emission from the phosphor.

Let's pause at this point to summarize briefly what we have learned of phosphor-target storage tube construction and operation. These tubes have a target composed of phosphor which can be written, i.e. lifted by a writing beam to a higher potential and will then attract electrons from a floodbeam whose landing energy is partly converted to light and partly used to dislodge secondary electrons. The secondary electrons find their way through gaps in the target to the storage target backplate which acts as a collector. The floodbeam is therefore used in the first place to make the written areas visible, but it also has the effect of shifting the target from whatever voltage it may have been left at by the writing beam or erase pulse to the upper or lower stable point, making this storage tube a bistable one. The beam originates from a floodgun and is deliberately dispersed to cover the whole target area. The writing beam comes from the writing gun which is so negative with respect to the target that when the writing beam lands it causes much secondary emission, thus lifting the target voltage. The writing beam is intensity-controlled, focussed and deflected in the normal manner.

With this basic picture in mind we must now go a little more deeply into the problems of target construction, since this will considerably increase our understanding of storage tube behavior. These are problems which are of concern at the design stage, but also have important effects on operating characteristics.

A suitable target material must be chosen. Then it must be decided whether to deposit particles according to figure 3A or 3B. In the first several years that Tektronix manufactured bistable storage tubes the semicontinuous method shown in figure 3A was predominantly used. More recently the target deposition process shown in figure 3B has become the most widely used technique. Having decided which material to use and which target deposition method to use we can then begin the process of optimizing the processes or materials to obtain the performance desired.

As target thickness increases a number of factors are affected in a beneficial way. Luminance increases fairly linearly, since the presence of additional material (and the higher operating voltage that this permits) generates additional light. Resolution increases rapidly at first: when the target is only molecules thick, wide spaces exist between particles and these fill in as thickness increases. Predictably, once a certain thickness has been reached, the increase in resolution levels off. But perhaps the most significant improvement resulting from greater target thickness is the increase in contrast, as shown in Figure 23-2.

Against this catalog of benefits resulting from increased target thickness we must set one factor which, after reaching a peak, decreases again. This is the stable range of collector operating voltages, and to understand what it is, and why it is so important to us that we sacrifice a great deal of contrast to it, we must consider one aspect of this storage tube which has been ignored to this point: the possibility of leakage from the target surface to the backplate on which it is deposited.

In unwritten screen areas there is in fact some leakage through the target, to the collector, which sits at a high positive voltage, lifting the phosphor surface above the lower stable point and causing a slight amount of light emission because of the increased landing energy of the floodbeam. It might seem to contradict basic theory that the target can rest at a point above the lower stable point, since the secondary emission ratio is then less than unity and it ought to gain electrons, but this effect is balanced by the migration of electrons through the target to the collector.

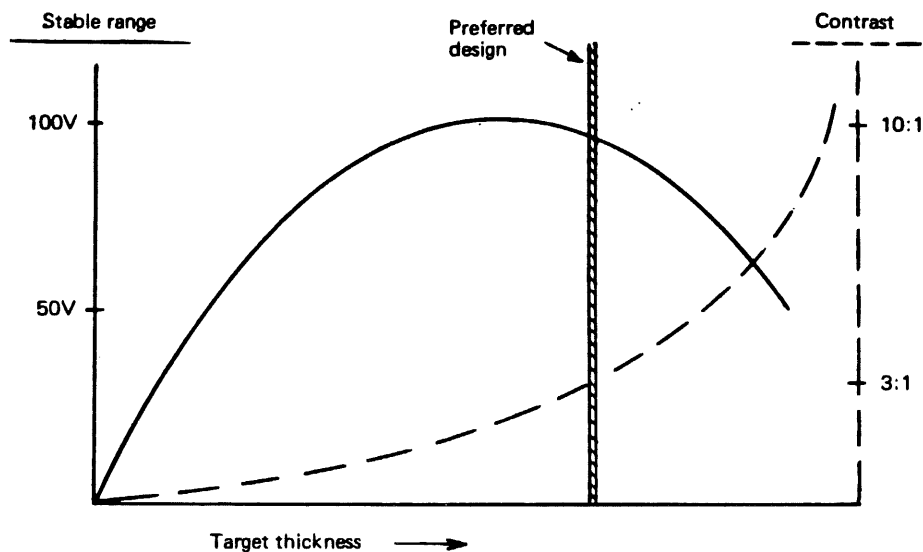


Figure 23-2

The amount of leakage will vary from point to point across the screen, since the phosphor layer is randomly semicontinuous, but some leakage will be observed almost everywhere and we can surmise that the rest potential might look something like the solid line RP in Figure 23-3. This will cause light emission to vary across the screen in a correlated manner. From normal viewing distances these variations average out and we simply observe an average background light level, corresponding to the average rest potential (ARP).

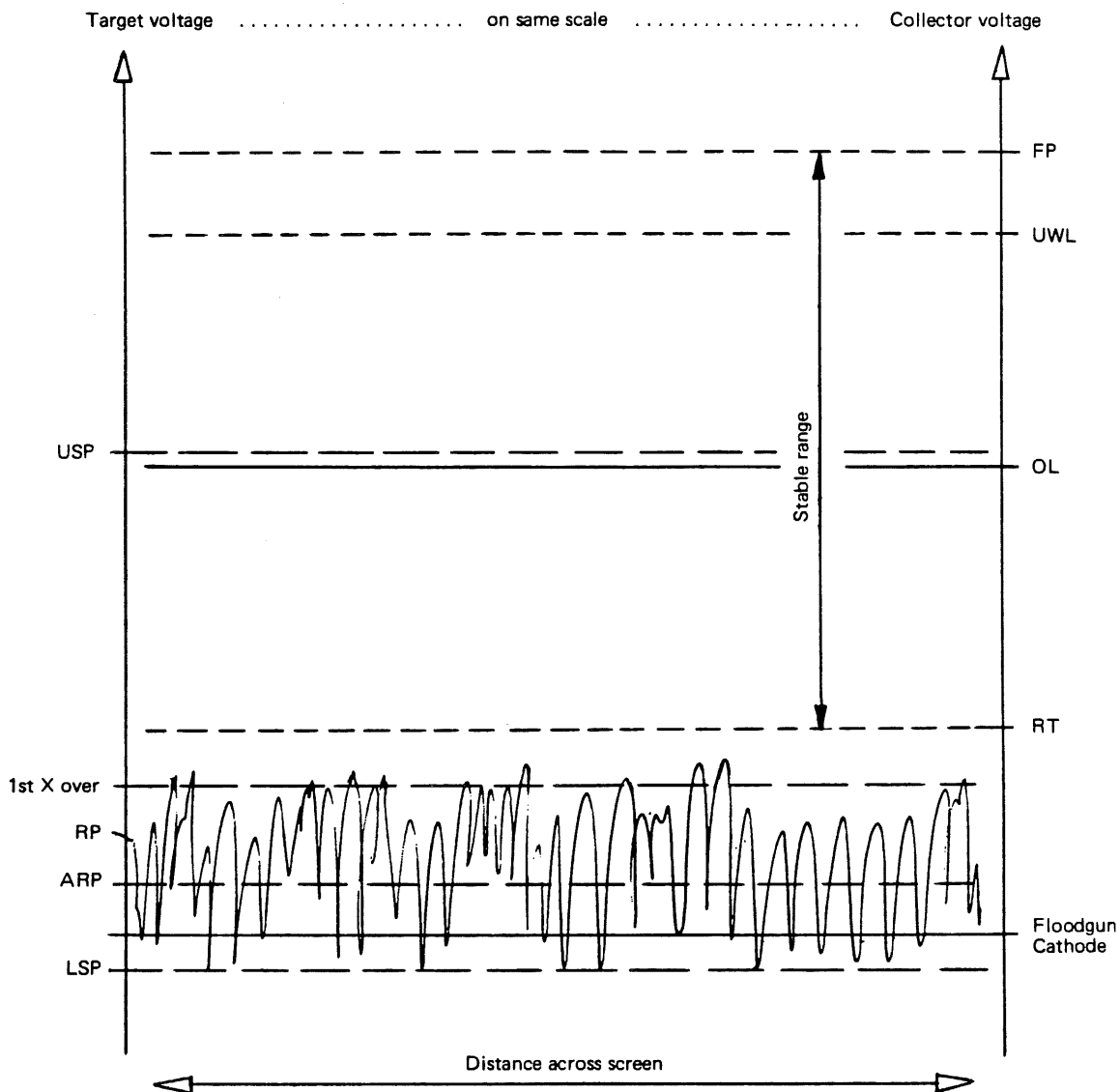


Figure 23-3

The solid line RP is no more than an artist's impression, but given such wide variations across the target, some points will inevitably exceed the first crossover level, and these points will therefore move to the upper stable point, a process which is often called "fading positive". Being individual, randomly distributed bright dots on a microscopic scale we can again see only their contribution to the average background light level.

Although on theoretical grounds one might wish to exclude these written dots from the calculation of the average rest potential, in practice this is not possible. The average rest potential is a purely theoretical value which cannot be measured directly since the target is floating. We assess the average rest potential on the basis of average light emission, and when making such light measurements we are bound to include the written dots as well as those in various unwritten states.

The full picture, then, is that dot by dot across the screen the rest potential varies in a random manner, causing a corresponding slight light output, with the exception that all those dots which happen to exceed the first crossover level will fade positive and emit the written light level. Only the average of all these light contributions can be perceived on a macroscopic scale, and from this average light level we can deduce the average rest potential.

The situation is illustrated in Figure 23-3, in a purely qualitative way, for the condition where the collector voltage is set to a typical operating level. Naturally, as the collector voltage is varied up and down, the amount of leakage also varies and the RP curve will shift up and down to some extent.

If we set the collector to increasingly positive levels, a point will be reached where spreading of the written trace occurs because areas adjacent to it are so near the crossover that capacitive effects or local dielectric breakdown are sufficient to make them fade positive. This collector voltage is known as the upper writing limit (UWL). At some still higher level, so much of the RP curve lies so near the first crossover that the whole screen will spontaneously fade positive. Both the collector voltage levels are shown in Figure 23-3.

Turning now to the consequences of decreasing the collector voltage below the operating level, we must recall that the upper stable point of the target always occurs at a voltage in the vicinity of the collector voltage, since it is the failure of the collector to collect which causes the abrupt drop in the target "balance sheet" curve of Figure 22-2. Now if the collector is lowered to the vicinity of the first crossover voltage, this will result in a curve as shown in Figure 23-4, and it is clear that under these conditions there is only one stable point, the lower stable point. The floodbeam will return all target areas to the lower stable point; written information is no longer retained. This collector voltage is therefore called the retention threshold.

Now we can define the stable range: it is the range of collector operating voltages between retention threshold and fade-positive. It is this stable range which is affected by the thickness of the target in the manner shown in Figure 23-2. In itself it will not concern us operationally, since we would be unwise to operate the collector near either of these extreme limits. But a large stable range will obviously provide a greater operating margin for the collector voltage. This margin is important to us for several reasons:

1. Setting the collector voltage operationally to the center of this range is a subjective procedure which will yield a certain spread from operator to operator;
2. In many instances the CRT heater is unregulated, and varying line voltages can cause performance changes (this is not as much of a concern in newer instrument designs as it was in earlier instruments);
3. Storage CRTs are subject to aging effects which might, if the operating margin is too small, require frequent recalibrations.

4. Even with the best manufacturing techniques there is usually some non-uniformity across the target, calling for different optimum collector voltage settings, and in the presence of a large operating margin the choice of a suitable compromise setting is much easier.

For all these reasons we consider a large stable range so important that we sacrifice much contrast to obtain it, as suggested by Figure 23-2.

When contrast was first mentioned as a significant factor in connection with Figure 23-2 you may have been puzzled since it is normally taken for granted in oscilloscopes that unwritten areas of the screen are practically black and the contrast therefore practically infinite. The discussion of the average rest potential will have explained why, on phosphor-target storage tubes, the contrast is quite limited. But although Figure 23-2 shows a typical contrast ratio of only 3:1, some improvement can in fact be expected after a few hundred operating hours. The reason is that much background light is contributed by those dots which have faded positive, and as these phosphor dots operate continually at full light output they will be the first to age and eventually turn dark, leaving the unwritten part of the screen much darker. On most tubes the contrast ratio will reach 20:1 after about 500 hours. Contrast ratios in the order of 100:1 are possible after several thousand hours of operation.

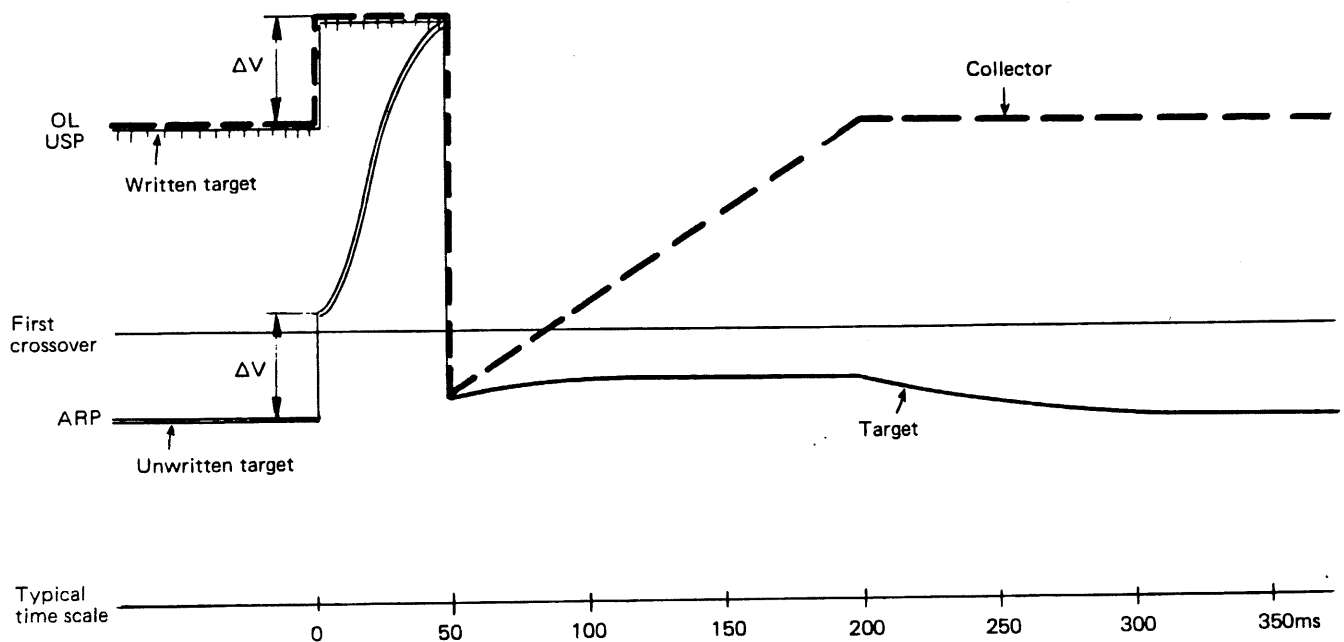


Figure 23-4

OPERATING CHARACTERISTICS OF THE PHOSPHOR-TARGET TUBE

One of the main limitations of a storage tube is its inability to store traces if the beam is moving too fast—if it exceeds the maximum writing speed. The bulk of this chapter will be concerned with the definition of writing speed, what factors influence it and how it can be improved. Then we shall return to the topic of erasing and see in detail how it is done.

In a bistable tube, writing, as we know, is the process of raising the voltage of those points on the target which are scanned by the writing beam above the first crossover despite the continuing attempts of the floodbeam to return them to the rest potential. (Once the critical first crossover level has been passed, the floodbeam will carry them to the written level even without any further contribution from the writing beam.) The effect of the floodbeam is to add a given number of electrons to unit target area in unit time. But this number depends on the secondary emission ratio and is highest where the “balance sheet” curve departs most from the $\delta = 1$ level, trailing off to zero as the first crossover is approached. Since we can neither measure the secondary emission in an actual CRT, nor even be sure from what rest potential the target must be lifted, it is impossible to quantify the demands made on the writing beam if it is to achieve storage.

But the effect of the writing beam itself is also far from straightforward. Consider first the situation of a stationary beam. Even though it is focussed, the spatial distribution of beam intensity follows the normal Gaussian distribution curve shown in Figure 24-1. At the point on the target where it peaks, the beam density per unit target area is greatest, hence the number of secondary electrons lost in unit time is highest.

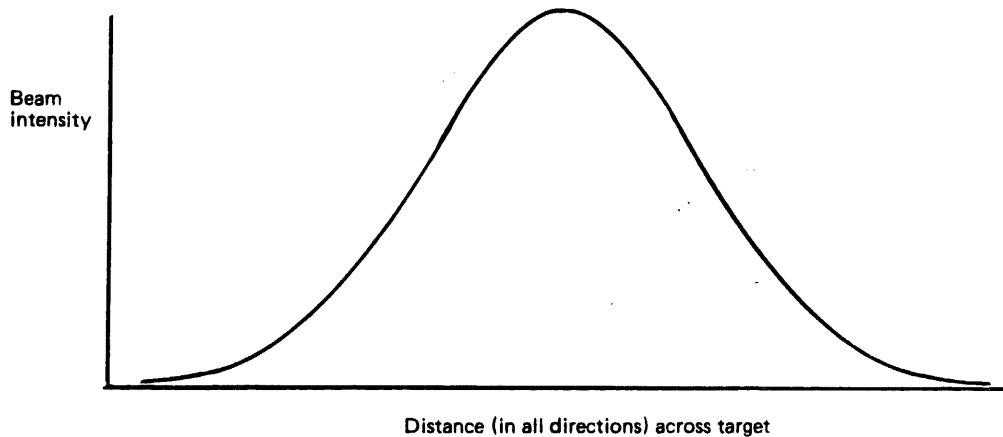


Figure 24-1

If this number exceeds the number gained from the floodbeam action the target will begin to charge up. However, the charging process takes time and relies on the continuing presence of the writing beam if it is to reach a successful conclusion, namely that the target voltage passes the first crossover. With greater beam density, the disparity between electron loss due to writing beam and gain due to floodbeam increases and a shorter beam dwell time is enough to achieve storage.

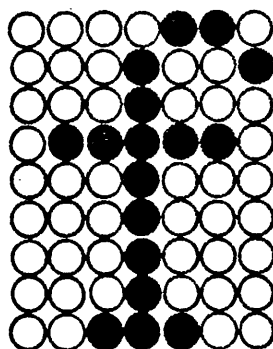
Away from the center of the writing beam, since the beam intensity decreases, the number of electrons lost per unit time by the target will also decrease. As long as it is still greater than the gains made from floodbeam action, the target will still move positive, but it will require a longer beam dwell time to reach a successful conclusion.

Let us review the picture given in the last three paragraphs, and assume for simplicity that the target rest potential is at point B of Figure 22-2. To achieve storage, the requirement is that the center of the writing beam (where its intensity is greatest) should cause the target to lose more electrons per unit time than it gains from the floodbeam, and that the writing beam should dwell long enough at that spot to cause the resulting positive target drift to reach the first crossover. We can instinctively feel that something like the product of dwell time and beam intensity is significant here, but there is a certain minimum intensity below which no amount of dwell time will achieve storage because the target gains more electrons from the floodbeam than it loses from the writing beam. It would be misleading to try to quantify this complicated situation in a formula, but we will refer to the dwell time-intensity product in this loose sense later in the text.

One last consideration, if we start with the minimum dwell time and beam intensity which will just achieve storage at the beam center, and then increase either factor, areas away from the center of the beam will also manage to reach the first crossover. As dwell time or intensity are increased we therefore obtain a stored dot of increasing diameter.

A stationary beam such as we have discussed is typical of information display devices. For instance, a computer readout monitor might display alpha-numeric characters, each of which is made up of selected written dots in a 7 X 9 dot matrix. Figure 24-2 shows an example.

If we want to specify the minimum requirement to achieve storage, we generally adjust the beam intensity to the maximum value before defocussing occurs, and then measure and quote the necessary dwell time. This specification is called "dot writing time", and a typical value is 5 microseconds or less. You will appreciate that the beam intensity setting is a somewhat subjective adjustment.



Lower-case f in a dot matrix

Figure 24-2

In oscilloscopes, the beam is normally moving and we must now study this new situation. If a given spot on the target lies in the path of this beam, then as the beam approaches, its intensity will increase in a manner which corresponds to the slopes of the beam current distribution curve. It will reach a peak when the beam is centered on the spot, and then decrease in a similar manner. But whether storage will take place depends on the same considerations which we enumerated previously, i.e. whether the maximum beam intensity is great enough and the dwell time is long enough. In this situation quantitative analysis is even more futile. Specifications are verified by again selecting the highest beam intensity before defocussing occurs, and increasing the beam velocity until the beam moves so fast that there is insufficient dwell time for storage to occur. This specification is called "writing speed" and is typically, for phosphor-target tubes $0.1 \text{ cm}/\mu\text{s}$.

For the moving beam we can say that if the dwell time is made longer by moving the beam more slowly, areas to the side of the central path of the beam will receive a sufficient dwell time-intensity product to become written. As the beam is slowed down we therefore get a progressively wider stored trace.

At the end of this discussion we hope that you will have an instinctive feeling for the principal factors affecting dot writing time and writing speed. We will now consider in what way the writing speed, and also the brightness and contrast of the stored display, are affected by the collector operating voltage.

The published specifications assume that the collector operating level (OL) is set normally, let us say to the center of the operating stable range in Figure 23-3. As we increase the collector voltage, leakage increases, the average rest potential increases, and consequently the target rests nearer to the first crossover. This means that a lesser dwell time-intensity product will suffice to achieve storage; holding the intensity constant we can increase the beam velocity and still store. The writing speed specification has been improved. But the improvement is not spectacular and the change of collector voltage has other side effects which are more important and which we will look at shortly.

If the collector voltage is decreased the opposite effect takes place. The ARP drops and the writing beam must linger longer to achieve writing. In fact, for a specified beam velocity, if the collector voltage is decreased sufficiently, a level will be reached at which the dwell time-intensity product is no longer enough to achieve writing. This collector voltage limit is called "writing threshold" (WT). Unlike all other collector voltage limits (FP, UWL, RT), this one is not a limit due to basic construction features of the tube; it is dependent on the beam velocity which we specified.

For such a specified velocity, the writing threshold represents the lower limit of the collector voltage operating margin to which we referred earlier. Neither can we operate successfully above the upper writing limit since trace spreading occurs. This defines the collector operating range and is shown in Figure 24-3. A writing speed specification is only realistic if it puts the writing threshold in approximately the position shown in Figure 24-3, giving a usefully large operating range (typically operating range is $>10 \text{ V}$).

Now to the other effects of departing from the normal collector operating level. We said that as the collector voltage is raised, the ARP goes up. Therefore the light level of the unwritten area will increase. But also, since the upper stable point follows the collector voltage up, the brightness of the written trace increases. The converse is true when the collector voltage is decreased. We must now consider whether, on the average, these effects produce traces with more or less contrast, and whether, if we have a choice, it is important to get the maximum possible contrast or the maximum possible absolute light output. (Contrast as defined here means the brightness ratio of written to unwritten areas.)

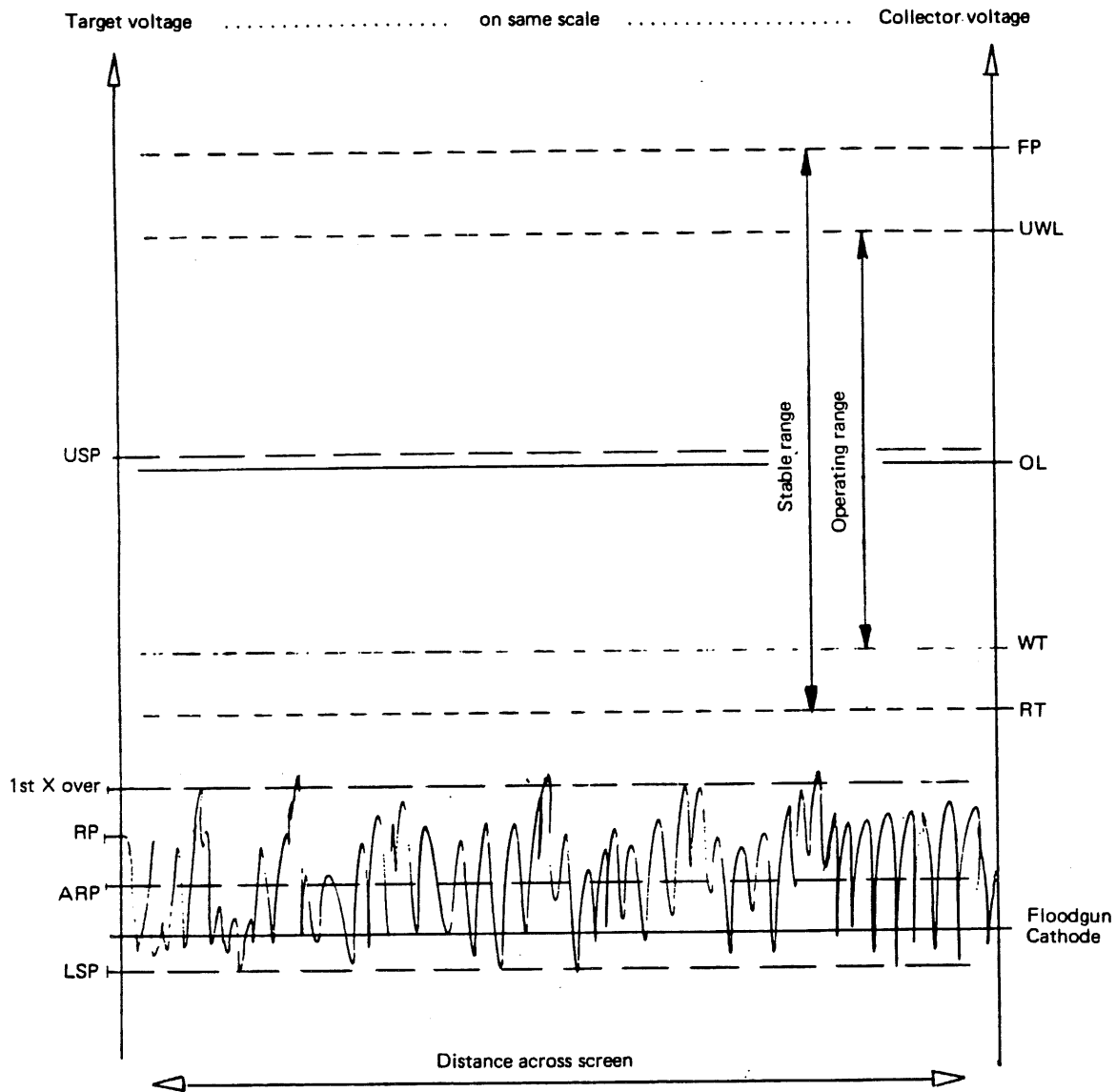


Figure 24-3

The simplest way to study this matter is by way of a numerical example. The figures in table 1 have been chosen for convenient mental arithmetic, but they are typical for the actual performance of phosphor-target tubes. The set of figures headed "in total darkness" shows the actual light output of the CRT. As you can see, the brightness of the unwritten areas increases more rapidly with increased collector voltage than the brightness of the written trace, so the contrast gets poorer. In the next two sets of figures, 6 and 100 candela /m² respectively have been added to the CRT light output figures to show what happens when these amounts of ambient light are reflected from the CRT. The contrast decreases, but it decreases least if the CRT light output is high, because the ambient light cannot swamp out the tube light as easily.

Collector Voltage	in total darkness			with 6 cd/m ² ambient light			with 100 cd/m ² ambient light		
	written trace cd/m ²	unwritten areas cd/m ²	Contrast	written trace cd/m ²	unwritten areas cd/m ²	Contrast	written trace cd/m ²	unwritten areas cd/m ²	Contrast
100 V	24	4	6 : 1	30	10	3.0 : 1	124	104	1.2 : 1
140 V	50	10	5 : 1	56	16	3.5 : 1	150	110	1.4 : 1
180 V	80	20	4 : 1	86	26	3.3 : 1	180	120	1.5 : 1

Table 1

Which is preferable? To see the trace at all, we need contrast and the more we have the better. But it turns out that for different ambient lighting conditions different collector voltages will give the best contrast, so no hard and fast rule is possible. Photography, of course, takes place in total darkness as the camera shuts out all ambient light, and would therefore benefit from a low collector voltage.

It has already been said that the improvement in writing speed which can be achieved with higher collector voltage is only marginal. There are two other techniques, however, which are capable of increasing the writing speed by a factor of 10 or more. These will now be discussed.

To understand how they work, we must first visualize what happens when the beam moves faster than the maximum writing speed and fails to store. In such a case, the dwell time-intensity product is not enough to raise the target voltage above the first crossover, and as soon as the writing beam has passed, the floodbeam begins the destructive process of moving the target back to its rest potential. Nevertheless, the writing beam did raise the target above the rest potential. The secret of the two techniques is to make use of this charge pattern before the floodbeam destroys it.

The first technique is useful on repetitive sweeps, and is called the "integrate" mode. By stopping the floodbeam altogether, the destructive process can be halted. Any charges laid down by the writing beam will remain on the target, if not indefinitely, at any rate for minutes. If the signal is repetitive, successive beam sweeps will scan the same target areas and will add to the charge pattern. This is a cumulative process which must eventually lead to the point where the written target areas cross the first crossover point. If the floodbeam is then restored it will move these areas to the written state and the trace can be seen.

For a given beam velocity it will take a given number of beam sweeps to build up this charge. We have already seen that these factors are not amenable to numerical analysis. In practice it is a matter of trial and error to find out how long the integrate mode has to be applied before a trace gets stored. There is unfortunately no way of knowing, while the mode operates, whether storage will be achieved, since without the floodbeam we cannot see a stored trace. When integration is stopped, and by the time we have inspected the display and perhaps decided we didn't integrate long enough, the portions of the trace which failed to write will have been moved back to rest potential. Any second attempt at integration will therefore be starting again from square one.

But imagine now that we wish to store a single transient, some unique event, at a speed exceeding the normal writing speed. Since we cannot repeat the event, the integration technique is useless. Yet even that one sweep did leave some charge behind. The second technique, called "enhance" mode, again attempts to salvage the situation. A positive pulse is applied to the collector, of such amplitude that capacitive coupling will lift the whole target by just the amount needed to bring the written area above the first crossover. Figure 24-4 makes this clear. The floodbeam will then immediately set to work separating the written and unwritten potential further. We maintain the positive pulse long enough to ensure that at its end the written areas do not drop back below the first crossover.

The curvatures recall the fact that the floodbeam is most effective at voltages where the secondary emission ratio departs most from unity, and floodbeam action slows down as a δ of 1 is approached.

Figure 24-4 also makes the point that immediately after the beam passage the floodbeam starts removing the laid-down charge. The enhance pulse must therefore be applied as soon as possible—in other words, as soon as the sweep is completed. But on slow sweeps, say $5 \mu\text{s}/\text{div.}$ or slower, even this may be too late. The enhance pulse will only rescue the later portions of the trace while those near the beginning of the sweep will already have been partly or wholly destroyed by the floodbeam.

Nevertheless, if enhancing were that simple one would have to ask why the technique is not made a permanent feature of fast sweeping storage, giving at a stroke a tenfold improvement in writing speed. But Figure 24-4 is oversimplified in an important aspect. The average rest potential is a fictitious level, and the actual target rests over a broad range of levels. When the writing beam adds a charge to this, the written areas, too, will end up over a broad range of levels. There will therefore be no one correct amplitude of enhance pulse which can raise all the written, and none of the unwritten areas above the first crossover.

In fact, the smaller the charge left behind by the writing beam, the more likely it will be that even with optimum enhance pulse amplitude some written parts will remain unstored, and some unwritten parts will become stored. The exact amplitude then becomes a matter of experimentation until the user subjectively feels that he has achieved the best compromise, making for the clearest display.

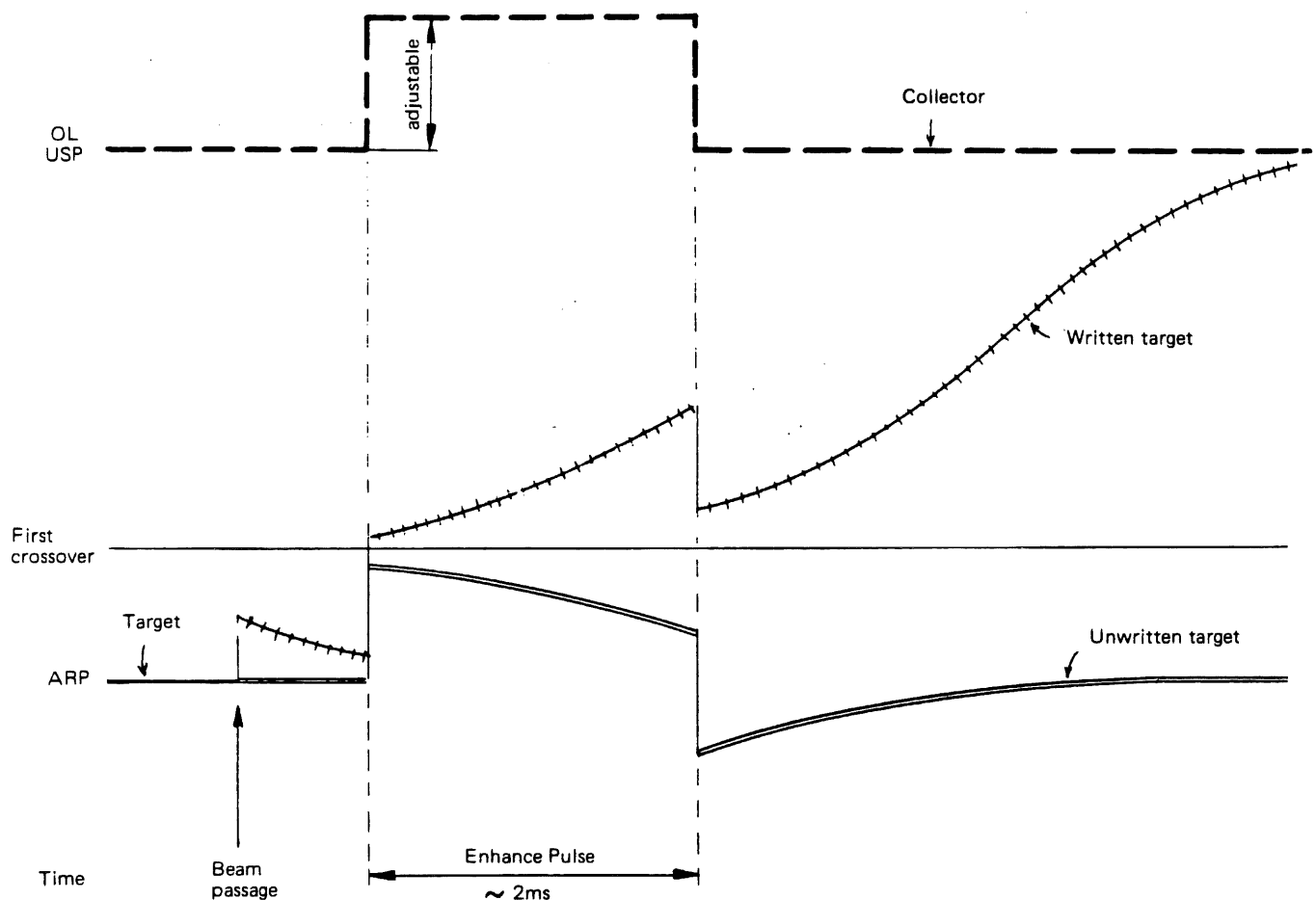


Figure 24-4

When we said that the enhance technique allowed a tenfold increase in writing speed, this was meant as a guideline only. In any given situation it depends on the kind of compromise the user finds acceptable. By contrast, the integrate technique really has no upper speed limit; it just depends on whether you can afford enough time to integrate long enough to accumulate enough charges to reach the first crossover. In cases where the signal repetition rate is 1 Hz or so and the required sweep speed is very fast, this can become a question of operator patience.

The next topic in this section is the erase process used in phosphor-target tubes. Basically, the erase pulse is a negative pulse applied to the collector, which capacitively moves the whole target negative. The aim is to move the written portions from the upper stable point to below the first crossover, after which the floodbeam can complete the erasure. But there are two problems. The first arises from the fact that sooner or later we will have to return the collector back to its normal operating level, and if we do this too fast we will capacitively move the target back up. This is true even if the negative pulse was long enough to give the floodbeam a chance to stabilize the target at the rest potential, because the voltage separating rest potential and first crossover is much smaller than that between first crossover and operating level through which the collector must move. The solution is to make the trailing edge of the erase pulse so slow that any capacitive coupling effects on the target can be countered by floodbeam action.

The other problem with erasing is that when small written areas are surrounded by large unwritten areas, and the target is capacitively lowered, the unwritten areas will move to a potential which is so greatly negative that the floodbeam is totally repelled from the target. The small written areas are in effect then shielded from the floodbeam and not returned to rest potential. At the end of the erase pulse they can easily become written again. Since small written areas among large unwritten ones are typical in normal storage tube use, this cannot be tolerated. Shielding effect of this kind can be avoided if the whole target is first written and then the erase pulse applied. So the erase pulse proper is preceded by a so-called fade-positive pulse large enough to lift the unwritten areas above the first crossover (V in Figure 24-5). Figure 24-5 shows the complete sequence.

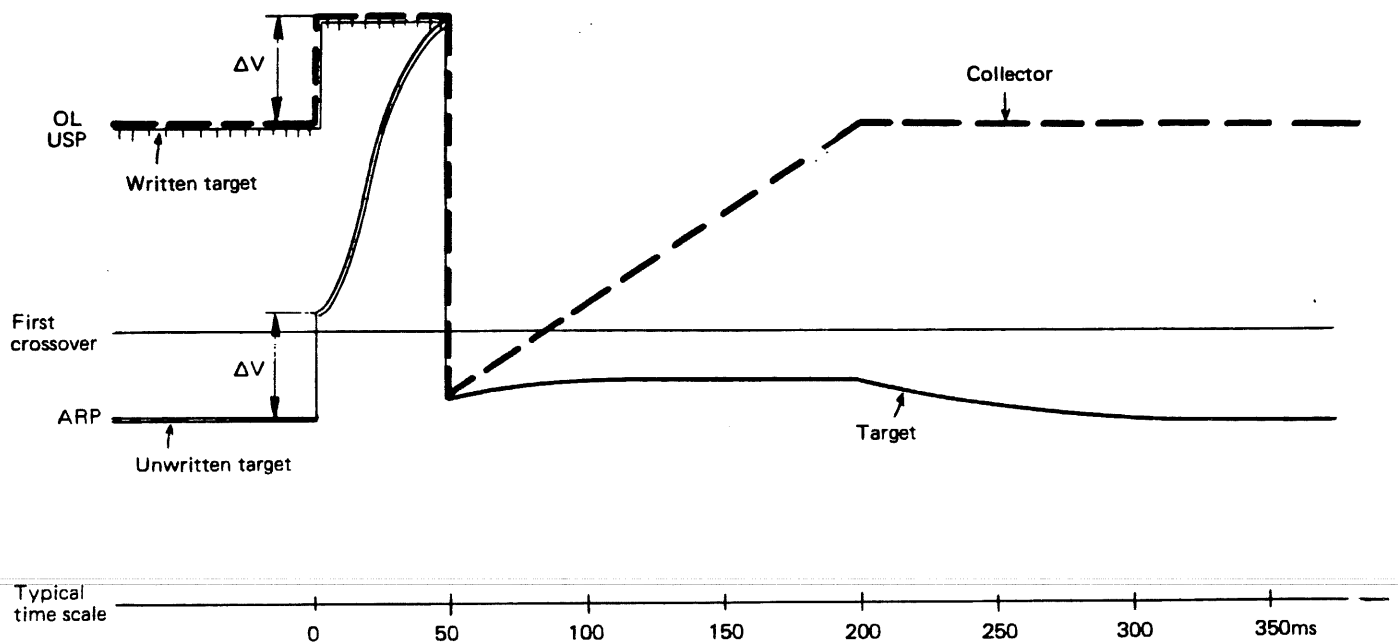


Figure 24-5

It sometimes happens that after the prolonged stored display of a trace the target resists erasure. During such periods the charge pattern becomes buried deep inside the target, rather than just on its surface. This is not to be confused with a phosphor burn in a conventional tube, where the phosphor is permanently damaged due to excessive heating of the phosphor during the passage of an intense writing beam. But though the phosphor is undamaged, unless the buried charge can be removed, an irritating residual image will remain. In the first place, to avoid buried charges, most instruction manuals give a time limit for storage, typically 1 hour. But if a buried charge does appear, and cannot be cleared by repeated erasures, the whole target may be written and left in this state for about 10 minutes, after which erasure should be successful.

The stored time limit just mentioned serves another purpose. As we said earlier, dots which sit at fade-positive for prolonged periods will obviously be the first ones to burn the phosphor. Parts of the screen which are frequently written will become dimmer and the tube will eventually fail for writing speed or poor appearance. One should avoid displaying the same waveform in the same position day after day. Second, it would be prudent for this reason to limit viewing time to no longer than is necessary.

An alternative solution is to reduce the floodbeam. This will result in a dimmer display and reduce the aging process somewhat but may still be sufficiently bright to be useful. Some oscilloscopes have a storage brightness control with which the floodbeam can be adjusted between 100% and 10%. (At the lower end, the floodbeam is so weak that it allows the target to accumulate charges from successive sweeps as in the "integrate" mode, provided the sweeps follow one another at intervals not much longer than 1 ms.) On information display monitors, viewing time at full brightness is often limited to 90 seconds, after which the display automatically goes into a low-brightness standby condition until the operator requests another viewing period. This condition is called the "hold" mode.

This completes our description of the storage characteristics of the phosphor target tube. But a word is in order about using it in the non-store mode. To stop the storage effect we simply have to set the collector below retention threshold. The tube then behaves like a conventional non-storage tube. No matter how high the writing beam charges the target, in a matter of milliseconds before the eye can see it the floodbeam returns it to the rest potential. With the collector below RT, leakage will be very small and the average rest potential so low that the screen is completely dark.

BISTABLE STORAGE OSCILLOSCOPE FEATURES

It is not the purpose of this booklet to list in detail all the features of bistable oscilloscopes. Users of such instruments will have a manual with full details, and intending purchasers will mainly want to study specifications sheets. A specific comparison chart of Tektronix storage oscilloscopes is given in appendix B. In this chapter we shall briefly look at some special techniques offered by many-but not all-bistable instruments. These are split-screen operation, write-through, locate mode and automatic erasure.

Split-screen operation is a technique where the storage target backplate, the collector, is split in two sections, covering the upper and the lower screen halves respectively. This permits the application of independent enhance and erase pulses and independent operation at non-store levels. The technique is extremely useful for comparative work, where a trace can be stored in one half, and repeatedly stored and erased; or displayed without storage, in the other half. Split-screen construction is only practical in phosphor-target tubes.

The write-through technique is also useful for comparative work. In this mode of operation the beam intensity is reduced to the level where the dwell time-intensity product is insufficient to achieve storage, but not to the level where the writing beam cannot be seen on screen. The margin between these two points depends greatly on the average rest potential. If it is too close to the first crossover, the slightest amount of writing beam will cause storage, and write-through will be tricky (if not impossible) to achieve. A very sharply focussed beam will also tend to store more readily, and it is sometimes useful to defocus the beam slightly or to wobble or dither it over a narrow area in order to achieve write-through conditions. Write-through is useful to position a trace to a desired location within an already stored display before turning on the full beam to add this new trace. In computer terminal applications write-through is often used to provide a cursor; this is in fact a case where instrument circuitry automatically selects the correct beam intensity and adds spot dithering. In most oscilloscopes the user must achieve the write-through condition by judicious manual adjustment of the beam intensity.

Another helpful arrangement for the purpose of positioning the trace before storing it is the "locate" zone. This is a narrow vertical strip at the extreme left side of the CRT which has no storage target or is run at an operating level so low that no storage will take place. When the LOCATE button is pushed the sweep is disconnected and the beam appears in the locate zone where it can be positioned vertically to the desired location.

Next we turn to automatic erasure-auto erase for short. This is an extremely useful feature of bistable oscilloscopes. Usually a single sweep is allowed to be recorded, after which further sweeps are prevented and a user selectable viewtime period starts. This is variable from the front panel between one-half and fifteen seconds. At the end of the viewtime erasure is initiated and after that a new sweep is allowed. The applications for such a system are too numerous to list and must be left to the reader's imagination.

It might be useful here to give the basic timing diagram of the scheme most frequently adopted. Figure 25-1 shows how, in addition to the conventional sweep holdoff which gives the sweep circuit time to reset, a lockout is introduced which prevents the recognition of new triggers until the viewtime and erasure are completed.

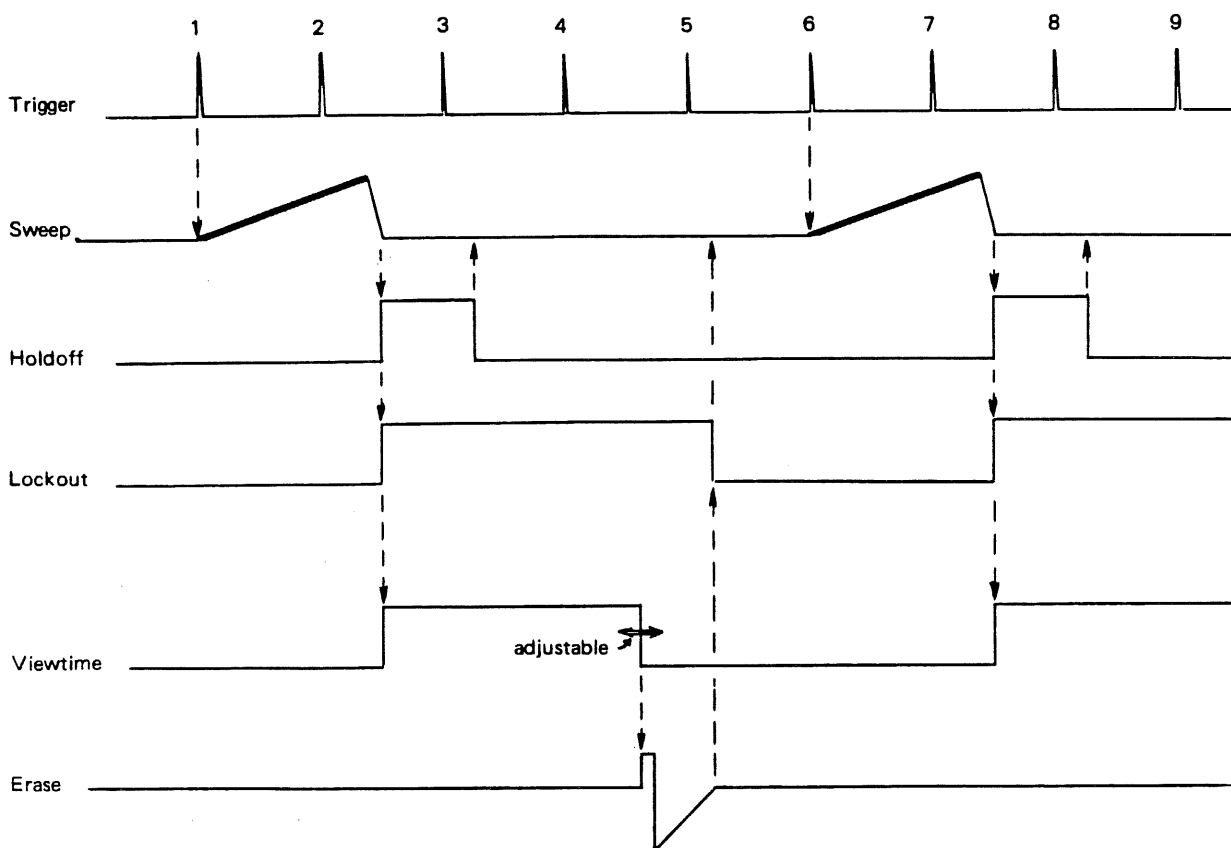


Figure 25-1

- Trigger 1 starts sweep
- Trigger 2 ignored because sweep in progress
- Trigger 3 ignored because conventional sweep holdoff operates
- Trigger 4, 5 ignored because viewtime/erase cycle in progress
- Trigger 6 starts next sweep

Another method used occasionally is to let the sweep circuits continue to function but to blank the CRT beam during the viewtime and erase periods. Unblanking then occurs at the beginning of the next full sweep after erasure is completed. The advantage is that the timebase circuits continue to provide sweep sawtooth and sweep gate outputs during the viewtime, with which ancillary equipment could be driven. But at very slow sweep speeds this method may entail long additional waiting periods if a sweep happens to be in progress when the viewtime/erase period ends.

Several other auto erase schemes are in use in different instruments, most of them (like the ones described above) permitting only one sweep to be recorded at a time. But some instruments allow the recording of further sweeps during the viewtime and these auto erase circuits are often called "periodic erase". If the periodic erase is interlocked with the sweep so that neither can start until the other is completed, then on slow sweeps it is still possible, by a suitable adjustment of the viewtime, to set up a "single-sweep followed by erase" sequence.

The Transfer Storage Tube

While the chief advantages of the phosphor-target tubes are their sturdiness and low cost, their brightness leaves much to be desired. The transmission storage tube offers the exact opposite, a very bright display at the expense of cost and ruggedness. In recent years the last two factors have been brought under control, and the transmission tube is a practical proposition for many applications.

The transfer storage tube Figure 26-1 will operate in a conventional (non-store) mode, a halftone storage mode, a bistable storage mode, or an enhanced (fast) bistable mode. The halftone mode offers a high contrast display of slower speed signals for viewing times of a few minutes. Operation in variable persistence is possible in the halftone mode. The bistable mode is also for slow speed signals but the display can be viewed for longer times; in fact, typically the storage can be viewed for hours. The transfer mode is essentially an enhanced mode of bistable operation with an enhance factor of around 3000. Typical writing speeds are 100×10^6 div/sec.

The halftone mode will be discussed first. The same principles of operation of the storage mesh in the halftone mode are applied to the high speed mesh in the transfer mode. The transfer mode will be discussed next. The final step in a transfer sequence is to store the information onto the storage mesh which is being operated in the bistable mode. Hence, the bistable mode is a fallout from the transfer mode and will be discussed last. The instrument may be considered as a classic halftone storage scope with an ultra fast enhance mode and a permanent storage bistable mode.

HALFTONE MODE:

The storage section includes everything from the floodguns forward. This includes a collimation system comprised of two floodguns, three wallbands (collimation electrodes) and a collector (ion repeller) mesh. This collector mesh is particularly required for collimation since the targets operate at low potentials and it is important that the flood electrons approach normally to the plane of the target mesh. The next mesh forward is the high speed target mesh which in the halftone mode is operated at the same potential as the collector. The storage mesh modulates the flood current and the differences in current are displayed on the phosphor screen which is at 7 kilovolts with respect to the floodgun cathode. This operation can be treated as a classic halftone tube.

The flood electrons approach the storage target. Electrons which pass through the mesh openings are accelerated by the 7 kV field to the phosphor and excite a visible display. The transmission of electrons through the mesh openings is described in the curve of Figure 26-2. The storage mesh potential on this curve actually is a potential determined by both the support wire potential and the dielectric surface potential. Controlling the storage potential along this curve is what the halftone mode is all about.

An operating point for the storage mesh is found by lowering the potential of this target until some section of the view screen begins to go dim. This indicates that this area has dropped off the flat upper part of the curve such as to point A of Figure 26-2. The operating point is selected 3 volts above this point to ensure that the entire target is at saturation.

The following waveform Figure 26-3 is then applied to the mesh to move the dielectric down the curve and prepare for writing:

TRANSFER STORAGE TUBE

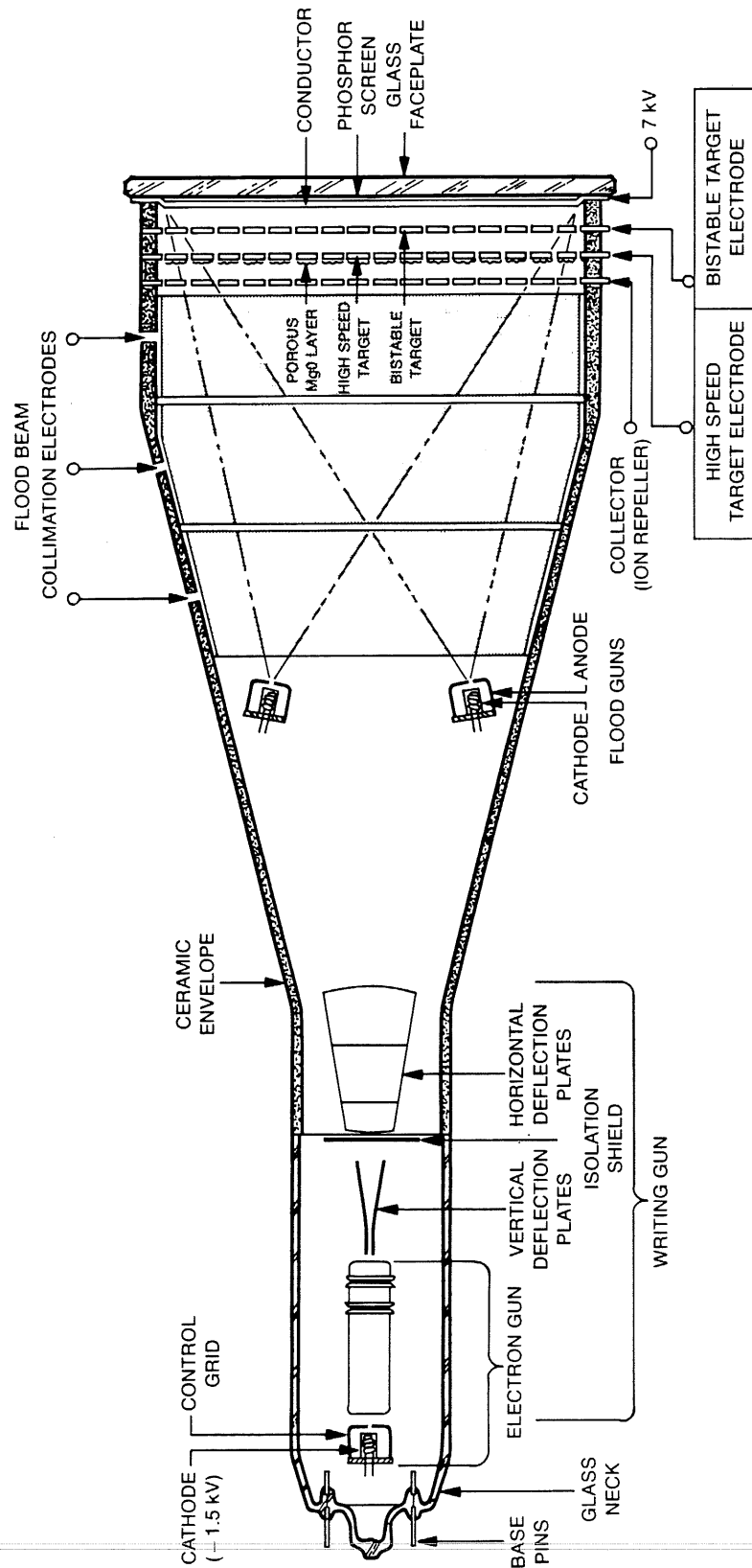


Figure 26-1

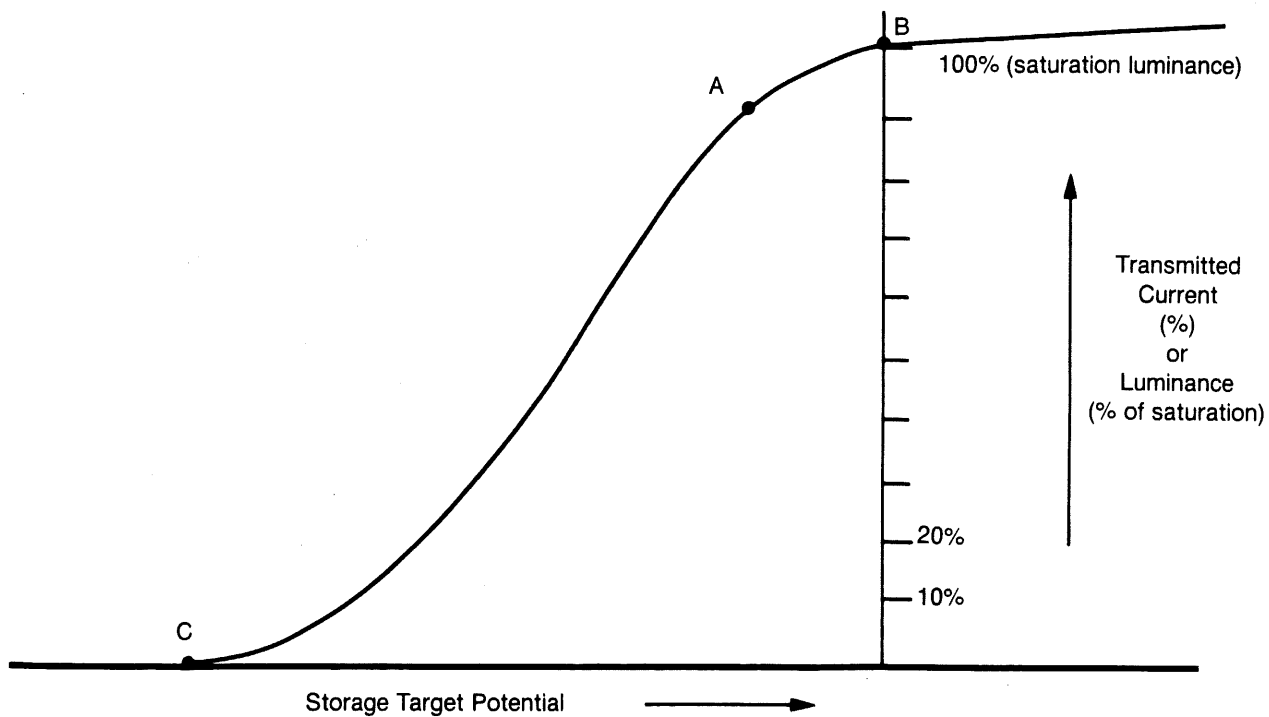


Figure 26-2

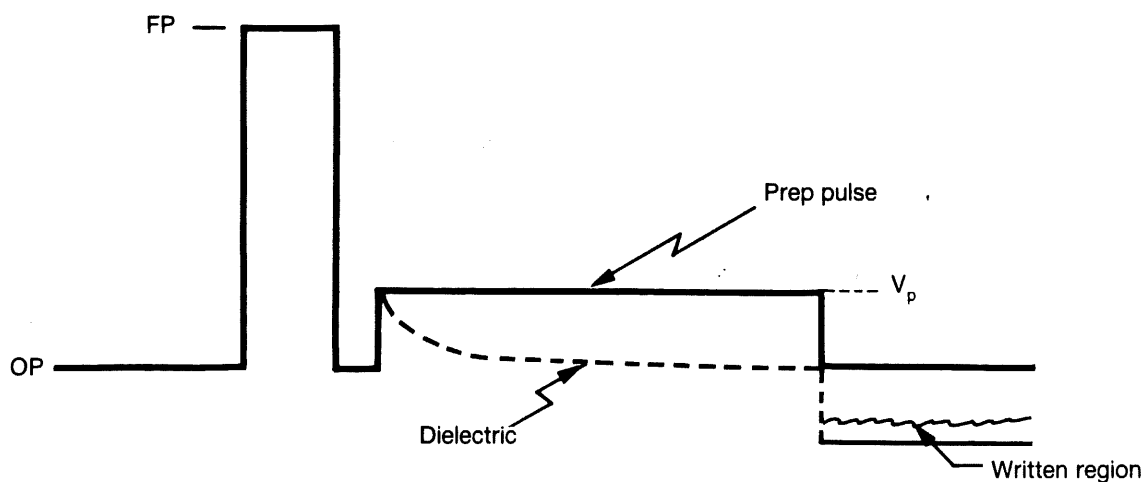


Figure 26-3

This discussion will follow the test set technique for achieving the above waveform rather than what is done in the instrument. The difference is that the test set adds a prep pulse to the operating point. The instrument has a pre-set voltage at the top of the prep pulse and the operating point will be varied to change the pulse height. The advantage of the latter is in versatility to the scope user and does not affect the way the tube operates.

The fade positive pulse breaks down the dielectric and establishes a uniform potential across the target. The dielectric surface changes positive with respect to the mesh wire during the fade positive pulse, but between the FP and prep pulse moves to approximately floodgun cathode potential.

The prep pulse height is below the first crossover potential. The dielectric charges down toward floodgun cathode. This moves the storage target potential negative approximately V_p volts. As V_p is increased and the cycle repeated, some area of the target goes dark. On our transmission curve this corresponds to Point C or cut-off. Due to a combination of target non-uniformities and collimation imperfections, different areas of the storage target have different transmission curves (Figure 26-4). Thus, to prep the entire target below cut-off, the prep pulse height must be increased until the last area goes dark, (Point D of Figure 26-4).

The difference in volts between that required to get the first area to go dark and what is required for the last area to go dark is a measure of uniformity and is called the differential cut-off (DCO).

The writing beam charges the dielectric positive by secondary emission. Halftones are achieved by charging the dielectric to any point along the transmission curve. For the writing speed measurement of the 7623A/7633, the slowest area is charged to 10% of saturation luminance. This corresponds to Point E of Figure 26-4 and represents enough charge deposited to move the surface potential from Point D to Point E. Writing speed is inversely proportional to the voltage from D to E and the DCO is a major part of this voltage.

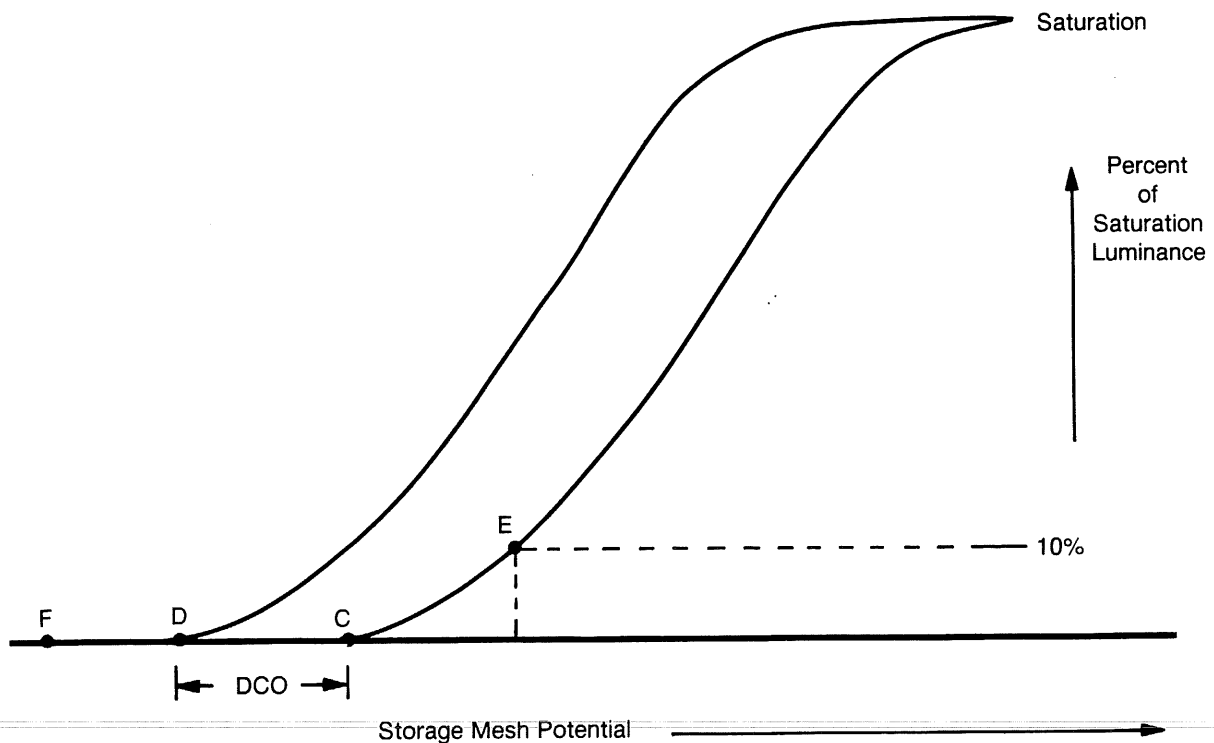


Figure 26-4

Following the prep pulse, the dielectric surface is below floodgun cathode and the most negative element in the storage system. Positive ions created by the flood beam preferentially strike this surface and drive it positive along the transmission curve. This decreases the contrast ratio which approaches 1:1 as the unwritten area approaches saturation. By erasing the target more negative (increasing the prep height) such as to Point F of Curve B, the dielectric has farther to charge to saturation and the view time is lengthened. However, now to write the target to 10% saturation requires enough charge to move the dielectric from Point F to Point E.

A writing speed versus viewtime curve is shown in Figure 26-5.

The equation for writing speed can be derived from the basic equation for charge storage on a dielectric: (1) $Q = CV$

$$\Delta Q = I_b (\delta - 1) \Delta T$$

$$A = \text{area} = \Delta L \times TW$$

$$d = \text{dielectric thickness}$$

$$E = \text{dielectric constant}$$

$$C = \frac{EA}{d}$$

ΔV = voltage shift required for writing

$$v = \text{writing speed} = \frac{\Delta L}{\Delta T}$$

$$\therefore A = v(TW \Delta T)$$

$$(2) I_b (\delta - 1) \Delta T = \left(\frac{EvTW\Delta T}{d} \Delta V \right)$$

$$v = \frac{I_b (\delta - 1) d}{TW \Delta V E}$$

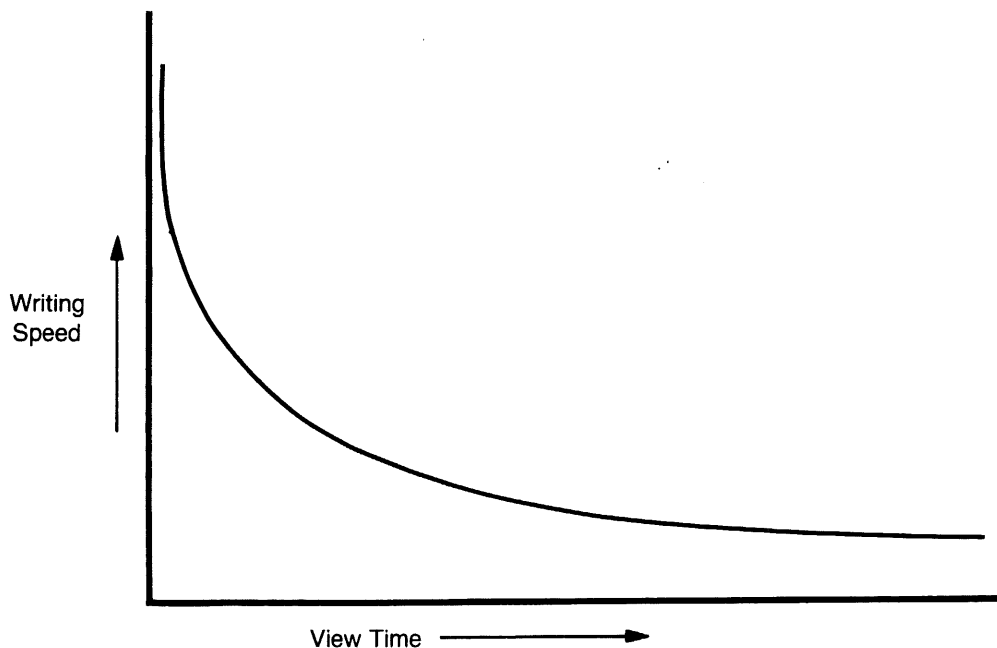


Figure 26-5

The value of this equation is that it becomes apparent what can be done to improve writing speed. The I_b/TW is a gun parameter. It is primarily limited by instrument requirements of bandpass and deflection voltages. The $(\delta-1)$ is the secondary emission gain in the target and is a material property. MgO has a high secondary emission gain and good stability through target processing. The last two parameters are dielectric structure properties. The dielectric thickness is obvious. The dielectric constant can be varied by changing the density of the structure.

Target deposition methods attempt to optimize writing speed by achieving a thick deposition (20 microns typically) and a low density (about 5% of bulk density) with a material which has a high secondary emission ratio (MgO). However, it turns out that these structure changes also increase the speed at which ions write up the target; thus, we move up on the view time curve to high writing speeds and short view times (Figure 26-5). The transfer mode provides a way to extend the view time and use the fast writing speeds that normally would be viewable only for a fraction of a second.

TRANSFER MODE:

In the transfer mode, the high speed target performs in the same manner that the storage mesh did in the halftone mode. One difference is that the target is at fade positive while the display is viewed and only drops into the halftone condition when the transfer cycle is initiated.

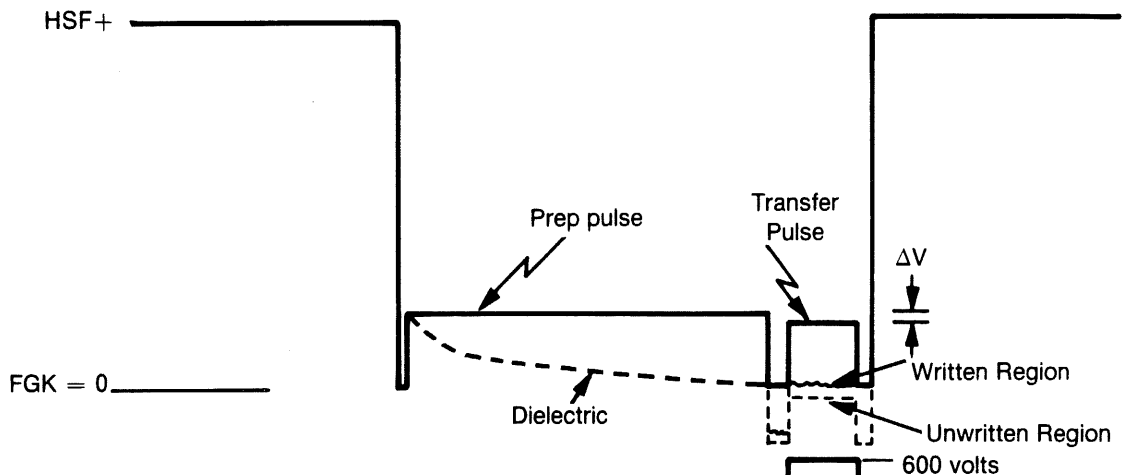
The classic bistable erase pulse is applied to the storage target while the high speed target is at fade positive (Figure 26-6). This ensures a maximum amount of transmitted current which is required for erasure. This erasure leaves the storage target dielectric at rest potential (Figure 26-7).

A prep voltage, V_p , is selected so that all areas of the high speed target are well above floodgun cathode and below first crossover. As in halftone, the dielectric charges down toward floodgun cathode. However, due to the low fields on either side of the high speed target (rest potential on the storage target and 125 volts on the collector), the charging has a self-leveling effect. That is, the areas of higher potential initially receive more flood current and consequently charge down more rapidly. The areas of low potential charge slowly. The net effect is that all areas approach a condition of uniform flood current density which implies uniform transmission of electrons over all of the target, or low DCO. The DCO is typically reduced to a few tenths of a volt. A considerable amount of writing speed of the transfer tube depends on this reduction of the DCO.

To establish V , we operate the tube with no writing beam. V moves the target along the transmission curves (Figure 26-8).

As before, the two curves correspond to the extreme areas of the target or the DCO. If the ΔV is set for a transmission at Point A of Figure 26-8, which was the last area of the target to cut-off, it establishes a charging rate on the corresponding area of the storage mesh of : $Q_a = I_a (\delta-1) T$. I_a is the current transmitted through the high speed mesh in Area A. Note in Figure 26-6 that the storage mesh during ΔV is pulsed to 600 volts to ensure a good secondary emission gain $(\delta-1)$. ΔT is the pulse width. This corresponds to view time in Figure 26-5 for the high speed target and is kept narrow. However, a lower limit exists that allows operation in the lower portion of the transmission curve where the slope is steeper (higher u). A typical value is 100 milliseconds.

A. Pulse train applied to high speed target:



B. Pulse train applied to storage target:

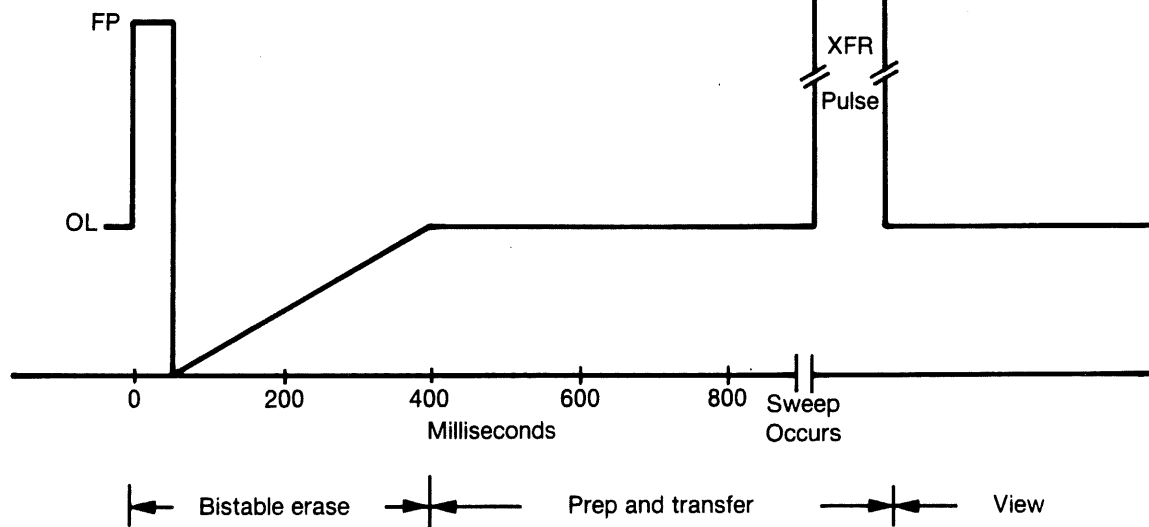


Figure 26-6

For any value of ΔV , ΔV_5 , Q_a is the area which charges most positive on the storage mesh. Any other area would have a charging rate less than Q_a but greater than Q_b . Q_b is the slowest charging area. ΔV is established so in the area on the storage target corresponding to A, 5% of the target is written above first crossover (Point A on Figure 26-7). This ensures that a minimum of increase in the charging rate (potential on high speed dielectric) will cause the storage mesh in this area to charge above first crossover. All other areas are charged to a point between A and B on Figure 26-7 and floodgun current will subsequently charge them to rest potentials.

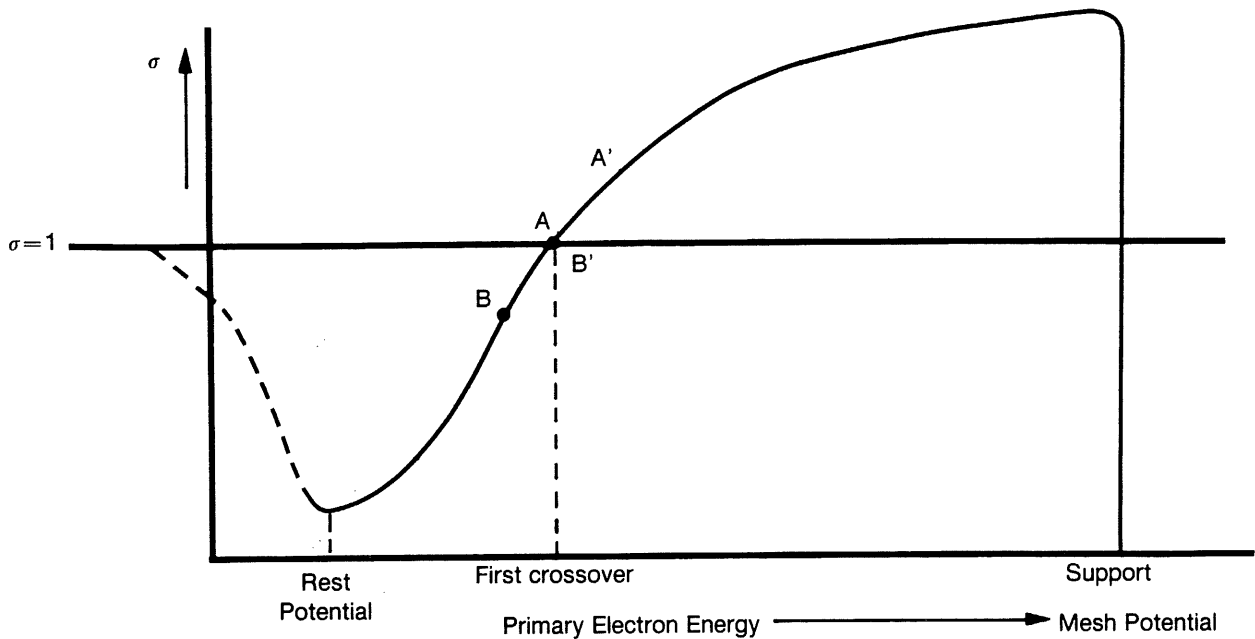


Figure 26-7

While the writing gun is off, DCO can be easily measured. If ΔV is decreased (transfer pulse on high speed target is raised), the charging rates of all areas of the target increase. At ΔV_{95} the charging rate of the slowest area, Area B, is great enough to charge a corresponding area of the storage mesh above first crossover (Point B on Figure 26-7). Now the fastest charging area, Area A, is well above first crossover, Point A on Figure 26-7, and all areas of the target are above first crossover. The floodguns subsequently charge all areas of the target toward the stable point at the storage mesh potential. Actually, ΔV_{95} is defined when 95% of the quality area is written. The DCO is the difference between ΔV_{95} and ΔV_5 .

For writing, the ΔV is set at ΔV_5 . To write the slowest area of the target, the writing beam must charge the dielectric enough to move the transmission of this area from Point B to Point C on Figure 26-8. The charging rate of the slowest area is now sufficient to move the storage target in the corresponding area above first crossover (Point A on Figure 26-7) since this charging rate is now equal to the initial charging rate of Area A.

The same equation used for halftone writing speed can be applied to the high speed target.

$$V = \frac{Ih}{TW}$$

$$\frac{I}{\Delta V}$$

$$\frac{(\delta-1)d}{E}$$

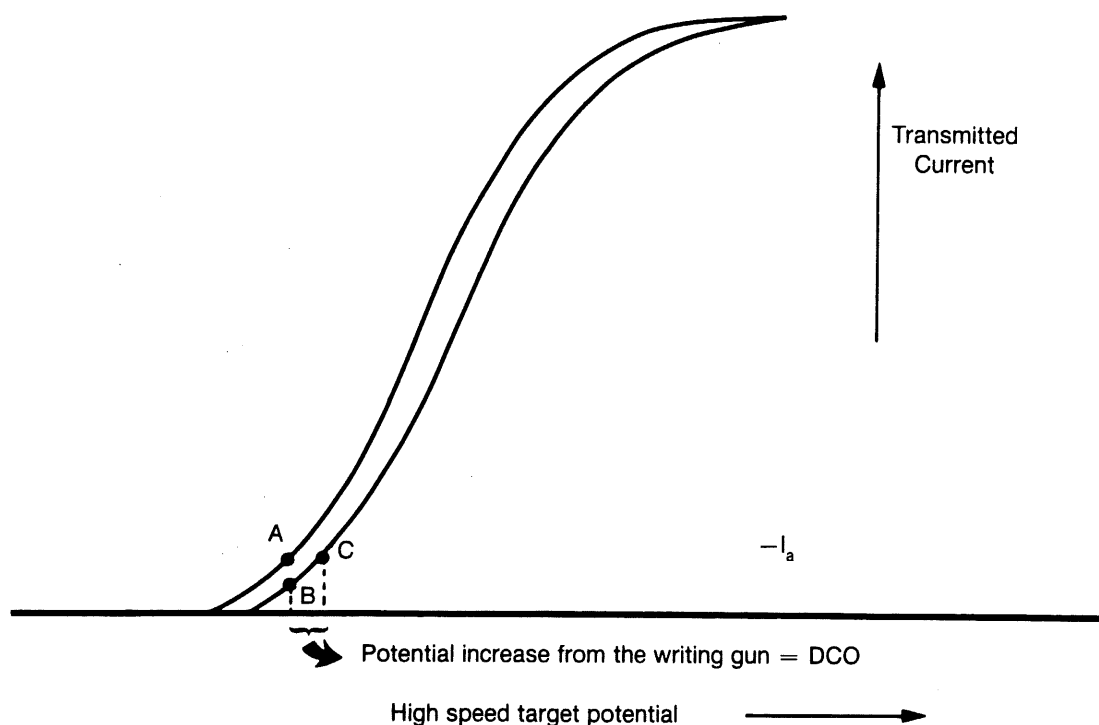


Figure 26-8

A sensitivity measurement is possible which measures $(\delta-1)$ (d/E.) Typical value is 3×10^6 volts/coulomb.nm². ΔV in this equation corresponds to the DCO. Ib/TW equal to $1 \mu\text{a}/\text{mil}$ is typical with the 7633 CRT. Plugging these values into the equation yields about 100×10^6 cm/sec per 120 millivolts of DCO. This is good agreement with measured writing speeds. The correlation improves if a factor is included for the density distribution of the writing beam.

Oscilloscope application revealed a basic problem. The problem is that the target must wait in the prep mode until the sweep is triggered. The dielectric is charging on a curve asymptotic to the floodgun cathode. There is no way to know when the sweep will trigger. Therefore, there is no way to know in advance to what potential the dielectric will prep. It is essential to know this so V5 can be established in advance. The solution to this is to stop the prepping of the dielectric at a certain level and hold it there. This is done with a holding pulse train as seen in Figure 26-9.

Each positive pulse (about $2 \mu\text{sec}$ pulse width at 100 Hz) pushes the dielectric above first crossover and a small, fixed amount of positive charge is added. (see inset of Figure 26-9). Between pulses, the dielectric is below first crossover and charges negatively toward floodgun cathode. The rate of negative charging is dependent on the dielectric potential (the lower the potential the slower the charging). When the prep pulse is initiated, the negative charging between pulses is greater than the positive charging during pulses. The net negative charge lowers the dielectric potential until the negative and positive charging is equal, equilibrium is established. The small potential shifts during each cycle of the holding pulses is small with respect to the DCO and have a minimum effect. Thus, the potential on the dielectric is stable and ΔV is set for this established potential. The cost of this stability in terms of performance is that the high speed target does not prep completely so the minimum DCO/maximum writing speed is not achieved. However, the writing speed loss without the pulses in the first minute is typically several orders of magnitude greater than that due to the increased DCO with the holding pulses.

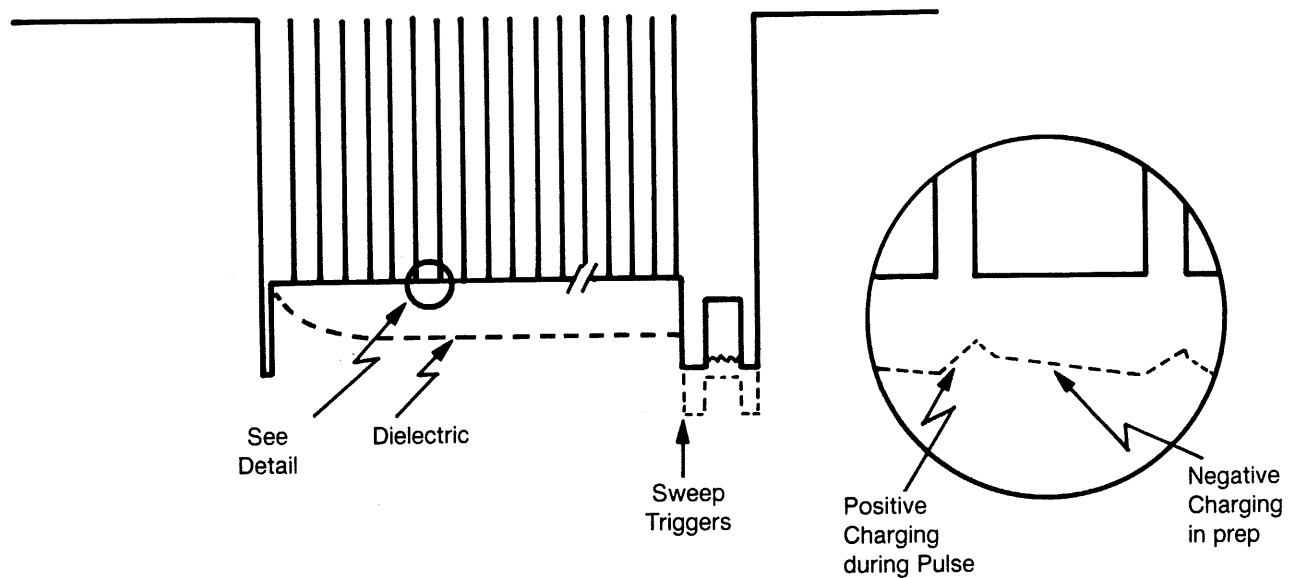


Figure 26-9

BISTABLE MODE:

The bistable mode is essentially the same as our classic bistable storage tubes. To write the storage target requires the writing beam to charge the dielectric from rest potential to first crossover (Figure 26-7). The writing speed is limited since the beam must pass through both the collector mesh and the high speed target.

VIEWING:

When a signal is written onto the storage target (either directly by the writing beam or transferred from the high speed mesh), the image is viewed on the phosphor screen as a bright area (high current density) with a dark border. Unlike the halftone mode in which the background is near cut-off (Figure 26-4, Point D) and the written area is the only area transmitting a significant current, the background in the bistable mode is transmitting near saturation. (Figure 26-10, Point A).

The bright area of the written information is viewable because it scavenges electrons from surrounding areas and focuses these on the phosphor. This is possible because of the relatively large difference in dielectric potential between written and unwritten area (Points A and B of Figure 26-10). The trace profile is shown in Figure 26-11. The dips adjacent to the trace reflect scavenged electrons.

One disconcerting effect of the lack of contrast when this scavenging cannot occur is that it is difficult to detect the difference between the unwritten and the fully written condition. The differences in transmission (Points A and B of Figure 26-10) are insignificant. However, with the focusing of the scavenged electrons, the trace is a brilliant several hundred footlamberts at a contrast ratio near 3:1

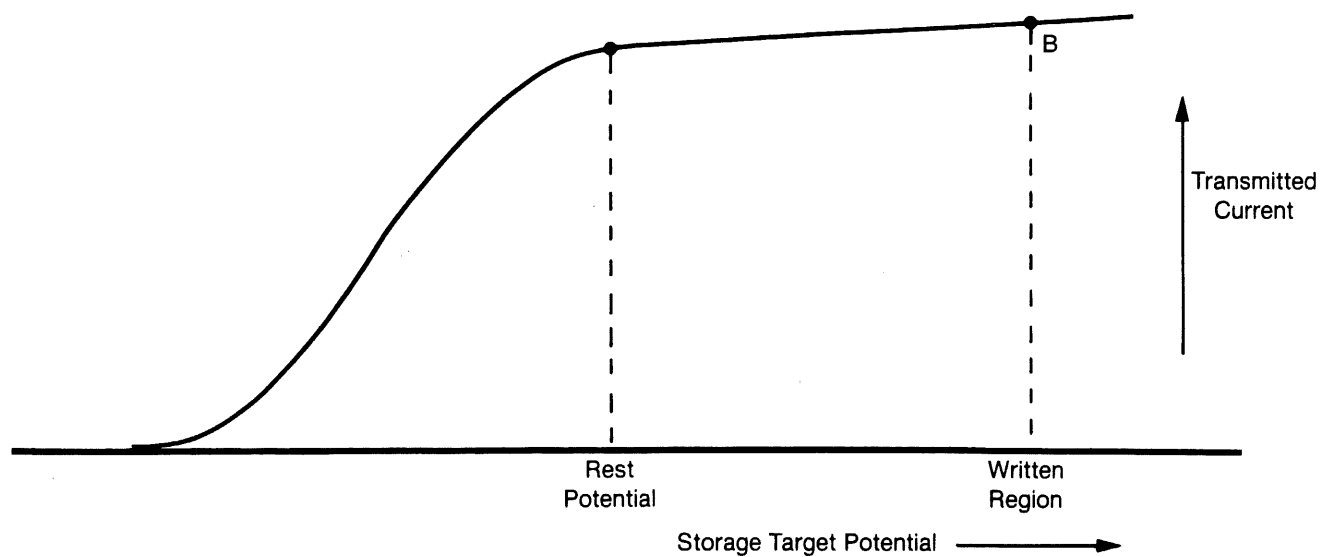


Figure 26-10

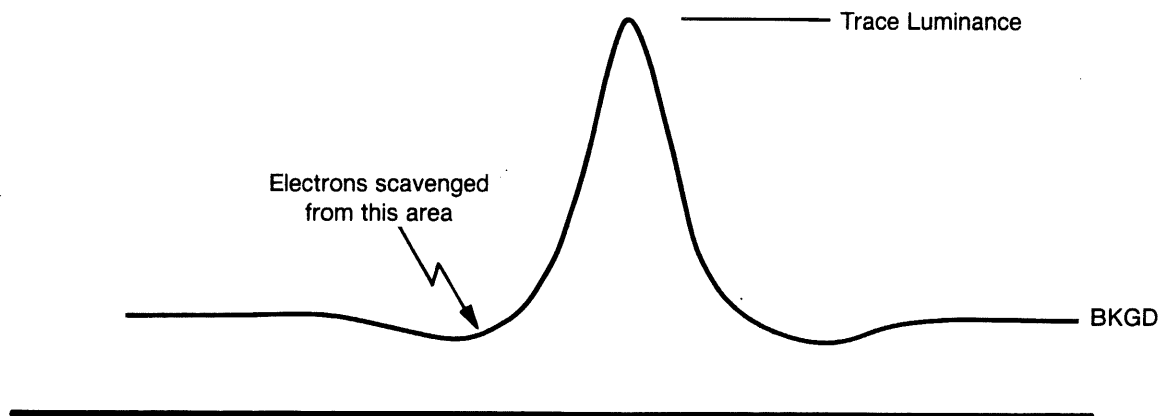


Figure 26-11

FEATURES OF THE TRANSFER STORAGE OSCILLOSCOPE

A few Tektronix oscilloscopes offer both transfer modes discussed in the previous chapter and a "reduced-scan mode" to be described in this chapter. Other instruments using transfer tubes each lack either the reduced-scan feature or one of the transfer modes. Here we shall discuss the features of the type 7633 and mention some of the innovations of the more recent 7834. For details of the controls available on other transfer instruments you should refer to their respective operating manuals.

Many of the facilities of the 7633 will be familiar to you from previous chapters. There is an auto erase circuit (here called PERIODIC ERASE) which operates in all storage modes, and there are the PERSISTENCE and STORAGE LEVEL controls. Erase and persistence are disabled when the SAVE pushbutton is selected, and the floodbeam can then be reduced or stopped with the "save time" control (here called SAVE INTENSITY). To operate the instrument as a normal bistable or variable persistence scope the appropriate store mode is selected. For transfer operation the store mode button and the FAST button must be pushed.

Before going on to discuss the reduced-scan feature, let us consider briefly the effect of the STORAGE LEVEL control in the various modes. In the conventional variable persistence mode it allows us to shift the target mesh voltage. We can thereby control the relative brightness of the recorded trace and the background, moving the display to the steepest part of the transfer curve when viewing very fast, faint traces, or moving the background well below cutoff for good contrast and long viewing times of solidly written traces.

In the fast variable persistence mode the principle mentioned in the previous paragraph obviously applies to both targets, and to optimize them for the very fastest writing speed both need to be adjusted carefully. A vernier screwdriver control marked FAST LEVEL CENTER, is provided so that the two targets can be made to track exactly at the desired STORAGE LEVEL setting. For details on how to adjust the FAST LEVEL CENTER control consult the calibration procedure in the 7633 instruction manual. (In recent instruments the control is located inside the instrument). In fast bistable operation the STORAGE LEVEL control allows us to pick a suitable fast mesh voltage as shown in Figure 27-1.

Turning now to the reduced-scan feature, you may recall that we mentioned the difficulty of achieving uniform storage target performance in transmission tubes. But the writing speed and thus the usefulness of an instrument is limited by the performance in the least sensitive part of the screen. During manufacturing we try to make the target as uniformly sensitive as possible but there are still areas on the target less sensitive than other areas. When the first transfer tube instrument, the 7623, was introduced, the writing speed specification was limited to the center 4×5 division area. This is inconvenient for users who generally prefer to have an 8×10 div graticule. To make measurement more convenient additional graticule markings were added to the face of the CRT, outlining 8×10 half-sized divisions within the center 4×5 standard divisions. When the REDUCED-SCAN mode is entered by pulling the appropriate knob, the deflection sensitivity of the instrument is exactly halved, so that the selected sweep speed and vertical sensitivity, as shown by the time/div and volts/div switch and as indicated on the CRT readout now apply directly to the new, smaller divisions, and in addition the negative cathode potential on the writing gun is doubled for a more intense writing beam. The combined effect of these changes is a six to eight times increase in writing speed.

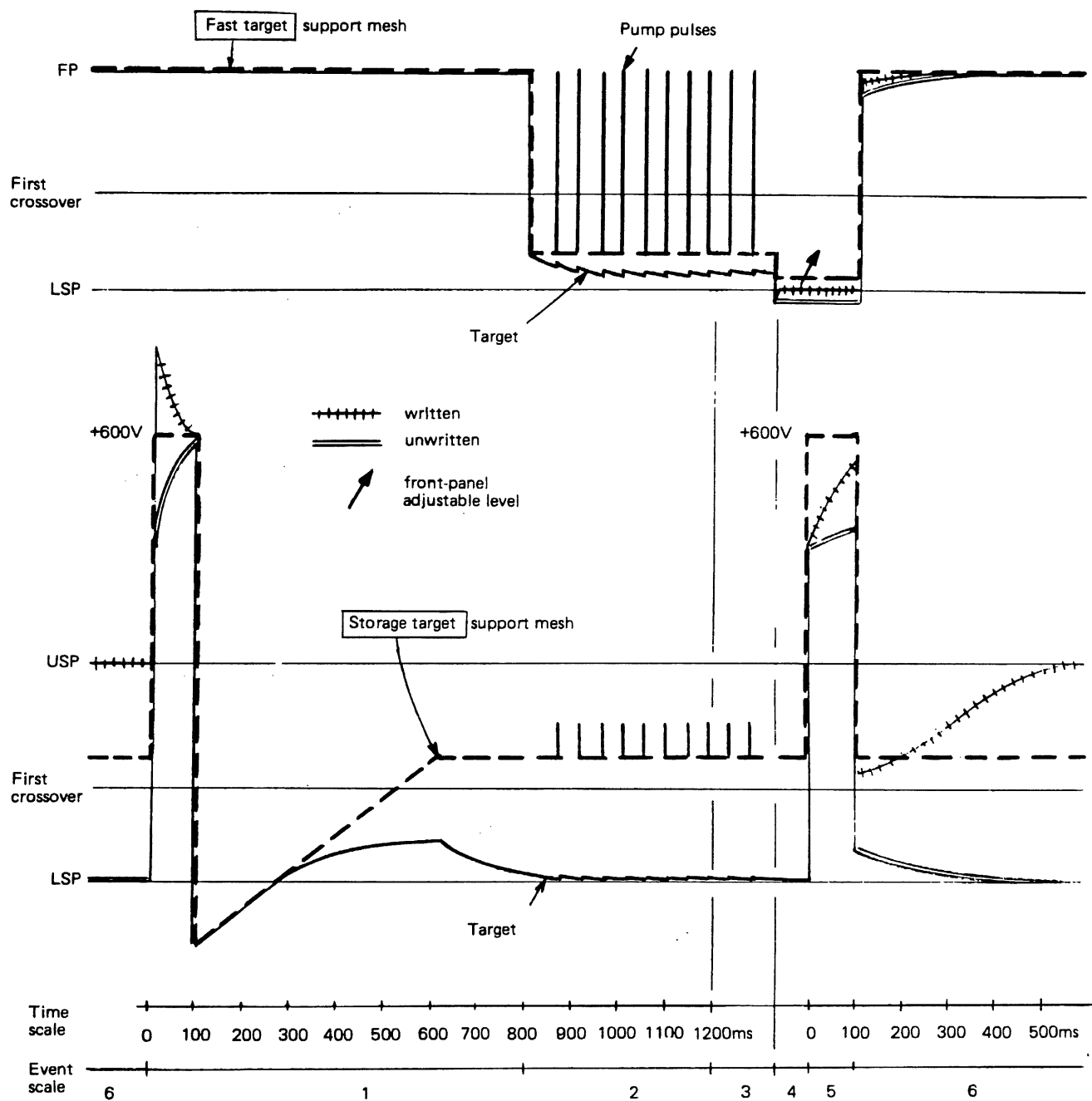


Figure 27-1

A further effect of the reduced-scan operation is that the writing beam spot size is decreased by a factor of about 1.5 and to this extent the resolution of the display becomes greater. This improvement in resolution is over and above that gained by the additional writing speed.

One more feature remains to be explained. You may remember that when the transfer mode is used a single sweep is recorded and transferred, and a new recording normally starts with the erase sequence. Now in some application it may be desirable to record several traces on top of one another for comparison purposes. This can be achieved by not erasing the storage target while going through the rest of the transfer mode sequence. In this way the new information can be added to the trace already existing on the storage target. In storing slow signals many traces can be added in this way, but if you are looking at very fast events where it is necessary to advance the STORAGE LEVEL control then you will notice that the background of the storage target brightens and each new trace adds to that background brightness. As a result it may not be possible to repetitively store more than one or two times before the target is fully written.

Such a mode of operation is referred to as the "multi" mode. To make multiple sweeps it is merely necessary to initiate a new sweep by pressing the single sweep RESET button on the normal oscilloscope timebase instead of the erase button. If you were using the periodic erase feature it might be wise to disable this before beginning multiple repetitive storage.

One of the innovations of the 7834 allows traces to be added in the "multi" mode on an automatic basis at intervals selected by the MULTI TRACE DELAY control. This could be useful, for instance, during calibration procedures when the operator wishes to superimpose the results of each of a series of adjustments. He would merely have to set the MULTI TRACE DELAY to the time required to make and observe each adjustment and recording the results then becomes a "hands-off" operation. The control might also be used to make the instrument ignore unwanted information in a long pulse train while automatically recording data occurring at specific intervals. In principle this is similar to the variable trigger holdoff feature offered by many oscilloscopes, but here the time scale is a different one: the MULTI TRACE DELAY is adjustable between 0.6 and 4 seconds.

Baby-sitting operation of the 7633 can be had by putting the timebase into the single-sweep mode, then initiating an erase cycle (after which the timebase will automatically be armed, as indicated by the RESET button lighting up), and finally entering the SAVE mode. One sweep will then be allowed before the timebase is locked out. If the instrument is used in either variable persistence mode and you want indefinite storage after the event, then, you must make sure that the SAVE INTENSITY control is at minimum. When returning to the instrument to view the trace recorded in your absence, all that is necessary is to turn up the SAVE INTENSITY control to the desired brightness. Baby-sitting is of course also available in the 7834.

The 7834 achieves the fastest writing speed of any storage tube instrument ($2500 \text{ cm}/\mu\text{s}$) by design improvements in the CRT gun assembly and deflection system, giving a smaller tracewidth and providing the target with a greater charge density. The instrument also features comprehensive remote control facilities.

If we compare the transfer tube oscilloscope with the first storage instrument introduced nearly 20 years ago the writing speed has been improved by a factor of 10 000 without employing any radically new principles, making possible the single shot storage of a 2 cm high sinewave of 400 MHz where previously as many kilohertz were completely out of reach.

STORAGE WRITING SPEED

In this book the term "writing speed" was used in the sense of "maximum stored writing speed"-in other words, the maximum beam velocity at which the tube is capable of producing a satisfactory stored trace. Several questions arise from this:

1. What criteria are used to define "satisfactory"?
2. How could the performance of a given instrument be verified?
3. What is the maximum beam velocity produced by a signal of a given shape and with given deflection factors?

We shall try to answer all these questions starting with the last one.

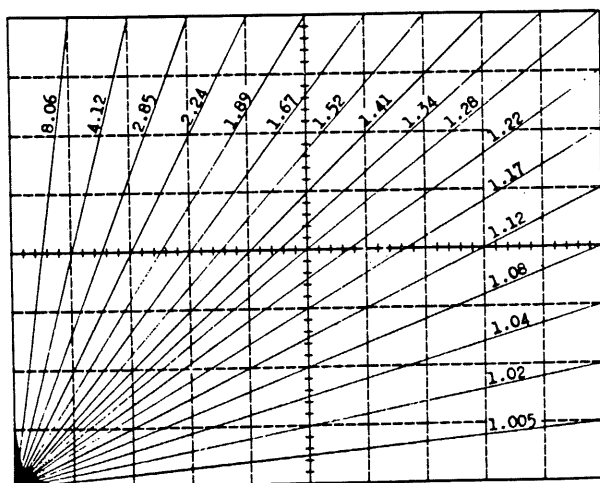
HORIZONTAL BEAM MOTION

The most trivial case is that of a straight horizontal trace, when the beam sweeps across the CRT without being deflected vertically. In this case the beam velocity is constant and is determined by the selected sweep speed factor. The beam velocity is usually quoted in $\text{div}/\mu\text{s}$, so if, for example, the sweep speed is $0.1 \mu\text{s}/\text{div}$, then the beam velocity would be its reciprocal, $10 \text{ div}/\mu\text{s}$.

COMBINED BEAM MOTION

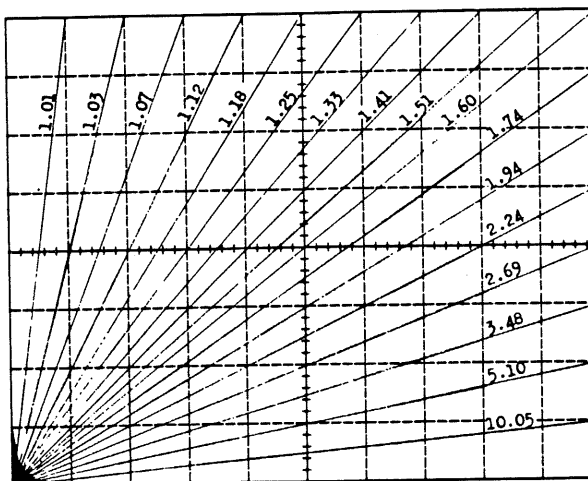
When vertical deflection is added, the beam velocity will be the vector sum of the horizontal and vertical motions. For a trace rising or falling at 45 degrees, for instance, the beam velocity will be $\sqrt{2}$ times the horizontal component. Elementary trigonometry will allow you to calculate, for any given trace angle, the factor by which the horizontal motion must be multiplied to obtain the true beam velocity. Figure 28-1 gives some selected values. So if you have an actual display in front of you and want to calculate the maximum beam velocity, look for the steepest part of the curve and multiply the horizontal beam motion by the appropriate factor.

This procedure will become impractical if the vertical motion is very much greater than the horizontal motion, making the trace nearly vertical, or if the horizontal sweep is uncalibrated. For some signals it may be possible to approach the problem the other way; to determine the vertical component of the beam motion from known facts about the signal, and then multiply it by a factor derived from trigonometry to allow for the horizontal component. Again, if the display rises at 45 degrees, the factor will be $\sqrt{2}$. Figure 28-2 gives a number of values for different angles. Obviously, the most accurate results are obtained if, for nearly vertical traces, you start off with a known vertical speed.



Factors by which horizontal motion must be multiplied to obtain combined motion

Figure 28-1



Factors by which vertical motion must be multiplied to obtain combined motion

Figure 28-2

VERTICAL BEAM MOTION

Since the vertical motion depends on the signal shape, no generally valid statement can be made. Each waveshape must be treated independently. The simplest case is that of a linear ramp, where the rate of rise directly expresses the vertical motion of the beam. For instance, a ramp rising at 2 div/ns has a vertical beam motion of just that — 2 div/ns. Such a ramp is shown in Figure 26-3, which also illustrates how the rate of rise of the ramp could be measured on an oscilloscope by selecting a sweep speed of 1 ns/div. Remember that the result of the measurement, 2 div/ns, is the vertical component of the beam motion only, and for the combined beam velocity you must now multiply this figure by a factor taken from Figure 28-2, in this case 1.12.

If the ramp is the leading edge of a pulse and if the risetime t of that pulse is quoted, it follows that the leading edge will run through 80% of its total amplitude during time t . The vertical component of the beam motion can be calculated from the total pulse amplitude A and the given risetime as

$$V_{\max} = \frac{K-A}{tr} = \frac{(0.8)(.5 \text{ div})}{2 \text{ ns}} = 2 \text{ div/ns}$$

The formula is expressed in general terms suitable for other kinds of step responses in which the velocity is not constant but will, at some point, reach a maximum. The constant k (in this case 0.8) simply states, for a given waveshape, through what fraction of the total pulse amplitude the leading edge would run if it maintained V_{\max} for the duration of t_r .

Figure 28-4 shows a Gaussian response for a step of the same amplitude and risetime as in Figure 28-3. Since parts of the curve between 10% and 90% rise less steeply than the linear ramp, it follows that in other parts (near the center) it must be steeper if the 90% level is to be reached in the same time. Not surprisingly, then, the constant k will be larger. For a true Gaussian response it is 1.023, but in practice a factor of 1 is usually employed.

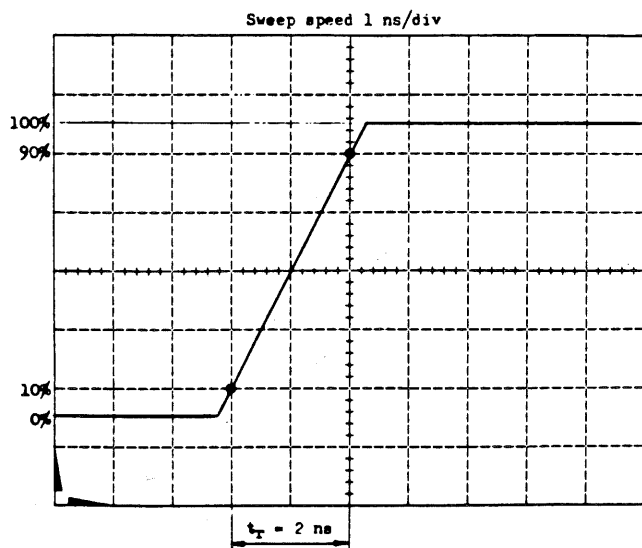


Figure 28-3

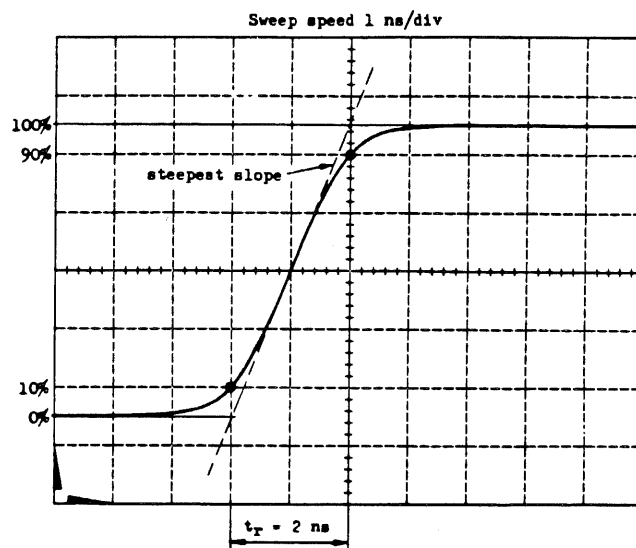
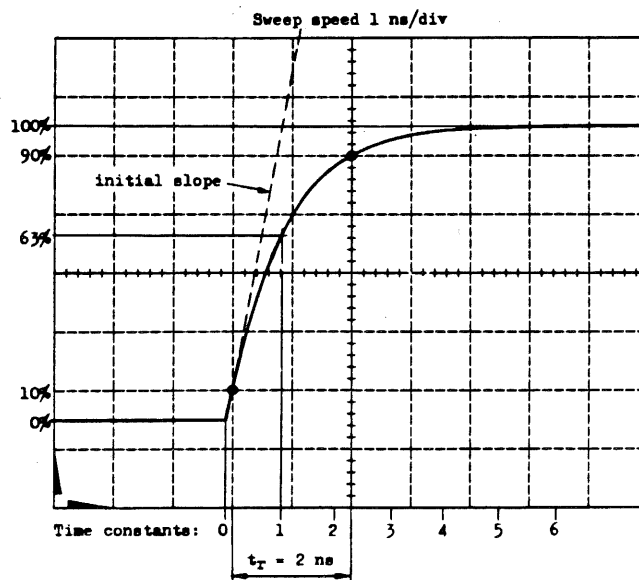


Figure 28-4

Figure 28-5 shows the exponential response of a single RC network to a step input. In this case, obviously, the fastest vertical motion occurs at the 100% level in one time constant, and (since $t_r = 2.2$ time constants) to 220% during t_r . Thus the scaling factor k becomes 2.2 for this waveshape.

To sum up, the k factor in the formula is 0.8 for linear ramps, about 1 for true Gaussian response, and increases to 2.2 for single-pole RC networks. Intermediate values for networks limited by a few poles can readily be guessed. We shall have more to say about the accuracy to which such calculations should be carried when we consider how a "satisfactory" stored trace is defined.



One more waveshape will be discussed here, that of the common sinewave. Its maximum vertical motion occurs at the center of the sinewave and is given by the simple formula:

$$V_{\max} = \pi A f$$

where A is the peak-to-peak amplitude and f is the frequency.

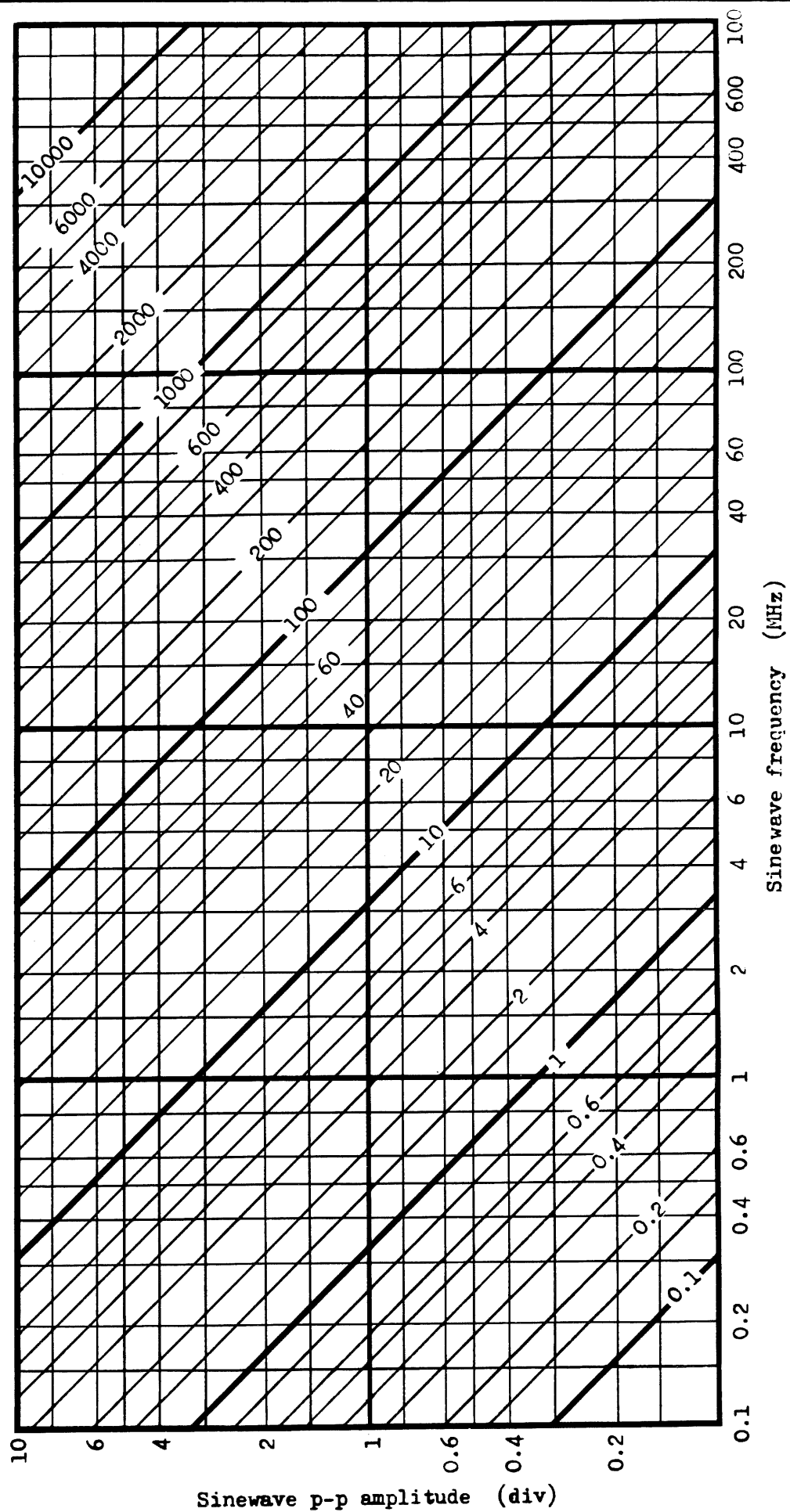
With amplitude in div and frequency in MHz, the result will be in div/ μ s.

To save calculations, the nomograph on the next page might be useful, in which, for a wide range of sinewave frequencies and amplitudes, the maximum writing speed can be read off directly.

Finally in this section we must remind you again that after determining the vertical beam velocity in this way you must then allow for the effect of the horizontal motion to obtain the actual velocity on the CRT screen.

MAXIMUM VERTICAL VELOCITY OF SINEWAVES

The diagonal lines are labelled in div/ μ s



HOW TO VERIFY THE WRITING SPEED PERFORMANCE OF AN INSTRUMENT

At its simplest, one could record a vertically undeflected beam and increase the sweep speed until the stored trace became unsatisfactory. But this would only check the tube performance at that particular vertical level, and would not show up vertical nonuniformity. Further traces in other positions could be recorded, but this would be rather tedious. Also, the calibrated sweep speeds progress in a 1-2-5 sequence, making intermediate measurements difficult.

A much more satisfactory method is to use a constant-amplitude sinewave generator as a signal source and set the amplitude for full-screen deflection. Now if at least 3 cycles of the sinewave are displayed, the waves will be steep enough in the center portion for the horizontal beam motion to be neglected, and while the vertical motion is exactly πAf at the center only, it will be within 10% of that speed over a 40% band on both sides of center, thus allowing the tube performance to be assessed over a reasonably wide region. The method is simply to increase the frequency of the sinewave generator, while repeatedly storing a trace, until the stored display becomes unsatisfactory and then plugging that particular frequency and the sinewave amplitude into the formula. As the frequency is increased, the sweep speed should also be increased occasionally so that the recorded individual sinewave cycles do not run into one another.

It may then be necessary to convert the result of your measurement from $\text{div}/\mu\text{s}$ to $\text{cm}/\mu\text{s}$ in order to compare it with published specifications.

WHAT CONSTITUTES A SATISFACTORY STORED TRACE?

The answer depends on whether the display is bistable or halftone. For bistable displays the evidence is fairly objective: the trace is either there or it isn't. As the writing speed increases, break-up of the trace because of failure to store may start in some screen areas first. At the factory, the stored trace is checked with suitable magnifying equipment and the writing speed defined as that speed at which no breaks greater than a certain fraction of an inch (typically 0.025") occur. For practical purposes the user can decide what, in his context, constitutes an unacceptable break. With the fairly uniform phosphor-target tubes he will find that at writing speeds not much greater than the one where such breaks first occur in one part of the screen, the whole screen area will be affected. Determining the maximum writing speed therefore becomes a reasonably repeatable experiment, giving results within 5 or 10% for different observers and different parts of the screen.

Transmission tubes, used bistably, are less uniform and will generally be optimized for best performance in the center portion of the screen. Where the writing speed is specified for the center 4×5 div area it would be best to ignore the tube performance outside this area.

Halftone tubes present a completely different problem. The trace will not visibly break-up, but rather it will become fainter and fainter until it becomes difficult to distinguish it from the background, and at the same time the storage time will become shorter and shorter. Because of the tube non-uniformity this may also happen at very different writing speeds in different parts of the screen. Restrictions to the center 4×5 div area must obviously be observed, but even so the writing speed evaluation can yield results that differ by several factors of 2 from observer to observer, unless the conditions of the experiment are very closely defined and the observers suitably trained.

You can see from the above discussion why it is perfectly reasonable practice, when testing writing speed with sinewaves, to ignore the error due to horizontal beam motion and the 10% speed variation within the inner 40% band of the sinewave, or to guess the k factor for non-Gaussian step responses.

Finally a word about writing speed in the context of photography rather than storage. The method of assessment is exactly the same, the preferred technique being to use sinewaves. As in the halftone tube a decision has to be made about the minimum acceptable contrast. But since non-store CRTs and photographic film are virtually uniform and the finished product can be measured with a densitometer or photometer, generally acceptable limits have been agreed on. A trace is considered satisfactory if the density difference in a transparency is at least 0.1, corresponding to a contrast ratio of 1.26:1.

APPENDIX A

Format EIA Phosphor Designation	Fluorescence	Phosphorescence	CIE Coordinates X Y		Persistence (20%)	Comparable WTDS Designations
P1	Yellowish Green	Yellowish Green	0.218	0.712	Medium	GJ
P2	Yellowish Green	Yellowish Green	0.279	0.534	Medium Short	GL
P3	Orange Yellow	Orange Yellow	0.523	0.469	Medium	YB
P4	White Screen for Monochrome TV and Data Display Tubes (11,000°K)					WW
P5	Blue	Blue	0.169	0.132	Medium Short	BJ
P6	White Screen for Monochrome Data Display Tubes (11,000°K)					WW
P7	Purplish Blue	Yellowish Green	0.151	0.032	Medium Short	GM
P8	(Reservation Cancelled)	0.357	0.537	Long		
P9	(Reservation Cancelled)					
P10	Dark Trace Screen (KCI)	Normally White				
P11	Blue	Blue	0.139	0.148	Medium Short	BE
P12	Orange	Orange	0.557	0.442	Long	LB
P13	Reddish Orange	Reddish Orange	0.670	0.329	Medium	RC
P14	Blue	Orange Yellow	0.150	0.093	Blue-Med Short	YC
			0.504	0.443	Orange-Medium	
P15	Green	Green	0.246	0.439	Short	GG
P16	Violet (UV)	Violet (UV)	0.199	0.016	Very Short	AA
P17	White	Yellow	0.302	0.390	Blue-Short	WF
					Yellow-Long	
P18	White Screen for Monochrome TV and Data Display Tubes (11,000°K)					WW
P19	Orange	Orange	0.572	0.422	Long	LF
P20	Yellow Green	Yellow Green	0.426	0.546	Medium Short	KA
					To Medium	
P21	Reddish Orange	Reddish Orange	0.539	0.373	Long	RD
P22	Tricolor Screen for Color TV and Display Tubes (R,G,B)					X
P23	White	White	0.364	0.377	Medium Short	WG
P24	Green	Green	0.245	0.441	Short	GE
P25	Orange	Orange	0.569	0.429	Medium	LJ
P26	Orange	Orange	0.513	0.426	Very Long	LC
P27	Reddish Orange	Reddish Orange	0.674	0.326	Medium	RE
P28	Yellow Green	Yellow Green	0.370	0.540	Long	KE
P29	Yellowish Green	Yellowish Green	0.279	0.534	Medium Short	SA
	Orange	Orange	0.569	0.429	Medium	
P30	(Reservation Cancelled)					
P31	Green	Green	0.226	0.528	Medium Short	GH
P32	Purplish Blue	Yellowish Green	0.340	0.515	Long	GB
P33	Orange	Orange	0.559	0.440	Very Long	LD
P34	Bluish Green	Yellowish Green	0.235	0.364	Very Long	ZB
P35	Yellowish Green	Greenish Blue	0.200	0.245	Medium Short	BG
P36	Yellow Green	Yellow Green	0.400	0.543	Very Short	KF
P37	Greenish Blue	Greenish Blue	0.143	0.208	Very Short	LK
P38	Orange	Orange	0.591	0.407	Very Long	LK
P39	Yellowish Green	Yellowish Green	0.223	0.698	Long	GR
P40	White	Yellowish Green	0.276	0.312	Blue-Med. Short	GA
					Yellow Green-Long	
P41	Orange Yellow	Orange Yellow	0.541	0.456	Long	YD
P42	Yellowish Green	Yellowish Green	0.238	0.568	Medium	GW
P43	Yellowish Green	Yellowish Green	0.333	0.556	Medium	GY
P44	Yellowish Green	Yellowish Green	0.300	0.596	Medium	GX
P45	White	White	0.253	0.312	Medium	WB
P46	Yellow Green	Yellow Green	0.365	0.595	Very Short	KG
P47	Purplish Blue	Purplish Blue	0.166	0.101	Very Short	BH
P48	Yellow Green	Yellow Green	0.365	0.615	Medium	KH
P49	Yellowish Green	Reddish Orange				VA
	Yellowish Green		0.315	0.615	Medium	
	Reddish Orange		0.672	0.327	Medium	
P50	Reddish Orange	Yellowish Green				VB
	Reddish Orange (8 KV)		0.655	0.340	Medium	VB
	Yellowish Green (15KV)		0.398	0.546	Medium Short	
P51	Reddish Orange	Yellow Green				VC
	Reddish Orange (6KV)		0.675	0.325	Medium	
	Yellowish Green (12 KV)		0.414	0.514	Medium Short	
P52	Purplish Blue	Purplish Blue	0.157	0.075	Medium Short	BL
P53	Yellow Green	Yellow Green	0.368	0.539	Medium	KJ
	Tri-Color Screen for Display (R,G, white)					B
P55	Blue	Blue	0.150	0.070	Medium Short	BM
P56	Red	Red	0.640	0.335	Medium	RF
P57	Yellowish Green	Yellowish Green	0.218	0.712	Medium	LL
		Orange	0.573	0.426	Very Long	

APPENDIX B

Types of storage

- P phosphor-target bistable
 B transmission bistable
 H halftone without variable persistence
 V variable persistence
 FB fast (transfer) and bistable
 FV fast (transfer) and variable persistence

Other abbreviations

- * optional feature
 Δ type RM564 only
 ∇ central 6x8 div only
 ° central 4x5 div only
 ‡ in reduced scan mode each division is half normal size
 † integration is also a natural property of all halftone and variable persistence tubes
 - not applicable or not available

Product	Y or Z resp. of instru- ment	CRT			Usable area		Internal graticule illuminated or non-illuminated
		Dual beam	Type of storage	Split screen	cm	div	
D1	Y2	-	P	S	10x12.5	8x10	N
DM53A	Y25	D	V	-	6x10	6x10	-
DM63	Y15	D	V	-	7.2x9	8x10	N
DM64	Y10	-	P	-	8x10	8x10	-
GMA-101A	Z7	-	P	-	26.6x35.5	-	-
GMA-102A	Z7	-	P	-	26.6x35.5	-	-
T912	Y10	-	P	-	8x10	8x10	N
214	Y0.5	-	P	-	3x5	6x10	N
314	Y10	-	P	-	5.1x6.3	8x10	N
434	Y25	-	P	S	7.8x9.8	8x10	N
434 opt 1	Y25	-	P	S	7.8x9.8	8x10	N
464	Y100	-	FV	-	7.2x9	8x10	I
466	Y100	-	FV	-	7.2x9	8x10	I
549	Y30	-	P	S	6x10	6x10	-
564	Y10	-	P	S	8x10	8x10	-
564B	Y10	-	P	S	8x10	8x10	-
564B Mod 08	Y10	-	P	S	8x10	8x10	-
601	Z1	-	P	-	8x10	-	-
603	Z5	-	P	-	10x12.5	8x10*	N*
603 opt 2	Z5	-	P	-	10x12.5	8x10*	N*
605	Z5	-	V	-	7.2x9	8x10*	N*
607	Z5	-	V	-	7.2x9	8x10*	N*
611	Z1.7	-	P	-	16.2x21	-	-
613	Z1.7	-	P	-	15x20	-	-
4501	Z5	-	P	-	7.5x10	-	-
5031	Y1	D	P	S	10x12.5	8x10	I
5111	Y2	-	P	S	10x12.5	8x10	N
5113	Y2	D	P	S	10x12.5	8x10	N
5113 opt 3	Y2	D	P	S	10x12.5	8x10	N
5115	Y2	-	P	S	10x12.5	8x10	N
5441	Y60	-	V	-	7.2x9	8x10	I
5441 opt 5	Y60	-	V	-	7.2x9	8x10	I
7313	Y25	-	P	S	7.8x9.8	8x10	I
7514	Y90	-	P	S	8x10	8x10	I
7613	Y100	-	V	-	7.2x9	8x10	I
7623	Y100	-	FB V	-	7.2x9	8x10	I
7623 opt 12	Y100	-	FB V	-	7.2x9	8x10	I
7623 A	Y100	-	FB V	-	7.2x9	8x10	I
7633	Y100	-	FB V	-	7.2x9	8x10	I
7834	Y400	-	FB TV	-	7.2x9	8x10	I

Fastest writing speed		Stored trace brightness	Integrate mode† (use reduced brightness)	Longest storage time of fastest recording		Longest erase cycle	Auto erase	Remote control (Erase only)	Locate zone or Write-through	Dot writing time	Resolution	Product
normal	enhanced or reduced scan†			normal brightness	reduced brightness							
cm/μs	cm/μs	fL		min	min	ms				μs	paired lines	
0.025	-	15	R	60	600	250	-	-	-	-	-	D1
0.05	E0.5	100	-	10	60	500	-	R	L	-	-	DM53A
0.045	E0.9	100	-	0.5	5	250	-	-	L	-	-	DM63
0.025	E0.25	6	I	60	-	250	A	E*	L	-	-	DM64
0.01	-	5	-	15	30	1800	-	R	W	5	368x490	GMA-101A
0.015	-	5	-	15	30	1800	-	R	W	5	420x560	GMA-102A
0.025	E0.25	6	I	60	-	600	-	-	-	-	-	T912
0.04	E0.25	8	-	60	-	500	-	-	-	-	-	214
0.05	E0.25	12	I	240	-	300	A	-	-	-	-	314
0.1	E0.4	10	I	240	-	300	-	-	L	-	-	434
0.75	E5	5	I	240	-	300	-	-	L	-	-	434 opt 1
100	-	80	-	0.25	6	1350	A	-	-	-	-	464
135	R1350	80	-	0.25	6	1350	A	-	-	-	-	466
0.5	E5	3.5	I	60	-	150	A	R	L	-	-	549
0.025	E0.25	6	I	60	-	250	-	E∇	L	-	-	564
0.025	E0.25	6	I	60	-	250	A*	R	L	-	-	564B
0.1	E0.5	2	I	60	-	250	A*	R	L	-	-	564B Mod 08
0.01	-	6	-	15	-	200	-	R	-	9	100x125	601
0.025	-	15	-	60	600	250	-	R	-	4	80x100	603
0.25	-	6	-	60	600	250	-	R	-	0.5	80x100	603 opt 2
0.9	-	100	-	5	60	500	-	R	-	-	80x100	605
0.72	-	200	-	1	10	500	-	R	-	-	144x180	607
0.025	-	6	-	15	300	500	-	R	W	.5	300x400	611
0.025	-	20	-	15	300	900	-	R	W	5	200x266	613
0.01	-	75	-	15	-	175	-	R	-	8	100x125	4501
0.025	E0.1	6	-	60	-	250	A	R	L	-	-	5031
0.025	-	15	R	60	600	250	A*	E*	-	-	-	5111
0.025	-	15	R	60	600	250	A*	E*	-	-	-	5113
0.25	-	6	R	60	600	250	A*	E*	-	-	-	5113 opt 3
0.25	E1	6	R	60	600	250	A*	E*	-	-	-	5115
4.5	-	100	-	5	60	500	-	-	-	-	-	5441
0.9	-	100	-	5	60	500	-	-	-	-	-	5441 opt 5
0.5	E5	10	I	240	-	300	A	E	L	-	-	7313
0.06	E1	6	I	60	-	1000	A	R	W	-	-	7514
4.5	-	100	-	5	60	500	-	E	-	-	-	7613
90° 0.45	-	100	-	∞ 0.25	∞ 60	1000	A	E	-	-	-	7623
200° 0.45	-	100	-	∞ 0.25	∞ 60	1000	A	E	-	-	-	7623 Opt 12
45° 135°	-	100	-	∞ 0.5	∞ 15	1300	A	E	-	-	-	7623A
45° 135°	R180 R1000	100	-	∞ 0.5	∞ 15	1300	A	E	-	-	-	7633
45° 270°	R350 R2500	135	-	30 0.5	∞ 15	1200	A	R	-	-	-	7834

APPENDIX C

STORAGE TUBE NOMENCLATURE

Nomenclature	Abbrev.	Definition
Aperture Burrs		Partial blockage of W.G. aperture which appears as small splattering of electrons around ECO dot/dots.
Background Luminance	Bkgd	The luminance of the storage target when completely erased at a specified operating voltage.
Backplate		See Storage Target Backplate.
Brightness		The attribute of visual perception in which an area appears to emit more or less light.
Collimation Lens		A low-voltage electrostatic lens used to adjust the trajectories of the flood gun electrons.
Collimation Electrode	CE	An element used in the collimation lens.
Contrast Enhancement		A method of altering electrode potentials to reduce background luminance.
Contrast Ratio	CR	The ratio of stored luminance to background luminance at a given operating voltage.
Conventional Mode (Non-Store)		The mode of operation that prevents storage of written information and permits the storage tube to operate as a conventional tube.
Enhance		To alter momentarily the electrode potentials to increase performance (n: Enhancement).
Erase		To change electrode potentials in such a manner that previously stored information is removed (n: Erasure).
Erase Cycle		The sequence of potential changes required to erase the storage target.
Fade Positive Level	F	The highest operating voltage at which stored information can be retained.
Fade Up		The failure of an unwritten area to remain at background brightness and spontaneously move to the stored brightness of some adjacent written area.
Flood Gun	FG	A low-energy electron gun directing a large cone of electrons toward the entire storage target.

Nomenclature	Abbrev.	Definition
Fully Written		The condition under which the entire storage target is stored.
Grid Emission		Small circle of emission or halo (approximately 1/8 in. diameter) around dot (Reject).
Luminance		The quantitative attribute of light that correlates with the sensation of brightness, commonly measured in foot-lamberts (Ft. L.)
Luminance Uniformity Ratio		The ratio of the luminance of the brightness to the dimmest area on the target when the target is fully stored.
Non-Store Level		The mode of operation that prevents storage of written information and permits the storage tube to operate as a conventional tube.
Operating Level	OL	The mid-point of the operating range.
Operating Point	OP	The voltage within the operating range established by the tube specifications.
Operating Range	OR	The voltage range within which information can be written and completely stored under given conditions of operation (upper writing limit minus writing threshold).
Operating Voltage (or Store Level)		The potential difference between the flood gun cathode and the storage target backplate.
Quality Area (or Graticule Area)		The storage target area over which given specifications apply.
Ready-to-write State		The state of the storage target immediately after erasure and before writing again.
Retention Threshold	RT & WT	The lowest operating voltage at which stored information can be retained anywhere within the quality area.
Raster		A series of vertical/horizontal lines used for testing parameters such as W.S. + O.R., used in storage mode.
Store		To retain the written information on the target after the writing beam has passed.
Stored Luminance		The luminance of stored information at a given operating voltage.

Nomenclature	Abbrev.	Definition
Storage Mode		The mode of operation that permits the storage target to retain written information.
Storage Target	ST	A surface having the ability to store information when bombarded by an electron beam.
Storage Target Backplate	STB	A conductive surface electrically coupled to and usually physically supporting the storage target.
Stored Resolution		A measure of the tube's capability to display discrete elements of stored information usually defined by the number of line pairs resolvable per centimeter on the tube face.
Stored Writing Rate	WR	The time rate; i.e., Cm/sec. at which the writing beam will register stored information when scanning the storage target, under stated conditions of operation.
Stored Writing Speed	WS	The speed; i.e., Cm/sec. at which the writing beam will register stored information when scanning the storage target, under stated conditions of operation.
Upper Writing Limit	UWL	The highest operating voltage at which a signal can be written and still maintain a given resolution under given conditions of operation.
Write		To bombard the storage target with writing gun electrons and produce luminescence.
Writing Gun	WG	A high-energy electron gun giving a narrow focused beam which can be deflected and is used to write the information to be stored.
Writing Speed Enhancement		A method of altering electrode potentials to increase the stored writing speed.
Writing Threshold	WT	The lowest operating voltage at which a signal can be written and completely stored under given conditions of operation.